

UCLA

UCLA Electronic Theses and Dissertations

Title

Determining the Role of Coenzyme A in Alternative Macrophage Activation

Permalink

<https://escholarship.org/uc/item/3vz327dq>

Author

Jones, Anthony

Publication Date

2022

Peer reviewed|Thesis/dissertation

UNIVERSITY OF CALIFORNIA

Los Angeles

Determining the Role of Coenzyme A in Alternative Macrophage Activation

A dissertation submitted in partial satisfaction of the requirements for the degree Doctor of
Philosophy in Molecular and Medical Pharmacology

by

Anthony Jones

2022

© Copyright by

Anthony Jones

2022

ABSTRACT OF THE DISSERTATION

Determining the Role of Coenzyme A in Alternative Macrophage Activation

by

Anthony Jones

Doctor of Philosophy in Molecular and Medical Pharmacology

University of California, Los Angeles, 2022

Professor Ajit S. Divakaruni, Chair

Macrophages are innate immune cells that execute a variety of functions including microbial clearance, antigen presentation, and tissue repair. When exposed to the cytokine interleukin 4 (IL-4), these cells express genes associated with alternative activation. Previous work had shown that etomoxir-mediated disruption of coenzyme A homeostasis decreases the macrophage IL-4 response, while exogenous addition of CoA enhances the presence IL-4-associated cell-surface markers. However, the mechanism by which etomoxir decreased intracellular CoA levels and how this ubiquitous metabolic cofactor could instruct alternative activation was entirely unclear. In this work, I show that etomoxir likely decreases intracellular CoA levels by thioester-mediated pantothenate kinase inhibition. Further, I demonstrate that exogenous CoA enhances the IL-4 response *in vitro* and *in vivo*. I determined that CoA acts as a weak toll-like receptor 4 agonist, which enhances the IL-4 response through activation of the MyD88 signaling cascade. Finally, I show that activation of the MyD88 pathway is sufficient to enhance alternative activation both *in vitro* and *in vivo*.

The dissertation of Anthony Jones is approved.

Steven J. Bensinger

Orian Shirihai

Robert M. Prins

Heather R. Christofk

Thomas G. Graeber

Ajit S. Divakaruni, Committee Chair

University of California, Los Angeles

2022

DEDICATION

This work is dedicated to my loving family. Additionally, I wish to dedicate this dissertation to my fiancé Eboni who has been the most supportive person in my life.

TABLE OF CONTENTS

ABSTRACT OF THE DISSERTATION.....	II
COMMITTEE PAGE	III
DEDICATION.....	IV
TABLE OF CONTENTS.....	V
LIST OF TABLES AND FIGURES	VI
ACKNOWLEDGEMENTS	VIII
INTRODUCTION: MACROPHAGE ACTIVATION AS AN ARCHETYPE OF MITOCHONDRIAL REPURPOSING	1
CHAPTER 1: A SINGLE LC-MS/MS ANALYSIS TO QUANTIFY COA BIOSYNTHETIC INTERMEDIATES AND SHORT-CHAIN ACYL COAS	61
CHAPTER 2: MYD88-LINKED TLRs ENHANCE THE IL-4 RESPONSE	97
CONCLUSIONS AND FUTURE DIRECTIONS.....	138

LIST OF TABLES AND FIGURES

INTRODUCTION: FIGURES AND TABLES	30
FIGURE 1: OVERVIEW OF TCA CYCLE BIOENERGETICS.....	30
FIGURE 2: OVERVIEW OF MITOCHONDRIAL BIOENERGETICS AND MEMBRANE POTENTIAL.....	31
FIGURE 3: NON-BIOENERGETIC ROLES OF TCA CYCLE METABOLITES.....	32
CHAPTER 1: FIGURES AND TABLES.....	80
FIGURE 1: THE COA BIOSYNTHETIC PATHWAY.....	80
FIGURE 2: THE COMMON MS/MS FRAGMENTATION PATTERN FOR ALL COA SPECIES.....	81
FIGURE 3: THE LC-MS/MS METHOD PRODUCES WELL-SEPARATED PEAKS FOR EACH ANALYTE.....	82
FIGURE 4: THE METHOD DISPLAYS A LINEAR DETECTION OF ANALYTES	83
FIGURE 5: SSA-BASED SAMPLE PREPARATION RESULTS IN HIGHER RECOVERY OF COA-RELATED METABOLITES.....	84
FIGURE 6: THE METHOD SUCCESSFULLY DETECTS EXPECTED PERTURBATIONS IN COA METABOLISM.	85
FIGURE 7: THE METHOD DETECTS CHANGES IN THE COA BIOSYNTHETIC PATHWAY OF ETOMOXIR TREATED MACROPHAGES.....	86
TABLE 1: PARENT AND DAUGHTER ION M/Z FOR SHORT-CHAIN ACYL COAS, DEPHOSPHO-COA, AND PANTOTHENATE	87
TABLE 2: SOLVENT AND CHROMATOGRAPHY PARAMETERS FOR SHORT-CHAIN ACYL COA DETECTION.....	88

TABLE 3: LOWER LIMITS OF DETECTION AND QUANTITATION OF ANALYZED SPECIES.....	89
TABLE 4: PRECISION AND ACCURACY DETERMINATION FOR THE DESCRIBED LC-MS/MS METHOD.	90
CHAPTER 2: FIGURE AND TABLES	116
FIGURE 1: EXOGENOUS COA ENHANCES ALTERNATIVE MACROPHAGE ACTIVATION	117
FIGURE 2: COA DOES NOT ENHANCE ALTERNATIVE MACROPHAGE ACTIVATION BY BOOSTING KNOWN METABOLIC HALLMARKS OF THE IL-4 RESPONSE.	119
FIGURE 3: EXOGENOUS COA INDUCES A PRO-INFLAMMATORY RESPONSE IN BMDMS.....	121
FIGURE 4: COA IS A TOLL-LIKE RECEPTOR 4 AGONIST	123
FIGURE 5. MYD88-LINKED TLR-LIGANDS ENHANCE IL-4 RESPONSE	125

ACKNOWLEDGEMENTS

The work for this dissertation was performed under the direction of Dr. Ajit S. Divakaruni.

Introduction

The introduction is adapted from Jones AE and Divakaruni AS. Macrophage activation as an archetype of mitochondrial repurposing. *Molecular Aspects of Medicine*. 2020 71:100838.

Chapter One

Chapter One is adapted from Jones AE et al. A Single LC-MS/MS Analysis to Quantify CoA Biosynthetic Intermediates and Short-Chain Acyl CoAs. *Metabolites*.11(8):468. PMID: 34436409.

VITA

EDUCATION

University of California, Los Angeles, Los Angeles, CA
Ph.D. (Expected, December 2022), Molecular and Medical Pharmacology

California State University, Dominguez Hills, Carson, CA
B.S. (2015), Biochemistry

Los Angeles Southwest Community College, Los Angeles, CA
Transfer (2011), Chemistry

RESEARCH EXPERIENCE

University of California, Los Angeles (2018-present)
Dept. of Molecular and Medical Pharmacology
Doctoral Dissertation: “*Determining the role of coenzyme A in anti-inflammatory macrophage polarization*”
Advisor: Ajit Divakaruni, Ph.D

University of California, Los Angeles. (2016-2018)
Dept. of Pulmonary and Critical Care
Project: “*In vivo Imaging of mitochondrial membrane potential in non-small-cell lung cancer*”
Advisor: David Shackelford, Ph.D

California State University, Dominguez Hills. (2012-2015)
Dept. of Chemistry and Biochemistry
Project: “*Separation and identification of phenolic compounds from aloe vera and nopal cactus*”
Advisor: Kenneth Rodriguez, Ph.D

PUBLICATIONS

Meriwether D, **Jones AE**, Ashby JW, Solorzano-Vargas RS, Dorreh N, Noori S, Grijalva V, Ball AB, Semis M, Divakaruni AS, Mack JJ, Herschman HR, Martin MG, Fogelman AM, Reddy ST. (2022) Macrophage COX2 Mediates Efferocytosis, Resolution Reprogramming, and Intestinal Epithelial Repair. *Cell Mol Gastroenterol Hepatol.* 13(4):1095-1120. PMID: 35017061

Jones AE, Arias NJ, Acevedo A, Reddy ST, Divakaruni AS, Meriwether D. (2021) A Single LC-MS/MS Analysis to Quantify CoA Biosynthetic Intermediates and Short-Chain Acyl CoAs. *Metabolites.* 11(8):468. PMID: 34436409

Tucci J, Chen T, Margulis K, Orgel E, Paszkiewicz RL, Cohen MD, Oberley MJ, Wahhab R, **Jones AE**, Divakaruni AS, Hsu C, Noll SE, Sheng X, Zare RN and Mittelman SD. (2021)

Adipocytes provide fatty acids to acute lymphoblastic leukemia cells. *Front in Oncol.* 11:665763. PMID: 33968771

Veliova M, Ferreira CM, Benador IY, **Jones AE**, Mahdaviani K, Brownstein AJ, Desousa BR, Acín-Pérez R, Petcherski A, Assali EA, Stiles L, Divakaruni AS, Prentki M, Corkey BE, Liesa M, Oliveira MF and Shirihai OS (2020) Blocking mitochondrial pyruvate import in brown adipocytes induces energy wasting via lipid cycling. *EMBO Rep.* 21(12): e49634. PMID: 33275313.

Jones AE, Sheng L, Acevedo A, Veliova M, Shirihai OS, Stiles L and Divakaruni AS (2020) Forces, fluxes, and fuels: tracking mitochondrial metabolism by integrating measurements of membrane potential, respiration, and metabolites. *Am J Physiol: Cell Physiol.* 320(1): C80-C91. PMID: 33147057.

Chella Krishnan K, Floyd RR, Sabir S, Jayasekera DW, Leon-Mimila PV, **Jones AE**, Cortez AA, Shrivah V, Péterfy M, Stiles L, Canizales-Quinteros S, Divakaruni AS, Huertas-Vazquez A and Lusic AJ (2020) Liver Pyruvate Kinase Promotes NAFLD/NASH in Both Mice and Humans in a Sex-Specific Manner. *Cell Mol Gastroenterol Hepatol.* 11(2): 389-406. PMID: 32942044.

Assali EA, **Jones AE**, Veliova M, Acín-Pérez R, Taha M, Miller N, Shum M, Oliveira MF, Las G, Liesa M, Sekler I and Shirihai OS (2020) NCLX prevents cell death during adrenergic activation of the brown adipose tissue. *Nat Commun.* 11(1): 3347. PMID: 32620768.

Jones AE and Divakaruni AS (2020) Macrophage activation as an archetype of mitochondrial repurposing. *Mol Aspects Med.* 71:100838. PMID: 31954522.

Cao DY, Spivia WR, Veiras LC, Khan Z, Peng Z, **Jones AE**, Bernstein EA, Saito S, Okwan-Duodu D, Parker SJ, Giani JF, Divakaruni AS, Van Eyk JE and Bernstein KE. (2019) ACE overexpression in myeloid cells increases oxidative metabolism and cellular ATP. *J Biol Chem.* 295(5): 1369-1384. PMID: 31871049.

Momcilovic M, **Jones A**, Bailey ST, Waldmann CM, Li R, Lee JT, Abdelhady G, Gomez A, Holloway T, Schmid E, Stout D, Fishbein MC, Stiles L, Dabir DV, Dubinett SM, Christofk H, Shirihai O, Koehler CM, Sadeghi S and Shackelford DB (2019) In vivo imaging of mitochondrial membrane potential in non-small-cell lung cancer. *Nature.* 575(7782): 380-384. PMID: 31666695.

Maric T, Mikhaylov G, Khodakivskyi P, Bazhin A, Sinisi R, Bonhoure N, Yevtodiyenko A, **Jones A**, Muhunthan V, Abdelhady G, Shackelford D, Goun E. (2019) Bioluminescent-based imaging and quantification of glucose uptake in vivo. *Nat Methods.* 16(6):526-532. PMID: 31086341.

Jones AE, Belmont B, Rodriguez KR. (2014) Evaluation of Freeze-dried aloe vera and nopal cactus for possible health treatments by comparison of antioxidant properties and free radical inhibition. *J Undergrad Chem Res.* 13(4):67-70. PMID: 27284273

Introduction: Macrophage Activation as an Archetype of Mitochondrial Repurposing

ABSTRACT

Mitochondria are metabolic organelles essential not only for energy transduction, but also a range of other functions such as biosynthesis, ion and metal homeostasis, maintenance of redox balance, and cell signaling. A hallmark example of how mitochondria can rebalance these processes to adjust cell function is observed in macrophages. These innate immune cells are responsible for a remarkable breadth of processes including pathogen elimination, antigen presentation, debris clearance, and wound healing. These diverse, polarized functions often include similarly disparate alterations in the metabolic phenotype associated with their execution. In this chapter, mitochondrial bioenergetics and signaling are viewed through the lens of macrophage polarization: both classical, pro-inflammatory activation and alternative, anti-inflammatory activation are associated with substantive changes to mitochondrial metabolism. Emphasis is placed on recent evidence that aims to clarify the essential – rather than associative – mitochondrial alterations, as well as accumulating data suggesting a degree of plasticity within the metabolic phenotypes that can support pro- and anti-inflammatory functions.

1. Introduction

1.1 Mitochondria in cell physiology

Mitochondria play essential roles in cell physiology including, and extending far beyond, serving as the sites of oxidative phosphorylation. In addition to synthesizing the majority of ATP in most cell types (Nicholls and Ferguson, 2013; Pagliarini and Rutter, 2013), mitochondria are also hubs for biosynthesis, Ca²⁺ handling, iron homeostasis, redox balance, and signal transduction (Chandel, 2014; Murphy and Hartley, 2018; Shadel, 2012). Mitochondrially derived signals can be as varied as protein release from the intermembrane space (Jiang and Wang, 2004), metabolite efflux (Ryan et al., 2019), redox signals [e.g. reactive oxygen species (ROS) production] (Finkel, 2011; Murphy, 2009; Reczek and Chandel, 2015), and release of damage-associated molecular patterns (DAMPs) (Grazioli and Pugin, 2018; Picca et al., 2017).

It is increasingly appreciated that the roles of mitochondria in energy metabolism and as a signaling organelle are not necessarily discrete. In fact, one purpose of mitochondria as a signaling organelle is as a communicator of metabolic health status, serving a checkpoint or feedback function to instruct nuclear gene expression and cellular function (Chandel, 2015). Perhaps reflective of this, some proteins with essential roles in energy transduction have dual functions in pathways associated with cell death and disease. For example, cytochrome c is an essential component of the electron transport chain, but also triggers caspase-mediated apoptosis when released to the cytoplasm upon mitochondrial outer membrane permeabilization (Jiang and Wang, 2004; Tait and Green, 2010). Similarly, the F₀F₁-ATP

synthase that generates ATP during oxidative phosphorylation also dimerizes to form the mitochondrial permeability transition pore, a channel causing inner membrane permeability and causative of pathologies such as ischemic heart injury and muscular dystrophy (Bernardi, 2013). This mitochondrial plasticity in shifting from energy powerhouse to signaling platform often involves a classical definition of reduced or impaired mitochondrial function (lowered oxidative phosphorylation, redox imbalance, etc.) (Jazwinski, 2013). Remarkably, however, emerging evidence in murine bone marrow-derived macrophages (BMDMs) suggests this does not necessarily translate to reduced or impaired cellular function.

1.2 Macrophage function and activation

Macrophages are cells of the innate immune system responsible for a remarkable breadth of functions essential to human health including killing pathogens, clearing subcellular debris, and repairing tissue (Adams and Hamilton, 1984). In addition to their role in healthy physiology, targeting macrophage function may lead to improved therapies for a variety of pathologies including tissue fibrosis, cancer, and metabolic disease (Wynn and Vannella, 2016).

Macrophages were first described over 130 years ago by Metchnikoff, who suggested that the observed phagocytosis by ameboid cells could be a means of host defense rather than a deleterious consequence of tissue damage or infection (Gordon, 2016). Specificity for the functional role and activation state of a macrophage at any given time is set by coordinating intrinsic, extrinsic, and environmental cues (Murray, 2017). This allows for the broad and sometimes opposing range of functions (i.e. “kill or repair”) these cells must execute. This so-

called polarization state is often simplified through the classification of pro-inflammatory “M1” and anti-inflammatory “M2” macrophages (Gordon and Taylor, 2005). The nomenclature is drawn from the response to cytokines secreted by subsets of CD4⁺ helper T (T_h) cells. A T_h1 response that is associated with immunity to bacteria and infections and secretion of IFN- γ and tumor necrosis factor- α (TNF- α), whereas a T_h2 response counteracts the microbicidal T_h1 response and is associated with allergy and helminth immunity along with production of interleukin-4 (IL-4), IL-10, and IL-13.

Pro-inflammatory activation can occur via detection of pathogens by pattern recognition receptors (PRRs), proteins present at both the plasma and endosomal membranes (O’Neill et al., 2013). PRRs bind subsets of molecular scaffolds typically associated with microbes [pathogen associated molecular patterns (PAMPs)] or tissue damage [damage associated molecular patterns (DAMPs)]. Innate PRRs are broadly classified in two classes: membrane-bound, including Toll-like receptors (TLRs) and C-type lectin receptors (CLRs), and cytoplasmic, such as NOD-like receptors (NLRs) and RIG-I-like receptors (RLRs) (Akira and Takeda, 2004). Regardless of their localization, PRRs function by receptor-mediated activation of broad transcriptional programs, resulting in an orchestrated inflammatory response to eliminate pathogens or damaged cells (Barton and Medzhitov, 2003).

In addition to activation by PAMPs and DAMPs, macrophages can also be polarized to a range of activation states by secreted cytokines. This can occur in both paracrine [e.g. pro-inflammatory interferon- γ (IFN- γ) or anti-inflammatory IL-4 secreted by lymphocytes] and

autocrine [e.g. pro-inflammatory interleukin-1 β (IL-1 β) or anti-inflammatory transforming growth factor- β (TGF- β)] manners upon receptor binding (Mosser and Edwards, 2008). In some cases, activation of PRR- and cytokine receptor-mediated activation integrate to amplify the inflammatory response. In the hallmark example, activation of TLR4, which recognizes the gram-positive bacterial membrane component lipopolysaccharide (LPS), synergizes with IFN- γ to create a powerful, composite pro-inflammatory signal (Held et al., 1999).

It is often accepted that the M1/M2 framework is based on rigidly prescribed conditions that rarely, if ever, occur physiologically, and do not necessarily reflect the spectral nature of macrophage activation (Martinez and Gordon, 2014). Nonetheless, the use of tightly controlled, *in vitro* polarization assays coupled with modern metabolic techniques has revealed profound and unexpected roles for several aspects of mitochondrial function in the control of the innate immune response.

An essential role for metabolism in macrophage function may be somewhat obvious in the traditional definition, as activation-induced phagocytosis, motility, and cytokine synthesis are all ATP-consuming processes that require commensurate changes in ATP production. Indeed, early biochemical studies showed that glucose consumption in naïve, unstimulated macrophages is far below its enzymatic capacity, suggesting a capacity to quickly upregulate metabolic pathways in response to external stimuli (Newsholme et al., 1986). Abundant genetic and pharmacologic evidence now exists to demonstrate several essential roles for metabolism in shaping macrophage function, and these are surveyed in multiple comprehensive reviews (Arts et al., 2016a; Benmoussa et al., 2018; Caputa et al., 2019;

Geeraerts et al., 2017; Langston et al., 2017; O'Neill and Pearce, 2016; Odegaard and Chawla, 2011; Russell et al., 2019; Van den Bossche et al., 2017; Viola et al., 2019; Weinberg et al., 2015). Such roles include increased and/or rerouted metabolic flux through specific pathways, post-translational modifications by metabolic intermediates, and signaling initiated by metabolites, redox triggers, or nucleic acids.

In the present manuscript, we focus on mitochondria as a hub for both energy transduction as well as metabolite and signal generation, and discuss how these different modes are used to shape macrophage function. It is unquestioned that, in murine macrophages, oxidative metabolism is associated with anti-inflammatory activation (stimulation with IL-4 ± IL-13), and classical inflammatory activation (LPS ± IFN- γ) involves the collapse of oxidative phosphorylation and repurposing of mitochondria towards accumulation of metabolites and other pro-inflammatory triggers. However, the essential, targetable metabolic requirements to adjust macrophage function may not be as black-or-white as initially thought. In fact, a crude analogy could be drawn to macrophage polarization itself. Similarly to how the M1/M2 paradigm is perhaps too bifurcated and discrete to reflect the graded nature of macrophage function (Martinez and Gordon, 2014; Murray, 2017), so too may be a one-size-fits-all approach that suggest 'polarized' metabolic phenotypes are indispensable for pro- or anti-inflammatory macrophage activation. Rather, accumulating evidence suggests bioenergetic and signaling roles for mitochondria in both pro- and anti-inflammatory macrophage activation, although these manifest in different ways.

2. Mitochondrial energy metabolism in macrophage activation

2.1 Overview of mitochondrial energy metabolism.

Of course, the best described function of mitochondria is energy metabolism and the production of ATP through oxidative phosphorylation (Nicholls and Ferguson, 2013). Mitochondria generate ATP through a series of energy transducing processes. The chemical energy in nutrients such as sugars, amino acids, and fatty acids is first harvested through the tricarboxylic acid (TCA) cycle (Figure 1). The TCA cycle (or Krebs cycle) is a series of eight consecutive enzymes that oxidize energy-rich substrates in order to generate the reduced electron carriers NADH and FADH₂. During oxidative TCA cycle metabolism (conventionally drawn clockwise as in Figure 1), three dehydrogenases – isocitrate dehydrogenase (IDH), α -ketoglutarate dehydrogenase (KGDH), and malate dehydrogenase (MDH) – generate NADH. Additionally, succinate dehydrogenase (SDH) activity generates FADH₂, and ATP is generated through substrate-level phosphorylation by the succinyl-CoA synthetase reaction.

The reduced NADH and FADH₂ generated by the TCA cycle and other mitochondrial dehydrogenases [e.g., pyruvate dehydrogenase (PDH), β -hydroxybutyrate dehydrogenase, glycerol-3-phosphate dehydrogenase] are then passed through the mitochondrial respiratory chain. The respiratory chain (or electron transport chain) is a series of energetically favorable electron transfer reactions that are coupled to pumping protons out of the matrix and against their concentration gradient (Rich and Maréchal, 2010). Respiratory complex I oxidizes NADH and transfers the electrons through a series of iron-sulfur clusters to ultimately reduce ubiquinone to ubiquinol (Q to QH₂). This energy harvesting reaction is used to drive the

translocation of protons out of the matrix (Hirst, 2013). Complex II (SDH) also generates QH₂ using the electrons stripped from succinate during its oxidation. Importantly, SDH activity is not directly linked to complex I activity and, unlike complexes I, III, and IV, does not result in net proton translocation (Iverson, 2013). The reduced ubiquinol generated from activity of complexes I and II activity is re-oxidized by respiratory complex III: the electrons from QH₂ are transferred to cytochrome c (Crofts, 2004). Finally, electron transfer from cytochrome c to reduce molecular oxygen ($\frac{1}{2}\text{O}_2$ to H₂O) at complex IV is in the last step of the respiratory chain.

The resulting potential energy harnessed from respiratory chain activity (10 H⁺ pumped for every electron pair passed from NADH to oxygen) is used to drive ATP synthesis during oxidative phosphorylation. Activity of the ATP synthase, often called respiratory complex V, relieves the proton gradient (i.e. H⁺ re-entry into the matrix) to catalyze phosphorylation of ADP (Walker, 2013). Best estimates currently show that per mole of glucose, oxidative phosphorylation generates a maximum of ~31.5 moles of ATP (Mookerjee et al., 2017).

Broadly, mitochondrial energetics can be considered as a balance between processes that generate this potential energy and those that consume it (Figure 2) (Divakaruni and Brand, 2011). Under most conditions, the mitochondrial electron transport chain is the dominant process that generates the proton motive force (pmf). As described earlier, the respiratory chain links exergonic (energetically “downhill”) electron transfer reactions, beginning with the oxidation of NADH by complex I or FADH₂ by complex II, to endergonic (energetically “uphill”) proton translocation. Importantly, though, many enzymes in mitochondria are reversible and

respond to thermodynamic cues (Murphy, 2015). For example, when the membrane potential drops below threshold levels, the ATP synthase and NAD(P) transhydrogenase can operate in the 'reverse' direction to help maintain the pmf (Nicholls and Ferguson, 2013; Nickel et al., 2015).

The pmf is used to drive a range of mitochondrial processes (Brand and Nicholls, 2011), some of which are presented here. During oxidative phosphorylation, the membrane potential is used to drive not just the rotary catalysis of the ATP synthase, but also the prerequisite import of inorganic phosphate and ADP into the matrix against the charge gradient (both are anionic) (LaNoue and Schoolwerth, 1979). The NAD(P) transhydrogenase, or nicotinamide nucleotide transhydrogenase, helps maintain reducing power in the matrix by oxidizing NADH to generate NADP(H), an energetically unfavorable process that consumes the potential energy across the inner membrane to proceed (Hoek and Rydstrom, 1988; Murphy, 2015). Mitochondrial import of nuclear encoded proteins also consumes the membrane potential (Wiedemann and Pfanner, 2017), as does the electrogenic exchange of glutamate and aspartate by SLC25A12 in the malate-aspartate shuttle (LaNoue and Tischler, 1974). Mostly, uptake of metabolites into the matrix is charge neutral due to exchange with other metabolites, although uniport of substrates such as pyruvate is aided by the pH gradient to bring anions into the matrix along with H⁺ co-transport (or OH⁻ antiport) (Palmieri, 2013; Taylor, 2017). Ion channels, notably the mitochondrial calcium uniporter (MCU), will rapidly consume the membrane potential to drive Ca²⁺ uptake (De Stefani et al., 2014; Duchen, 2000). Additionally, uncoupling proteins are H⁺ channels that dissipate the membrane potential to

unlink (or 'uncouple') the activity of the respiratory chain to ATP synthesis (Divakaruni and Brand, 2011). UCP1 activity drives non-shivering thermogenesis in brown adipose tissue (Cannon and Nedergaard, 2004), and it remains contested as to whether other annotated UCPs catalyze so-called proton leak (Vozza et al., 2014). Clearly, a role for the mitochondrial membrane potential includes, but importantly extends far beyond, mitochondrial ATP synthesis.

2.2 Energy metabolism and inflammatory macrophage activation

Although perhaps the best studied feature of classical inflammatory macrophage activation is a striking increase in glycolytic flux (Cramer et al., 2003; Haschemi et al., 2012; Tannahill et al., 2013), profound mitochondrial remodeling occurs as well. Experiments since the 1970s have sought to link inflammatory triggers such as LPS to altered mitochondrial function (Kato, 1972), though recent appreciation of the integration of metabolism and signaling (Chandel, 2015) coupled to breakthrough technologies that increased the scope of functional mitochondrial measurements in their cellular context (Buescher et al., 2015; Divakaruni et al., 2014) have brought exponential progress. A landmark study in 2010 noticed similarities between the signaling pathways activated upon growth factor ligation to their cognate receptors and those activated during TLR ligation (Krawczyk et al., 2010). Given that activation of signaling pathways downstream of growth factor receptors leads to altered cellular metabolism (Christofk et al., 2008; Shaw, 2006), it was hypothesized that similar metabolic changes would also be observed upon activation of dendritic cells (DCs, antigen-presenting innate immune cells). Upon activation with LPS, DCs increase glycolysis and

decrease respiration (Krawczyk et al., 2010). This hallmark metabolic shift is also observed upon classic inflammatory activation with LPS \pm IFN- γ in BMDMs. This was initially demonstrated at the level of gene expression (Rodríguez-Prados et al., 2010) and later reinforced with functional assays that showed that metabolic changes can present as early as 4 hours (Haschemi et al., 2012; Tannahill et al., 2013).

There are likely multiple mechanisms that cause the reduction in mitochondrial ATP production. A contributing factor is undoubtedly the production of high concentrations of nitric oxide upon activation. Induction of inducible nitric oxide synthase (iNOS, the *Nos2* gene), which catalyzes NO production via metabolism of arginine to citrulline (Leone et al., 1991), is dramatically upregulated upon activation with LPS \pm IFN- γ (Han et al., 1999). Nitric oxide production is important for the bactericidal and tumoricidal function of macrophages (Adams et al., 1990; MacMicking et al., 1997; Stuehr and Nathan, 1989). Moreover, it also inhibits oxidative phosphorylation in BMDMs and DCs, as rates of ATP-linked mitochondrial respiration are rescued (to varying degrees) upon both genetic ablation or pharmacologic inhibition of iNOS (Bailey et al., 2019; Everts et al., 2012; Garedew and Moncada, 2008; Van den Bossche et al., 2017). Inhibitory effects of NO on oxidative mitochondrial metabolism can manifest via direct inhibition of respiratory complexes, such as competitive inhibition of respiratory complex IV by NO or S-nitrosation of respiratory complex I (Chouchani et al., 2013; Cleeter et al., 1994; Clementi et al., 1998). Additionally, nitric oxide may affect expression of mitochondrial proteins, as expression of the NADH-binding domain of complex I *Ndufv2* is reduced upon activation with LPS + IFN- γ in wild-type BMDMs but unchanged on a *Nos2*^{-/-}

background (Bailey et al., 2019). However, in many cases the respiratory inhibition upon inflammatory activation is only partially rescued with genetic or pharmacologic inhibition of iNOS (Bailey et al., 2019; Van den Bossche et al., 2016), suggesting nitric oxide-independent means of reprogramming mitochondrial metabolism during inflammatory activation.

Additional mechanisms likely include disruption of oxidative TCA cycle metabolism. Of course, an inability to generate NADH or FADH₂ due to decreased expression/activity of TCA cycle dehydrogenases necessarily slows respiratory chain activity and, as a result, oxidative phosphorylation. LPS stimulation results in a decrease in gene expression of both IDH and MDH in BMDMs (Jha et al., 2015; Tannahill et al., 2013), and changes observed with metabolomics and stable isotope tracing confirm reduced IDH activity and a bonafide break in the TCA cycle (De Souza et al., 2019; Jha et al., 2015). Multiple mechanisms likely contribute to the reduced IDH activity observed during pro-inflammatory activation. IDH expression is reportedly repressed by the orphan nuclear receptor Nur77 (Koenis et al., 2018) as well as type I interferon signaling (De Souza et al., 2019). Although genetic downregulation does not always manifest in altered IDH protein abundance (Bailey et al., 2019), it is well established that enzyme activity is decreased. Other TCA cycle enzymes and mitochondrial dehydrogenases show reduced activity upon pro-inflammatory activation as well (Cordes et al., 2016; Palmieri et al., 2018), and the extent to which control over respiratory inhibition is distributed among these various enzymes is not completely understood.

Additionally, mitochondrial reactive oxygen species (ROS) production may be another mechanism by which mitochondrial ATP production is reduced. In addition to microbicidal

superoxide produced by the plasma membrane-bound NADPH oxidase (Cathcart, 2004), mitochondrial ROS production is thought to be an important signal during inflammatory macrophage activation (West et al., 2011). Mitochondrial adaptations that support ROS production may necessarily involve reductions in oxidative phosphorylation. Of course, mitochondrial ROS production is directly affected by the bioenergetic status of mitochondria, though it is important to draw a distinction between ROS production associated with mitochondrial dysfunction (Adam-Vizi and Starkov, 2010) versus broader programs that reappropriate mitochondria away from oxidative phosphorylation and towards a generation of ROS as a signal. For example, mitochondria alter respiratory chain supercomplex assembly upon bacterial recognition in a way that may support mitochondrial ROS production but reduce oxidative capacity through specific pathways over time (Garaude et al., 2016). Moreover, during LPS activation, BMDM mitochondria are repurposed away from oxidative phosphorylation and towards production of reactive oxygen species. In fact, mitochondria remarkably maintain an elevated membrane potential despite a profound collapse of oxidative phosphorylation, suggesting a reset balance between pmf production and consumption and perhaps hydrolysis of glycolytically-derived ATP to help maintain the membrane potential (Mills et al., 2016).

Although it is well established that profound respiratory inhibition occurs in murine BMDMs upon activation with LPS (\pm IFN- γ) treatment, the functional reason for this remains somewhat unclear. For example, a reduced respiratory rate during inflammatory activation could be necessary for (i) enhancing glycolytic flux to fuel cytoplasmic NADPH production and

anabolism, (ii) generating redox signals such as ROS from reverse electron transport, or (iii) increasing abundance of TCA cycle-associated signaling metabolites by slowing Krebs cycle turnover. However, each of these processes can occur, in principle, without the near-total collapse of respiratory chain activity observed during LPS + IFN- γ treatment.

Moreover, it is likely that our current models for mitochondrial repurposing during classical pro-inflammatory macrophage activation may not be one-size-fits-all. For example, inflammatory stimuli such as IFN- γ treatment (without LPS) (Wang et al., 2018a), the TLR4 agonist monophospholipid A (Fensterheim et al., 2018), or low concentrations of LPS (10 ng/mL) (Cordes et al., 2016) do not elicit similarly dramatic reductions in mitochondrial ATP production in BMDMs. Moreover, maximal respiratory capacity is actually increased early upon bacterial recognition (Garaude et al., 2016) or LPS + IFN- γ stimulation (Cameron et al., 2019), and genetic models that blunt NO production (thereby enhancing respiration) increase production of succinate and itaconate in response to LPS + IFN- γ stimulation. The mitochondrial bioenergetic changes observed in murine BMDMs upon LPS activation are also largely absent in human peripheral blood monocyte (PBMC)-derived macrophages (Vijayan et al., 2019). As such, the precise functional role of mitochondria during inflammatory activation in murine BMDMs, and whether the same mechanisms are present in human macrophages, are not fully understood.

2.3 Energy metabolism and anti-inflammatory activation

Given the array of different macrophage functions coupled with the requisite role of metabolism in macrophage activation, it follows that there is tremendous diversity in the metabolic phenotypes as well. Of course, the most straightforward examples of this are the almost entirely disparate phenotypes observed between LPS- and IL-4-polarized macrophages (Van den Bossche et al., 2017). While LPS \pm IFN- γ -activated macrophages depress oxidative phosphorylation, anti-inflammatory activation with IL-4 is associated with increased respiratory capacity and mitochondrial metabolism.

The first indication that mitochondrial metabolism was associated with IL-4-driven (or “alternative”) activation was increased expression of enzymes associated with the TCA cycle, fatty acid oxidation genes, and drivers of mitochondrial biogenesis such as *Pgc1b* (Haschemi et al., 2012; Vats et al., 2006). Mitochondrial mass increases, as does maximal respiratory capacity upon IL-4 activation (Huang et al., 2014; Vats et al., 2006). Additionally, biochemical and functional evidence is supported by genetic evidence for an essential role for mitochondria and/or lipid metabolism, as the nuclear receptor PPAR- γ , a master transcription factor regulating lipid homeostasis, is essential for IL-4-driven polarization (Odegaard et al., 2007).

It is unquestionable that enhanced mitochondrial metabolism is associated with anti-inflammatory activation, and multiple metabolic pathways likely fuel this phenotype. For example, glucose-driven oxidative phosphorylation increases in response to IL-4 (Covarrubias et al., 2016; Huang et al., 2016; Vats et al., 2006). The inhibitory analog 2-deoxyglucose (2-DG), which blocks glucose oxidation after its cellular uptake, also decreases many markers of

IL-4 polarization *in vitro* and blunts the *in vivo* response to infection with the gastrointestinal helminth *H. polygyrus* (Covarrubias et al., 2016; Huang et al., 2016; Tan et al., 2015). Indeed, data suggests that some process dependent on mitochondrial glucose oxidation, rather than glycolysis, may explain the dependency. 2-DG blocks the IL-4-response, but cells grown in medium supplemented with galactose can polarize normally (Wang et al., 2018b). Moreover, knockdown of the pyruvate dehydrogenase kinase-1 (PDK1), which relieves kinase-mediated repression of PDH activity (Harris et al., 1997), also can reportedly boost expression of some anti-inflammatory markers (Tan et al., 2015). Likewise, inhibition of the mitochondrial pyruvate carrier, which blocks uptake of glucose-derived pyruvate into mitochondria, lowers expression of the IL-4 associated markers resistin-like molecule alpha (RELM α) and programmed cell death 1 ligand 2 (PD-L2) (Huang et al., 2016).

In addition to increases in glucose metabolism, increased oxidation of glutamine and fatty acids are also enhanced in BMDMs upon alternative activation. IL-4 enhances expression of the plasma membrane glutamine transporter ASCT2 and steady-state glutamine levels (Palmieri et al., 2017; Tavakoli et al., 2017). Glutamine withdrawal from the experimental medium or inhibition of glutaminase also blunt the IL-4 response (Jha et al., 2015; Liu et al., 2017). Increased fatty acid oxidation (FAO) is also universally recognized as a being strongly associated with anti-inflammatory macrophage activation (Gonzalez-Hurtado et al., 2017; Namgaladze and Brüne, 2014; Odegaard et al., 2007; Vats et al., 2006). A suite of genes related to lipid metabolism and oxidation increase in response to IL-4, and functional assays

with radiolabeled long chain fatty acids also show a substantial increase in fatty acid uptake and oxidation (Gonzalez-Hurtado et al., 2017; Vats et al., 2006).

Whether this fatty acid oxidation is an essential and targetable feature of the IL-4 response, however, has been the subject of debate and may be context-dependent (Van den Bossche and van der Windt, 2018). Indeed, the carnitine palmitoyltransferase-1 (CPT-1) inhibitor etomoxir can block IL-4-driven polarization at 200 μ M (Covarrubias et al., 2016; Huang et al., 2016, 2014). However, accumulating pharmacologic and genetic evidence suggests this is likely due to an off target effect of the drug, a reactive epoxide with several non-specific effects (Ceccarelli et al., 2011; Nomura et al., 2016; Raud et al., 2018). Lower concentrations of the drug that demonstrably block fatty acid oxidation do not inhibit the IL-4 response (Divakaruni et al., 2018; Namgaladze and Brüne, 2014; Tan et al., 2015), and high concentrations of etomoxir block IL-4-driven activation even in models where CPT-1a or CPT-2 have been genetically ablated (Divakaruni et al., 2018; Nomura et al., 2016).

The association between enhanced activities of multiple metabolic pathways with IL-4-associated differentiation suggests a degree of metabolic plasticity with IL-4-polarized macrophages (Wang et al., 2018b), and raises the question of whether the role of mitochondria is primarily bioenergetic or more closely aligned with biosynthesis and signaling. Indeed, IL-4 polarization can proceed when BMDMs are cultured in galactose (Wang et al., 2018b), which will increase reliance on oxidative phosphorylation for ATP production and in the presence of a range of respiratory chain inhibitors (which will result in glycolysis needing to meet almost all of the cellular ATP demand) (Divakaruni et al., 2018). These results suggest a threshold

requirement of ATP, irrespective of the pathway used for its generation. However, this is not without contradictory data. Multiple, independent reports have shown that chemical inhibition of oxidative phosphorylation or blocking the expression of mitochondrial proteins via reduced hypusination of the translation factor eukaryotic initiation factor 5A (eIF5A) reduces markers of the IL-4 response (Puleston et al., 2019; Van den Bossche et al., 2016; Vats et al., 2006).

Multiple, non-exclusive reasons might underlie the discrepancy. Importantly, it is well accepted that metabolic regulation of alternative activation is mosaic, as metabolic modulators frequently only regulate a subset of IL-4-associated genes (Covarrubias et al., 2015; Divakaruni et al., 2018; Sanin et al., 2018). As such, varying results may be due to differential readouts of genes and/or markers which are used to classify the IL-4 response. For example, it is possible that respiratory chain inhibition could affect the abundance of individual cell surface markers, but perhaps change neither gene expression nor the population of cells positive for multiple markers. Results may also be less reflective of the role of oxidative phosphorylation but rather attributable to different macrophage preparations and their glycolytic capacity to meet a threshold ATP demand. The broader use of functional assays or larger-scale -OMICS data beyond expression of select genes and proteins could therefore prove powerful in linking essential metabolic processes to alternative macrophage activation. Additional clarity could also come from using standardized, minimal concentrations of tool compounds to avoid potential off-target effects of respiratory chain inhibitors, which are often used at concentrations far exceeding the concentrations required for maximal effects. Nonetheless, our current understanding remains that mitochondrial metabolism is crucial to

the IL-4 response, though this dependence may not be solely attributable to bioenergetic function.

3. Mitochondrial signaling and macrophage activation

3.1 Mitochondrial signaling in cell physiology

One of the more exciting and remarkable developments in mitochondrial biology over the past decade has been appreciation of the myriad of ways in which the organelle links metabolism to cell physiology via TCA cycle metabolites (Dang and Su, 2017; Lu and Thompson, 2012; Mills et al., 2017; Ryan et al., 2019; Sciacovelli and Frezza, 2017; Sivanand et al., 2018). Much like bioenergetics, early inspiration likely came from the field of cancer metabolism following the discovery that cancers linked to TCA cycle mutations accumulate metabolites that can alter transcription factor activation and epigenetic remodeling (Lu et al., 2012; Selak et al., 2005; Xiao et al., 2012; Xu et al., 2011). Indeed, some of these same principles underly how TCA cycle metabolites can promote genetic and epigenetic changes during macrophage activation (Covarrubias et al., 2016; Liu et al., 2017; Tannahill et al., 2013).

However, the unique induction of the immunometabolite itaconate upon inflammatory macrophage activation stands out as an archetypal example of repurposing mitochondrial metabolism towards metabolite production to execute cell-specific functions (Cordes et al., 2015; O'Neill and Artyomov, 2019). In addition to TCA cycle metabolites, ROS (Garaude et al., 2016; West et al., 2011) and release of nucleic acids (Dhir et al., 2018; Shimada et al., 2012; Zhong et al., 2018) are also emerging as mitochondrially derived signals that can shape the immune response.

3.2 Mitochondrial signaling in inflammatory macrophage activation

Roles for many TCA cycle metabolites have been identified as important in shaping macrophage phenotypes (Figure 3) (Arts et al., 2016b; Infantino et al., 2011; Liu et al., 2017), and production of the immunomodulatory metabolites itaconate and succinate are hallmark examples of how mitochondria can be repurposed to support macrophage function (Cordes et al., 2015; Mills and O'Neill, 2014; O'Neill and Artyomov, 2019). The anti-microbial properties of itaconic acid have well known for decades as an inhibitor of the isocitrate lyase, an enzyme in the glyoxylate shunt (McFadden and Purohit, 1977). This pathway, non-functional or absent in mammals but necessary for long-term persistence of some bacterial infections (Muñoz-Elías and McKinney, 2005), allows biosynthesis and anaplerotic reactions to occur from acetyl-CoA-producing nutrients such fatty acids, thereby allowing bacterial survival under glucose-limiting conditions (Dolan and Welch, 2018). Additionally, the coenzyme A ester of itaconate (itaconyl-CoA) can inhibit bacterial methylmalonyl-CoA mutase, an integral enzyme in bacterial strains which catabolize propionate as an energy source (Ruetz et al., 2019).

Multiple findings were integrated to reveal *Irg1* as the gene encoding the enzyme generating itaconate as an offshoot of the mitochondrial TCA cycle (Michelucci et al., 2013). Previous work had identified *Irg1* as heavily transcribed upon LPS activation (Lee et al., 1995), and later work showed macrophages produced itaconate upon infection (Shin et al., 2011; Strelko et al., 2011; Sugimoto et al., 2012). Finally, using sequence homology with *Aspergillus* cis-aconitase decarboxylase (CAD), *Irg1* was identified and characterized as the mammalian CAD responsible for itaconate production (Michelucci et al., 2013).

In addition to a putative role as a bactericidal metabolite, itaconate may also have anti-inflammatory roles via posttranslational modification and direct effects on macrophage metabolism. The electrophilic metabolite, which is produced at millimolar concentrations upon activation (Cordes et al., 2016; Michelucci et al., 2013), can act as a Michael acceptor and affect the cellular oxidative stress response. Itaconate can alkylate a critical cysteine on Kelch-like ECH-associated protein 1 (KEAP1) (E. L. Mills et al., 2018), an endogenous repressor of the transcription factor NRF2 (Nuclear factor erythroid 2-related factor 2). This slows the degradation of NRF2, thereby increasing its activity and promoting an anti-inflammatory phenotype (Ahmed et al., 2017). Moreover, by reacting with glutathione as a Michael acceptor, itaconate can also decrease I κ B ζ pathway activity and, in turn, lower pro-inflammatory gene expression (Bambouskova et al., 2018).

Itaconate is also directly responsible for the increase in succinate observed during pro-inflammatory activation, as itaconate (methylene succinate) is a competitive inhibitor of succinate dehydrogenase (Cordes et al., 2016; Lampropoulou et al., 2016). The orders-of-magnitude increase in itaconate upon LPS activation is coupled to an increase in succinate, both of which are absent in *Irg^{-/-}* BMDMs (Lampropoulou et al., 2016). Much like itaconate, succinate can also shape macrophage activation in multiple distinct ways.

Increased levels of succinate observed during LPS activation can adjust pro-inflammatory gene expression via altered stability of hypoxia inducible factor-1 α (HIF-1 α) (Tannahill et al., 2013). Inhibition of prolyl hydroxylases by the altered succinate/ α -ketoglutarate ratio allows continued transcription of the inflammatory cytokine interleukin-1 β

(IL-1 β) due to a hypoxia response element on the IL-1 β promoter (Tannahill et al., 2013; Zhang et al., 2006). Adjusting succinate levels with cell permeant succinate analogs can also support a pro-inflammatory function for the metabolite, as these decrease expression of the anti-inflammatory IL-1RA and IL-10 (Mills et al., 2016).

In addition to stabilization of prolyl hydroxylases, succinate can regulate cell signaling via activation of extracellular receptors. It is an endogenous ligand for the G-protein coupled receptor GPR91 (or SUCNR1) (He et al., 2004). First identified in the kidney as a mediator of hypertension (He et al., 2004), SUCNR1 is also expressed in DCs and BMDMs (Littlewood-Evans et al., 2016; Rubic et al., 2008). Its activation enhances the pro-inflammatory effect of LPS, and cells from *Gpr91*^{-/-} mice have reduced HIF-1 α and IL-1 β production upon activation relative to wild-type controls (Littlewood-Evans et al., 2016).

Efflux of mitochondrially-derived citrate by the mitochondrial citrate carrier (CiC) is also important for aspects of pro-inflammatory macrophage activation. Citrate released from mitochondria is converted to malonyl CoA by first generating cytoplasmic acetyl CoA via ATP citrate lyase (ACLY) and subsequent conversion of acetyl CoA to malonyl CoA by acetyl CoA carboxylase (ACC). Inhibition of both the mitochondrial citrate carrier (CiC) responsible for efflux as well as ACLY decrease markers of pro-inflammatory activation such as NO production (Infantino et al., 2013, 2011). Malonyl CoA is primarily considered as a building block for fatty acid synthesis, as well as an endogenous CPT-1 inhibitor that slows fatty acid oxidation upon increased mitochondrial pyruvate metabolism (Hue and Taegtmeyer, 2009; McGarry et al., 1978). However, recent work shows that the glycolytic enzyme glyceraldehyde-

3-phosphate dehydrogenase (GAPDH) can be malonylated, and this post-translational modification relieves GAPDH-mediated repression of TNF α mRNA thereby enhancing translation (Galván-Peña et al., 2019). Regardless of the TCA cycle metabolite, it appears as if the pronounced changes in abundance are dynamic, as the increased levels of itaconate, succinate, and citrate observed during pro-inflammatory activation are restored to basal levels after 48 hours (Seim et al., 2019).

ROS is also a well-established signal for mitochondrial control of macrophage activation, and may be an additional, essential link between succinate levels and macrophage activation. Production of superoxide is, of course, tightly associated with inflammatory macrophage activation given the important role of the plasma membrane NADPH oxidase in pathogen clearance (Cathcart, 2004). Mitochondrial superoxide and ROS production was initially linked to macrophage activation through genetic studies with proteins indirectly associated with oxidative stress (Arsenijevic et al., 2000; Kizaki et al., 2002; Tal et al., 2009), and direct evidence came from studies linking cytokine signaling and TLR activation to mitochondrial ROS production and microbial clearance (Sonoda et al., 2007; West et al., 2011).

Succinate is strongly associated with mitochondrial ROS production through mitochondrial reverse electron transport (RET) (Murphy, 2009). Under conditions of a high membrane potential along with reduced NADH and quinone pools, succinate oxidation is associated with RET (Robb et al., 2018). These conditions can push electrons in the 'backwards' direction through complex I and generate substantial superoxide (Chouchani et

al., 2016). This form of ROS production is thought to underlie much of the damage associated with cardiac ischemia reperfusion injury – where succinate also increases upon ischemia and is oxidized upon reperfusion (Chouchani et al., 2014) – and occurs at physiologically relevant membrane potentials and quinone reduction states (Robb et al., 2018).

Indeed, the mitochondrial membrane potential increases upon inflammatory activation in a subpopulation of macrophages (Mills et al., 2016), linking the bioenergetic phenotype observed during inflammatory activation with increased succinate oxidation and RET. Moreover, bacterial recognition causes a shift away from reliance on complex I and towards a phenotype with enhanced complex II (succinate dehydrogenase) activity and sensitive to blocking mitochondrial ROS production, further establishing the respiratory chain as a link between TLR activation and enhanced mitochondrial ROS (Garaude et al., 2016). A requirement for RET in the LPS-induced regulation of IL-1 β production is given by blunting the response with rotenone (a complex I inhibitor that will block RET-driven superoxide from complex I), FCCP (an uncoupler that will dissipate the pmf), and heterologous expression of alternative oxidase [AltOx, an enzyme found in some plants that will re-oxidize the quinone pool (El-Khoury et al., 2014)] (Mills et al., 2016). Remarkably, mice expressing AltOx are resistant to LPS-induced toxicity, demonstrating the *in vivo* relevance of mitochondrial redox status in mediating the inflammatory response.

Recent work also suggests that ROS production by respiratory complex III may play a role in pro-inflammatory activation: the complex III inhibitor myxothiazol can blunt increases in cell surface marker expression and cytokine release upon LPS + IFN- γ treatment (Cameron

et al., 2019). However, the exact links between enhanced mitochondrial superoxide production and nuclear gene expression remain unclear. Release of oxidized mitochondrial nucleic acids, though, is a likely mechanism (Shimada et al., 2012; West and Shadel, 2017; Zhong et al., 2018).

3.3 Mitochondrial signaling in anti-inflammatory activation

Given the association between IL-4 polarization and increased oxidative metabolism, a role for mitochondrial signaling has been somewhat overshadowed by bioenergetic function. Nonetheless, mitochondrially derived metabolites can play important roles in regulating the anti-inflammatory response, particularly via epigenetics. Glutamine-derived α -ketoglutarate has been shown to be important as a co-factor for the histone demethylase Jumonji domain-containing protein D3 (Jmjd3) (Liu et al., 2017), which regulates epigenetic modification during IL-4-driven activation. Similarly to pro-inflammatory macrophage activation, acetyl CoA derived from mitochondrial citrate is also important for the IL-4 response. In addition to its role in lipogenesis, genetic and pharmacologic evidence support a role for ACLY-derived acetyl CoA in histone acetylation during alternative activation (Covarrubias et al., 2016).

Unexpectedly, the metabolic co-factor coenzyme A (CoA) has also emerged as an essential mediator of IL-4-driven macrophage activation. CoA is a ubiquitous metabolite facilitating acetyl transfer reactions and is essential to a range of physiological processes, most notably carbohydrate and lipid metabolism (Leonardi et al., 2005). Initial links between CoA and alternative activation were discovered while exploring which of the many off-target effects of etomoxir was responsible for its efficacy in blocking anti-inflammatory activation

(Divakaruni et al., 2018). Exogenous delivery of CoA to macrophages restored the etomoxir-induced decrease in intracellular CoA levels, as well as the rescue the expression of IL-4-associated cell surface markers, even in models with genetic disruption of long-chain fatty acid oxidation. Importantly, exogenous supplementation of CoA to the assay medium enhances the IL-4-associated cell surface markers above IL-4-treatment alone. The result suggests that intracellular CoA levels may be limiting, and therefore regulatory and targetable, in anti-inflammatory polarization. However, the precise mechanism by which CoA affects alternative activation, and whether this involves mitochondrial metabolism, remain unclear. A mechanism could be as straightforward as CoA abundance directly affecting acetyl CoA levels and histone acetylation (Covarrubias et al., 2016), or rather CoA levels could be limiting for a host of oxidative or biosynthetic metabolic reactions necessary for the IL-4 response.

Similarly unclear is whether mitochondrial reactive oxygen species, a pro-inflammatory trigger, plays any role in dampening the anti-inflammatory response. Supportive evidence at the level of gene expression comes from the use of different mitochondrial inhibitors. For example, complex I inhibition with rotenone, which blocks reverse electron transport and IL-1 β production upon LPS activation (Mills et al., 2016), remarkably increases some markers of the IL-4 response (Divakaruni et al., 2018). Moreover, rotenone and the ATP synthase inhibitor oligomycin both inhibit oxidative phosphorylation but can have markedly different effects on anti-inflammatory activation, perhaps suggesting this may be due to differential effects on the mitochondrial membrane potential and downstream redox triggers (Divakaruni et al., 2018). Clearly, more work is needed to better understand the precise role of mitochondria in anti-

inflammatory activation, particularly in the discovery of signals that reciprocally regulate pro- and anti-inflammatory markers and work within the graded, spectral nature of macrophage activation.

4. Concluding Remarks

In addition to autoimmune diseases that may be expected to have a dysregulated balance in the macrophage polarization state, it is now well accepted that an imbalance between pro- and anti-inflammatory function can underlie a range of diseases as varied as diet-induced obesity (Lumeng et al., 2008), insulin resistance (Olefsky and Glass, 2010), cardiovascular disease (Bolego et al., 2013; Zhou and Tian, 2018), non-alcoholic steatotic hepatitis (Kazankov et al., 2019), neurodegeneration (Baik et al., 2019), and cancer (Noy and Pollard, 2014). It therefore follows that 're-polarizing' the macrophage population may be a therapeutic strategy (Sica and Mantovani, 2012), and pre-clinical studies have investigated pharmacologic and biologic means to repolarize macrophages to adjust disease progression (Chen et al., 2018; Georgoudaki et al., 2016). Given the requisite metabolic changes that occur during macrophage activation, and that mitochondrial changes may explain limitations in reprogramming macrophages after initial polarization (Van den Bossche et al., 2016), mitochondrial metabolism is an attractive therapeutic target (Murphy and Hartley, 2018). Strategies could include not only repurposing existing drugs that target metabolic enzymes and transcriptional programs, but also cell-permeant metabolite analogs (Martin et al., 2019; E. A. Mills et al., 2018) given the dramatic effects of TCA cycle metabolites on macrophage function. Indeed, application of these concepts to targeting macrophage metabolism is likely

to only further enhance our appreciation for the breadth of mitochondrial repurposing upon macrophage activation.

Lastly, additional studies devoted to understanding how metabolism impacts both pro- and anti-inflammatory macrophage activation must be undertaken. Precise analyses that reveal how decreases in mitochondrial oxidative phosphorylation can directly instruct changes in the expression of pro-inflammatory genes are of particular interests. Regarding anti-inflammatory activation, further investigation of the mechanism by which exogenous CoA controls alternative macrophage activation are necessary. More specifically, studies determining if addition of “free” CoA in culture media increases the synthesis of particular intracellular acyl-CoAs are needed. These studies are important because some CoA thioesters have the ability to alter the epigenetic landscape and transcription factor activity during anti-inflammatory macrophage activation. Taken together, the above-mentioned studies may reveal therapeutic options for diseases including rheumatoid arthritis and cancer.

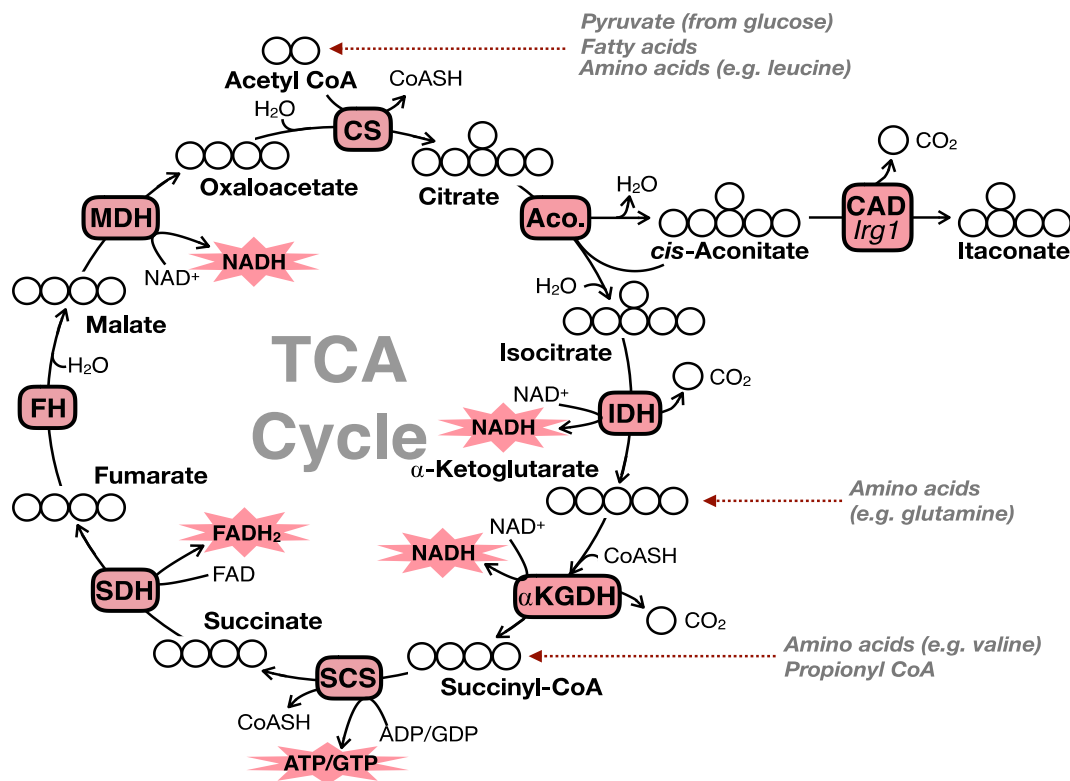


Figure 1: Overview of TCA cycle bioenergetics.

The TCA cycle is a series of 8 reactions which, from a bioenergetic perspective, provide electrons to respiratory chain in the form of the reduced electron carriers NADH and FADH₂. Isocitrate dehydrogenase, α -ketoglutarate dehydrogenase, and malate dehydrogenase generate NADH (when driven in the oxidative direction) for oxidation and reduction of the quinone pool by complex I. Succinate dehydrogenase (respiratory complex II) oxidizes succinate to reduce the quinone pool and using FADH₂ as an intermediate.

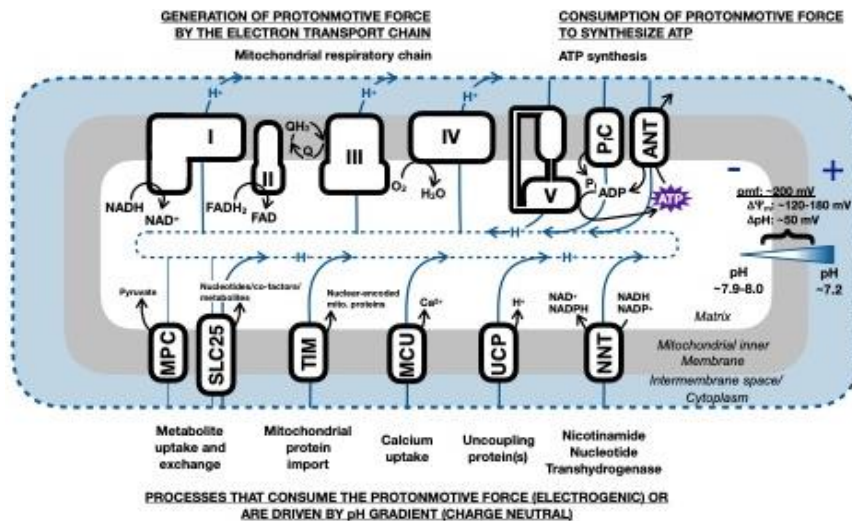


Figure 2: Overview of mitochondrial bioenergetics and membrane potential.

A reservoir of potential energy exists across the mitochondrial inner membrane due to the H⁺ gradient across the inner membrane. This consists of both an electrical component ($\Delta\Psi_m$), due to disparate charge across the membrane, and a chemical inner component, due to the differential pH ($\Delta\Psi_m$). The resulting proton motive force (ρmf) can be used to drive a range of energy-demanding reactions central to mitochondrial activity. I-V, mitochondrial respiratory complexes I-IV and the ATP synthase (complex V); PiC, inorganic phosphate carrier; ANT, adenine nucleotide translocase; NNT, nicotinamide nucleotide transhydrogenase [also NAD(P) transhydrogenase]; UCP, uncoupling protein; MCU, mitochondrial calcium uniporter; TIM, translocase

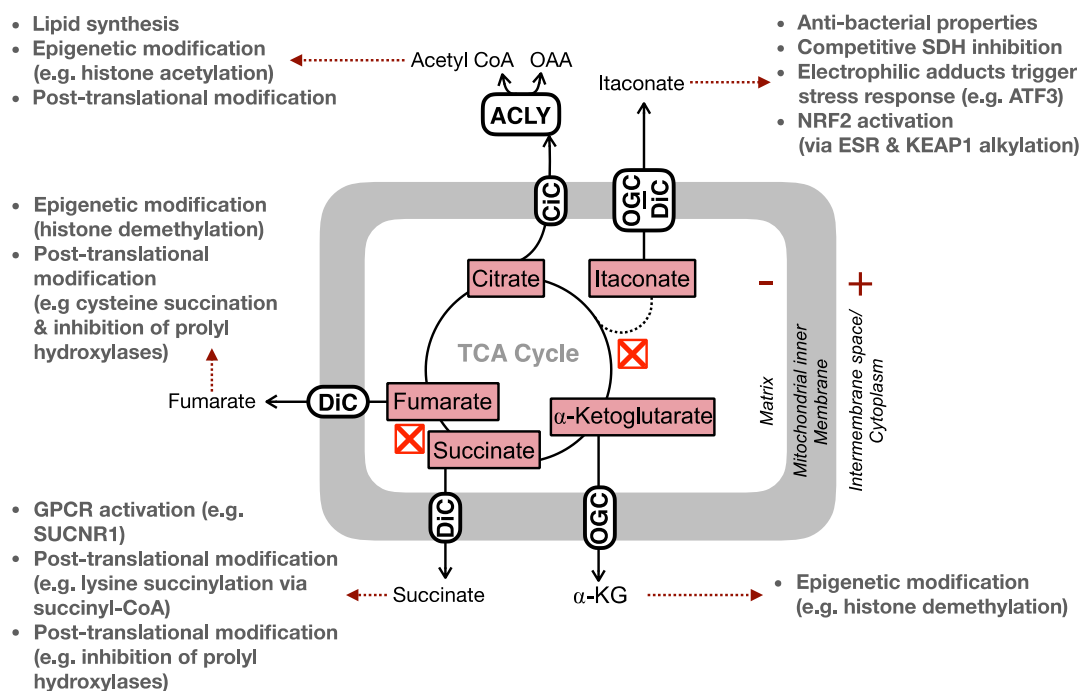


Figure 3: Non-bioenergetic roles of TCA cycle metabolites.

In addition to linking substrate oxidation to the respiratory chain, TCA cycle metabolites also serve critical roles in regulating cell function independently of direct effects on energy metabolism. These include post-translational modifications (e.g. hydroxylation, acetylation, alkylation, etc.), epigenetic modifications, ligand-mediated alterations of protein activity, and even direct functional effects such as microbicidal itaconate. ACLY, ATP citrate lyase; DiC, dicarboxylate carrier; OGC, oxoglutarate carrier; CiC, citrate carrier.

References

- Adam-Vizi, V., Starkov, A.A., 2010. Calcium and mitochondrial reactive oxygen species generation: How to read the facts. *J. Alzheimer's Dis.* <https://doi.org/10.3233/JAD-2010-100465>
- Adams, D.O., Hamilton, T.A., 1984. The Cell Biology of Macrophage Activation. *Annu. Rev. Immunol.* <https://doi.org/10.1146/annurev.iy.02.040184.001435>
- Adams, L.B., Hibbs, J.B., Taintor, R.R., Krahenbuhl, J.L., 1990. Microbiostatic effect of murine-activated macrophages for *Toxoplasma gondii*. Role for synthesis of inorganic nitrogen oxides from L-arginine. *J. Immunol.*
- Ahmed, S.M.U., Luo, L., Namani, A., Wang, X.J., Tang, X., 2017. Nrf2 signaling pathway: Pivotal roles in inflammation. *Biochim. Biophys. Acta - Mol. Basis Dis.* <https://doi.org/10.1016/j.bbadis.2016.11.005>
- Akira, S., Takeda, K., 2004. Toll-like receptor signalling. *Nat. Rev. Immunol.* <https://doi.org/10.1038/nri1391>
- Arsenijevic, D., Onuma, H., Pecqueur, C., Raimbault, S., Manning, B.S., Miroux, B., Couplan, E., Alves-Guerra, M.C., Goubern, M., Surwit, R., Bouillaud, F., Richard, D., Collins, S., Ricquier, D., 2000. Disruption of the uncoupling protein-2 gene in mice reveals a role in immunity and reactive oxygen species production. *Nat. Genet.* <https://doi.org/10.1038/82565>
- Arts, R.J.W., Joosten, L.A.B., Netea, M.G., 2016a. Immunometabolic circuits in trained immunity. *Semin. Immunol.* <https://doi.org/10.1016/j.smim.2016.09.002>
- Arts, R.J.W., Novakovic, B., ter Horst, R., Carvalho, A., Bekkering, S., Lachmandas, E.,

Rodrigues, F., Silvestre, R., Cheng, S.C., Wang, S.Y., Habibi, E., Gonçalves, L.G., Mesquita, I., Cunha, C., van Laarhoven, A., van de Veerdonk, F.L., Williams, D.L., van der Meer, J.W.M., Logie, C., O'Neill, L.A., Dinarello, C.A., Riksen, N.P., van Crevel, R., Clish, C., Notebaart, R.A., Joosten, L.A.B., Stunnenberg, H.G., Xavier, R.J., Netea, M.G., 2016b. Glutaminolysis and Fumarate Accumulation Integrate Immunometabolic and Epigenetic Programs in Trained Immunity. *Cell Metab.* <https://doi.org/10.1016/j.cmet.2016.10.008>

Baik, S.H., Kang, S., Lee, W., Choi, H., Chung, S., Kim, J.-I., Mook-Jung, I., 2019. A Breakdown in Metabolic Reprogramming Causes Microglia Dysfunction in Alzheimer's Disease. *Cell Metab.* <https://doi.org/10.1016/j.cmet.2019.06.005>

Bailey, J.D., Diotallevi, M., Nicol, T., McNeill, E., Shaw, A., Chuaiphichai, S., Hale, A., Starr, A., Nandi, M., Stylianou, E., McShane, H., Davis, S., Fischer, R., Kessler, B.M., McCullagh, J., Channon, K.M., Crabtree, M.J., 2019. Nitric Oxide Modulates Metabolic Remodeling in Inflammatory Macrophages through TCA Cycle Regulation and Itaconate Accumulation. *Cell Rep.* <https://doi.org/10.1016/j.celrep.2019.06.018>

Bambouskova, M., Gorvel, L., Lampropoulou, V., Sergushichev, A., Loginicheva, E., Johnson, K., Korenfeld, D., Mathyer, M.E., Kim, H., Huang, L.H., Duncan, D., Bregman, H., Keskin, A., Santeford, A., Apte, R.S., Sehgal, R., Johnson, B., Amarasinghe, G.K., Soares, M.P., Satoh, T., Akira, S., Hai, T., De Guzman Strong, C., Auclair, K., Roddy, T.P., Biller, S.A., Jovanovic, M., Klechevsky, E., Stewart, K.M., Randolph, G.J., Artyomov, M.N., 2018. Electrophilic properties of itaconate and derivatives regulate the I κ B ζ -ATF3 inflammatory axis. *Nature.* <https://doi.org/10.1038/s41586-018-0052-z>

Barton, G.M., Medzhitov, R., 2003. Toll-like receptor signaling pathways. *Science* (80-).

<https://doi.org/10.1126/science.1085536>

Benmoussa, K., Garaude, J., Acín-Pérez, R., 2018. How Mitochondrial Metabolism
Contributes to Macrophage Phenotype and Functions. *J. Mol. Biol.*

<https://doi.org/10.1016/j.jmb.2018.07.003>

Bernardi, P., 2013. The mitochondrial permeability transition pore: A mystery solved? *Front. Physiol.* <https://doi.org/10.3389/fphys.2013.00095>

Bolego, C., Cignarella, A., Staels, B., Chinetti-Gbaguidi, G., 2013. Macrophage function and
polarization in cardiovascular disease a role of estrogen signaling? *Arterioscler. Thromb.*

Vasc. Biol. <https://doi.org/10.1161/ATVBAHA.113.301328>

Brand, M.D., Nicholls, D.G., 2011. Assessing mitochondrial dysfunction in cells. *Biochem. J.*
<https://doi.org/10.1042/BJ20110162>

Buescher, J.M., Antoniewicz, M.R., Boros, L.G., Burgess, S.C., Brunengraber, H., Clish,
C.B., DeBerardinis, R.J., Feron, O., Frezza, C., Ghesquiere, B., Gottlieb, E., Hiller, K.,
Jones, R.G., Kamphorst, J.J., Kibbey, R.G., Kimmelman, A.C., Locasale, J.W., Lunt, S.Y.,
Maddocks, O.D.K., Malloy, C., Metallo, C.M., Meillet, E.J., Munger, J., Nöh, K., Rabinowitz,
J.D., Ralser, M., Sauer, U., Stephanopoulos, G., St-Pierre, J., Tennant, D.A., Wittmann, C.,
Vander Heiden, M.G., Vazquez, A., Vousden, K., Young, J.D., Zamboni, N., Fendt, S.M.,
2015. A roadmap for interpreting 13 C metabolite labeling patterns from cells. *Curr. Opin.*
Biotechnol. <https://doi.org/10.1016/j.copbio.2015.02.003>

Cameron, A.M., Castoldi, A., Sanin, D.E., Flachsmann, L.J., Field, C.S., Puleston, D.J., Kyle,

R.L., Patterson, A.E., Hässler, F., Buescher, J.M., Kelly, B., Pearce, E.L., Pearce, E.J., 2019. Inflammatory macrophage dependence on NAD⁺ salvage is a consequence of reactive oxygen species-mediated DNA damage. *Nat. Immunol.*

<https://doi.org/10.1038/s41590-019-0336-y>

Cannon, B., Nedergaard, J., 2004. Brown Adipose Tissue: Function and Physiological Significance. *Physiol. Rev.* <https://doi.org/10.1152/physrev.00015.2003>

Caputa, G., Castoldi, A., Pearce, E.J., 2019. Metabolic adaptations of tissue-resident immune cells. *Nat. Immunol.* <https://doi.org/10.1038/s41590-019-0407-0>

Cathcart, M.K., 2004. Regulation of Superoxide Anion Production by NADPH Oxidase in Monocytes/Macrophages: Contributions to Atherosclerosis. *Arterioscler. Thromb. Vasc. Biol.*

<https://doi.org/10.1161/01.ATV.0000097769.47306.12>

Ceccarelli, S.M., Chomienne, O., Gubler, M., Arduini, A., 2011. Carnitine palmitoyltransferase (CPT) modulators: A medicinal chemistry perspective on 35 years of research. *J. Med. Chem.* <https://doi.org/10.1021/jm100809g>

Chandel, N.S., 2015. Evolution of Mitochondria as Signaling Organelles. *Cell Metab.*

<https://doi.org/10.1016/j.cmet.2015.05.013>

Chandel, N.S., 2014. Mitochondria as signaling organelles. *BMC Biol.*

<https://doi.org/10.1186/1741-7007-12-34>

Chen, D., Xie, J., Fiskesund, R., Dong, W., Liang, X., Lv, J., Jin, X., Liu, J., Mo, S., Zhang, T., Cheng, F., Zhou, Y., Zhang, H., Tang, K., Ma, J., Liu, Y., Huang, B., 2018. Chloroquine modulates antitumor immune response by resetting tumor-associated macrophages toward

M1 phenotype. *Nat. Commun.* <https://doi.org/10.1038/s41467-018-03225-9>

Chouchani, E.T., Methner, C., Nadtochiy, S.M., Logan, A., Pell, V.R., Ding, S., James, A.M., Cochemé, H.M., Reinhold, J., Lilley, K.S., Partridge, L., Fearnley, I.M., Robinson, A.J., Hartley, R.C., Smith, R.A.J., Krieg, T., Brookes, P.S., Murphy, M.P., 2013. Cardioprotection by S-nitrosation of a cysteine switch on mitochondrial complex i. *Nat. Med.*

<https://doi.org/10.1038/nm.3212>

Chouchani, E.T., Pell, V.R., Gaude, E., Aksentijević, D., Sundier, S.Y., Robb, E.L., Logan, A., Nadtochiy, S.M., Ord, E.N.J., Smith, A.C., Eyassu, F., Shirley, R., Hu, C.H., Dare, A.J., James, A.M., Rogatti, S., Hartley, R.C., Eaton, S., Costa, A.S.H., Brookes, P.S., Davidson, S.M., Duchon, M.R., Saeb-Parsy, K., Shattock, M.J., Robinson, A.J., Work, L.M., Frezza, C., Krieg, T., Murphy, M.P., 2014. Ischaemic accumulation of succinate controls reperfusion injury through mitochondrial ROS. *Nature.* <https://doi.org/10.1038/nature13909>

Chouchani, E.T., Pell, V.R., James, A.M., Work, L.M., Saeb-Parsy, K., Frezza, C., Krieg, T., Murphy, M.P., 2016. A unifying mechanism for mitochondrial superoxide production during ischemia-reperfusion injury. *Cell Metab.* <https://doi.org/10.1016/j.cmet.2015.12.009>

Christofk, H.R., Vander Heiden, M.G., Harris, M.H., Ramanathan, A., Gerszten, R.E., Wei, R., Fleming, M.D., Schreiber, S.L., Cantley, L.C., 2008. The M2 splice isoform of pyruvate kinase is important for cancer metabolism and tumour growth. *Nature.*

<https://doi.org/10.1038/nature06734>

Cleeter, M.W.J., Cooper, J.M., Darley-Usmar, V.M., Moncada, S., Schapira, A.H.V., 1994. Reversible inhibition of cytochrome c oxidase, the terminal enzyme of the mitochondrial

respiratory chain, by nitric oxide. Implications for neurodegenerative diseases. *FEBS Lett.*

[https://doi.org/10.1016/0014-5793\(94\)00424-2](https://doi.org/10.1016/0014-5793(94)00424-2)

Clementi, E., Brown, G.C., Feelisch, M., Moncada, S., 1998. Persistent inhibition of cell respiration by nitric oxide: Crucial role of S-nitrosylation of mitochondrial complex I and protective action of glutathione. *Proc. Natl. Acad. Sci. U. S. A.*

<https://doi.org/10.1073/pnas.95.13.7631>

Cordes, T., Michelucci, A., Hiller, K., 2015. Itaconic Acid: The Surprising Role of an Industrial Compound as a Mammalian Antimicrobial Metabolite. *Annu. Rev. Nutr.*

<https://doi.org/10.1146/annurev-nutr-071714-034243>

Cordes, T., Wallace, M., Michelucci, A., Divakaruni, A.S., Sapcariu, S.C., Sousa, C., Koseki, H., Cabrales, P., Murphy, A.N., Hiller, K., Metallo, C.M., 2016. Immunoresponsive gene 1 and itaconate inhibit succinate dehydrogenase to modulate intracellular succinate levels. *J. Biol. Chem.*

<https://doi.org/10.1074/jbc.M115.685792>

Covarrubias, A.J., Aksoylar, H.I., Horng, T., 2015. Control of macrophage metabolism and activation by mTOR and Akt signaling. *Semin. Immunol.*

<https://doi.org/10.1016/j.smim.2015.08.001>

Covarrubias, A.J., Aksoylar, H.I., Yu, J., Snyder, N.W., Worth, A.J., Iyer, S.S., Wang, J., Ben-Sahra, I., Byles, V., Polynne-Stapornkul, T., Espinosa, E.C., Lamming, D., Manning, B.D., Zhang, Y., Blair, I.A., Horng, T., 2016. Akt-mTORC1 signaling regulates Acly to integrate metabolic input to control of macrophage activation. *Elife.*

<https://doi.org/10.7554/eLife.11612>

Cramer, T., Yamanishi, Y., Clausen, B.E., Förster, I., Pawlinski, R., Mackman, N., Haase, V.H., Jaenisch, R., Corr, M., Nizet, V., Firestein, G.S., Gerber, H.P., Ferrara, N., Johnson, R.S., 2003. HIF-1 α is essential for myeloid cell-mediated inflammation. *Cell*.

[https://doi.org/10.1016/S0092-8674\(03\)00154-5](https://doi.org/10.1016/S0092-8674(03)00154-5)

Crofts, A.R., 2004. The Cytochrome bc 1 Complex: Function in the Context of Structure .

Annu. Rev. Physiol. <https://doi.org/10.1146/annurev.physiol.66.032102.150251>

Dang, L., Su, S.-S.M., 2017. Isocitrate Dehydrogenase Mutation and (R)-2-

Hydroxyglutarate: From Basic Discovery to Therapeutics Development . *Annu. Rev.*

Biochem. <https://doi.org/10.1146/annurev-biochem-061516-044732>

De Souza, D.P., Achuthan, A., Lee, M.K.S., Binger, K.J., Lee, M.C., Davidson, S., Tull, D.L.,

McConville, M.J., Cook, A.D., Murphy, A.J., Hamilton, J.A., Fleetwood, A.J., 2019. Autocrine

IFN-I inhibits isocitrate dehydrogenase in the TCA cycle of LPS-stimulated macrophages. *J.*

Clin. Invest. <https://doi.org/10.1172/JCI127597>

De Stefani, D., Patron, M., Rizzuto, R., 2014. Structure and function of the mitochondrial

calcium uniporter complex. *Biochim. Biophys. Acta - Mol. Cell Res.*

<https://doi.org/10.1016/j.bbamcr.2015.04.008>

Dhir, A., Dhir, S., Borowski, L.S., Jimenez, L., Teitell, M., Rötig, A., Crow, Y.J., Rice, G.I.,

Duffy, D., Tamby, C., Nojima, T., Munnich, A., Schiff, M., de Almeida, C.R., Rehwinkel, J.,

Dziembowski, A., Szczesny, R.J., Proudfoot, N.J., 2018. Mitochondrial double-stranded RNA

triggers antiviral signalling in humans. *Nature.* <https://doi.org/10.1038/s41586-018-0363-0>

Divakaruni, A.S., Brand, M.D., 2011. The regulation and physiology of mitochondrial proton

leak. *Physiology* (Bethesda). <https://doi.org/10.1152/physiol.00046.2010>

Divakaruni, A.S., Hsieh, W.Y., Minarrieta, L., Duong, T.N., Kim, K.K.O., Desousa, B.R., Andreyev, A.Y., Bowman, C.E., Caradonna, K., Dranka, B.P., Ferrick, D.A., Liesa, M., Stiles, L., Rogers, G.W., Braas, D., Ciaraldi, T.P., Wolfgang, M.J., Sparwasser, T., Berod, L., Bensinger, S.J., Murphy, A.N., 2018. Etomoxir Inhibits Macrophage Polarization by Disrupting CoA Homeostasis. *Cell Metab.* <https://doi.org/10.1016/j.cmet.2018.06.001>

Divakaruni, A.S., Paradyse, A., Ferrick, D.A., Murphy, A.N., Jastroch, M., 2014. Analysis and interpretation of microplate-based oxygen consumption and pH data, in: *Methods in Enzymology.* <https://doi.org/10.1016/B978-0-12-801415-8.00016-3>

Dolan, S.K., Welch, M., 2018. The Glyoxylate Shunt, 60 Years On. *Annu. Rev. Microbiol.* <https://doi.org/10.1146/annurev-micro-090817-062257>

Duchen, M.R., 2000. Mitochondria and calcium: From cell signalling to cell death. *J. Physiol.* <https://doi.org/10.1111/j.1469-7793.2000.00057.x>

El-Khoury, R., Kemppainen, K.K., Dufour, E., Szibor, M., Jacobs, H.T., Rustin, P., 2014. Engineering the alternative oxidase gene to better understand and counteract mitochondrial defects: State of the art and perspectives. *Br. J. Pharmacol.* <https://doi.org/10.1111/bph.12570>

Everts, B., Amiel, E., Van Der Windt, G.J.W., Freitas, T.C., Chott, R., Yarasheski, K.E., Pearce, E.L., Pearce, E.J., 2012. Commitment to glycolysis sustains survival of NO-producing inflammatory dendritic cells. *Blood.* <https://doi.org/10.1182/blood-2012-03-419747>

Fensterheim, B.A., Young, J.D., Luan, L., Kleinbard, R.R., Stothers, C.L., Patil, N.K.,

McAtee-Pereira, A.G., Guo, Y., Trenary, I., Hernandez, A., Fults, J.B., Williams, D.L., Sherwood, E.R., Bohannon, J.K., 2018. The TLR4 Agonist Monophosphoryl Lipid A Drives Broad Resistance to Infection via Dynamic Reprogramming of Macrophage Metabolism. *J. Immunol.* <https://doi.org/10.4049/jimmunol.1800085>

Finkel, T., 2011. Signal transduction by reactive oxygen species. *J. Cell Biol.* <https://doi.org/10.1083/jcb.201102095>

Galván-Peña, S., Carroll, R.G., Newman, C., Hinchy, E.C., Palsson-McDermott, E., Robinson, E.K., Covarrubias, S., Nadin, A., James, A.M., Haneklaus, M., Carpenter, S., Kelly, V.P., Murphy, M.P., Modis, L.K., O'Neill, L.A., 2019. Malonylation of GAPDH is an inflammatory signal in macrophages. *Nat. Commun.* <https://doi.org/10.1038/s41467-018-08187-6>

Garaude, J., Acín-Pérez, R., Martínez-Cano, S., Enamorado, M., Ugolini, M., Nistal-Villán, E., Hervás-Stubbs, S., Pelegrín, P., Sander, L.E., Enríquez, J.A., Sancho, D., 2016. Mitochondrial respiratory-chain adaptations in macrophages contribute to antibacterial host defense. *Nat. Immunol.* <https://doi.org/10.1038/ni.3509>

Garedew, A., Moncada, S., 2008. Mitochondrial dysfunction and HIF1 α stabilization in inflammation. *J. Cell Sci.* <https://doi.org/10.1242/jcs.034660>

Geeraerts, X., Bolli, E., Fendt, S.M., Van Ginderachter, J.A., 2017. Macrophage metabolism as therapeutic target for cancer, atherosclerosis, and obesity. *Front. Immunol.* <https://doi.org/10.3389/fimmu.2017.00289>

Georgoudaki, A.M., Prokopec, K.E., Boura, V.F., Hellqvist, E., Sohn, S., Östling, J., Dahan,

R., Harris, R.A., Rantalainen, M., Klevebring, D., Sund, M., Brage, S.E., Fuxe, J., Rolny, C.,

Li, F., Ravetch, J. V., Karlsson, M.C.I., 2016. Reprogramming Tumor-Associated

Macrophages by Antibody Targeting Inhibits Cancer Progression and Metastasis. *Cell Rep.*

<https://doi.org/10.1016/j.celrep.2016.04.084>

Gonzalez-Hurtado, E., Lee, J., Choi, J., Selen Alpergin, E.S., Collins, S.L., Horton, M.R.,

Wolfgang, M.J., 2017. Loss of macrophage fatty acid oxidation does not potentiate systemic metabolic dysfunction. *Am. J. Physiol. - Endocrinol. Metab.*

<https://doi.org/10.1152/ajpendo.00408.2016>

Gordon, S., 2016. Phagocytosis: The Legacy of Metchnikoff. *Cell.*

<https://doi.org/10.1016/j.cell.2016.08.017>

Gordon, S., Taylor, P.R., 2005. Monocyte and macrophage heterogeneity. *Nat. Rev.*

Immunol. <https://doi.org/10.1038/nri1733>

Grazioli, S., Pugin, J., 2018. Mitochondrial damage-associated molecular patterns: From inflammatory signaling to human diseases. *Front. Immunol.*

<https://doi.org/10.3389/fimmu.2018.00832>

Han, B., Dubois, D.C., Boje, K.M.K., Free, S.J., Almon, R.R., 1999. Quantification of iNOS mRNA with reverse transcription polymerase chain reaction directly from cell lysates. *Nitric*

Oxide - Biol. Chem. <https://doi.org/10.1006/niox.1999.0240>

Harris, R.A., Hawes, J.W., Popov, K.M., Zhao, Y., Shimomura, Y., Sato, J., Jaskiewicz, J.,

Hurley, T.D., 1997. Studies on the regulation of the mitochondrial α -ketoacid dehydrogenase complexes and their kinases, in: *Advances in Enzyme Regulation.*

[https://doi.org/10.1016/S0065-2571\(96\)00009-X](https://doi.org/10.1016/S0065-2571(96)00009-X)

Haschemi, A., Kosma, P., Gille, L., Evans, C.R., Burant, C.F., Starkl, P., Knapp, B., Haas,

R., Schmid, J.A., Jandl, C., Amir, S., Lubec, G., Park, J., Esterbauer, H., Bilban, M.,

Brizuela, L., Pospisilik, J.A., Otterbein, L.E., Wagner, O., 2012. The sedoheptulose kinase

CARKL directs macrophage polarization through control of glucose metabolism. *Cell Metab.*

<https://doi.org/10.1016/j.cmet.2012.04.023>

He, W., Miao, F.J.P., Lin, D.C.H., Schwandner, R.T., Wang, Z., Gao, J., Chen, J.L., Tlan, H.,

Ling, L., 2004. Citric acid cycle intermediates as ligands for orphan G-protein-coupled

receptors. *Nature*. <https://doi.org/10.1038/nature02488>

Held, T.K., Weihua, X., Yuan, L., Kalvakolanu, D. V., Cross, A.S., 1999. Gamma interferon

augments macrophage activation by lipopolysaccharide by two distinct mechanisms, at the

signal transduction level and via an autocrine mechanism involving tumor necrosis factor

alpha and interleukin-1. *Infect. Immun.*

Hirst, J., 2013. Mitochondrial Complex I. *Annu. Rev. Biochem.*

<https://doi.org/10.1146/annurev-biochem-070511-103700>

Hoek, J.B., Rydstrom, J., 1988. Physiological roles of nicotinamide nucleotide

transhydrogenase. *Biochem. J.* <https://doi.org/10.1042/bj2540001>

Huang, S.C.C., Everts, B., Ivanova, Y., O'Sullivan, D., Nascimento, M., Smith, A.M., Beatty,

W., Love-Gregory, L., Lam, W.Y., O'Neill, C.M., Yan, C., Du, H., Abumrad, N.A., Urban, J.F.,

Artyomov, M.N., Pearce, E.L., Pearce, E.J., 2014. Cell-intrinsic lysosomal lipolysis is

essential for alternative activation of macrophages. *Nat. Immunol.*

<https://doi.org/10.1038/ni.2956>

Huang, S.C.C., Smith, A.M., Everts, B., Colonna, M., Pearce, E.L., Schilling, J.D., Pearce, E.J., 2016. Metabolic Reprogramming Mediated by the mTORC2-IRF4 Signaling Axis Is Essential for Macrophage Alternative Activation. *Immunity*.

<https://doi.org/10.1016/j.immuni.2016.09.016>

Hue, L., Taegtmeyer, H., 2009. The Randle cycle revisited: A new head for an old hat. *Am. J. Physiol. - Endocrinol. Metab.* <https://doi.org/10.1152/ajpendo.00093.2009>

Infantino, V., Convertini, P., Cucci, L., Panaro, M.A., Di Noia, M.A., Calvello, R., Palmieri, F., Iacobazzi, V., 2011. The mitochondrial citrate carrier: A new player in inflammation.

Biochem. J. <https://doi.org/10.1042/BJ20111275>

Infantino, V., Iacobazzi, V., Palmieri, F., Menga, A., 2013. ATP-citrate lyase is essential for macrophage inflammatory response. *Biochem. Biophys. Res. Commun.*

<https://doi.org/10.1016/j.bbrc.2013.09.037>

Iverson, T.M., 2013. Catalytic mechanisms of complex II enzymes: A structural perspective.

Biochim. Biophys. Acta - Bioenerg. <https://doi.org/10.1016/j.bbabbio.2012.09.008>

Jazwinski, S.M., 2013. The retrograde response: When mitochondrial quality control is not enough. *Biochim. Biophys. Acta - Mol. Cell Res.*

<https://doi.org/10.1016/j.bbamcr.2012.02.010>

Jha, A.K., Huang, S.C.C., Sergushichev, A., Lampropoulou, V., Ivanova, Y., Loginicheva, E., Chmielewski, K., Stewart, K.M., Ashall, J., Everts, B., Pearce, E.J., Driggers, E.M.,

Artyomov, M.N., 2015. Network integration of parallel metabolic and transcriptional data

reveals metabolic modules that regulate macrophage polarization. *Immunity*.

<https://doi.org/10.1016/j.immuni.2015.02.005>

Jiang, X., Wang, X., 2004. Cytochrome C -Mediated Apoptosis . *Annu. Rev. Biochem.*

<https://doi.org/10.1146/annurev.biochem.73.011303.073706>

Kato, M., 1972. Site of action of lipid A on mitochondria. *J. Bacteriol.*

Kazankov, K., Jørgensen, S.M.D., Thomsen, K.L., Møller, H.J., Vilstrup, H., George, J.,

Schuppan, D., Grønbaek, H., 2019. The role of macrophages in nonalcoholic fatty liver disease and nonalcoholic steatohepatitis. *Nat. Rev. Gastroenterol. Hepatol.*

<https://doi.org/10.1038/s41575-018-0082-x>

Kizaki, T., Suzuki, K., Hitomi, Y., Taniguchi, N., Saitoh, D., Watanabe, K., Onoé, K., Day,

N.K., Good, R.A., Ohno, H., 2002. Uncoupling protein 2 plays an important role in nitric oxide production of lipopolysaccharide-stimulated macrophages. *Proc. Natl. Acad. Sci. U. S. A.*

<https://doi.org/10.1073/pnas.142206299>

Koenis, D.S., Medzikovic, L., van Loenen, P.B., van Weeghel, M., Huvneers, S., Vos, M.,

Evers-van Gogh, I.J., Van den Bossche, J., Speijer, D., Kim, Y., Wessels, L., Zelcer, N.,

Zwart, W., Kalkhoven, E., de Vries, C.J., 2018. Nuclear Receptor Nur77 Limits the Macrophage Inflammatory Response through Transcriptional Reprogramming of

Mitochondrial Metabolism. *Cell Rep.* <https://doi.org/10.1016/j.celrep.2018.07.065>

Krawczyk, C.M., Holowka, T., Sun, J., Blagih, J., Amiel, E., DeBerardinis, R.J., Cross, J.R.,

Jung, E., Thompson, C.B., Jones, R.G., Pearce, E.J., 2010. Toll-like receptor-induced changes in glycolytic metabolism regulate dendritic cell activation. *Blood*.

<https://doi.org/10.1182/blood-2009-10-249540>

Lampropoulou, V., Sergushichev, A., Bambouskova, M., Nair, S., Vincent, E.E., Loginicheva, E., Cervantes-Barragan, L., Ma, X., Huang, S.C.C., Griss, T., Weinheimer, C.J., Khader, S., Randolph, G.J., Pearce, E.J., Jones, R.G., Diwan, A., Diamond, M.S., Artyomov, M.N., 2016.

Itaconate Links Inhibition of Succinate Dehydrogenase with Macrophage Metabolic Remodeling and Regulation of Inflammation. *Cell Metab.*

<https://doi.org/10.1016/j.cmet.2016.06.004>

Langston, P.K., Shibata, M., Horng, T., 2017. Metabolism supports macrophage activation.

Front. Immunol. <https://doi.org/10.3389/fimmu.2017.00061>

LaNoue, K.F., Schoolwerth, A.C., 1979. Metabolite Transport in Mitochondria. *Annu. Rev.*

Biochem. <https://doi.org/10.1146/annurev.bi.48.070179.004255>

LaNoue, K.F., Tischler, M.E., 1974. Electrogenic characteristics of the mitochondrial glutamate aspartate antiporter. *J. Biol. Chem.*

Lee, C.G.L., Jenkins, N.A., Gilbert, D.J., Copeland, N.G., O'Brien, W.E., 1995. Cloning and analysis of gene regulation of a novel LPS-inducible cDNA. *Immunogenetics.*

<https://doi.org/10.1007/BF00172150>

Leonardi, R., Zhang, Y.M., Rock, C.O., Jackowski, S., 2005. Coenzyme A: Back in action.

Prog. Lipid Res. <https://doi.org/10.1016/j.plipres.2005.04.001>

Leone, A.M., Palmer, R.M.J., Knowles, R.G., Francis, P.L., Ashton, D.S., Moncada, S.,

1991. Constitutive and inducible nitric oxide synthases incorporate molecular oxygen into both nitric oxide and citrulline. *J. Biol. Chem.*

Littlewood-Evans, A., Sarret, S., Apfel, V., Loesle, P., Dawson, J., Zhang, J., Muller, A., Tigani, B., Kneuer, R., Patel, S., Valeaux, S., Gommermann, N., Rubic-Schneider, T., Junt, T., Carballido, J.M., 2016. GPR91 senses extracellular succinate released from inflammatory macrophages and exacerbates rheumatoid arthritis. *J. Exp. Med.*

<https://doi.org/10.1084/jem.20160061>

Liu, P.S., Wang, H., Li, X., Chao, T., Teav, T., Christen, S., Di Conza, G., Cheng, W.C., Chou, C.H., Vavakova, M., Muret, C., Debackere, K., Mazzone, M., Huang, H. Da, Fendt, S.M., Ivanisevic, J., Ho, P.C., 2017. α -ketoglutarate orchestrates macrophage activation through metabolic and epigenetic reprogramming. *Nat. Immunol.*

<https://doi.org/10.1038/ni.3796>

Lu, C., Thompson, C.B., 2012. Metabolic regulation of epigenetics. *Cell Metab.*

<https://doi.org/10.1016/j.cmet.2012.06.001>

Lu, C., Ward, P.S., Kapoor, G.S., Rohle, D., Turcan, S., Abdel-Wahab, O., Edwards, C.R., Khanin, R., Figueroa, M.E., Melnick, A., Wellen, K.E., O'Grourke, D.M., Berger, S.L., Chan, T.A., Levine, R.L., Mellinghoff, I.K., Thompson, C.B., 2012. IDH mutation impairs histone demethylation and results in a block to cell differentiation. *Nature.*

<https://doi.org/10.1038/nature10860>

Lumeng, C.N., Delproposto, J.B., Westcott, D.J., Saltiel, A.R., 2008. Phenotypic switching of adipose tissue macrophages with obesity is generated by spatiotemporal differences in macrophage subtypes. *Diabetes.* <https://doi.org/10.2337/db08-0872>

MacMicking, J., Xie, Q., Nathan, C., 1997. NITRIC OXIDE AND MACROPHAGE

FUNCTION. *Annu. Rev. Immunol.* <https://doi.org/10.1146/annurev.immunol.15.1.323>

Martin, J.L., Costa, A.S.H., Gruszczuk, A. V., Beach, T.E., Allen, F.M., Prag, H.A., Hinchy,

E.C., Mahbubani, K., Hamed, M., Tronci, L., Nikitopoulou, E., James, A.M., Krieg, T.,

Robinson, A.J., Huang, M.M., Caldwell, S.T., Logan, A., Pala, L., Hartley, R.C., Frezza, C.,

Saeb-Parsy, K., Murphy, M.P., 2019. Succinate accumulation drives ischaemia-reperfusion

injury during organ transplantation. *Nat. Metab.* <https://doi.org/10.1038/s42255-019-0115-y>

Martinez, F.O., Gordon, S., 2014. The M1 and M2 paradigm of macrophage activation: Time

for reassessment. *F1000Prime Rep.* <https://doi.org/10.12703/P6-13>

McFadden, B.A., Purohit, S., 1977. Itaconate, an isocitrate lyase directed inhibitor in

Pseudomonas indigofera. *J. Bacteriol.*

McGarry, J.D., Takabayashi, Y., Foster, D.W., 1978. The role of malonyl-CoA in the

coordination of fatty acid synthesis and oxidation in isolated rat hepatocytes. *J. Biol. Chem.*

Michelucci, A., Cordes, T., Ghelfi, J., Pailot, A., Reiling, N., Goldmann, O., Binz, T., Wegner,

A., Tallam, A., Rausell, A., Buttini, M., Linster, C.L., Medina, E., Balling, R., Hiller, K., 2013.

Immune-responsive gene 1 protein links metabolism to immunity by catalyzing itaconic acid

production. *Proc. Natl. Acad. Sci. U. S. A.* <https://doi.org/10.1073/pnas.1218599110>

Mills, E., O'Neill, L.A.J., 2014. Succinate: A metabolic signal in inflammation. *Trends Cell*

Biol. <https://doi.org/10.1016/j.tcb.2013.11.008>

Mills, E.A., Ogrodnik, M.A., Plave, A., Mao-Draayer, Y., 2018. Emerging understanding of

the mechanism of action for dimethyl fumarate in the treatment of multiple sclerosis. *Front.*

Neurol. <https://doi.org/10.3389/fneur.2018.00005>

Mills, E.L., Kelly, B., Logan, A., Costa, A.S.H., Varma, M., Bryant, C.E., Tourlomousis, P., Däbritz, J.H.M., Gottlieb, E., Latorre, I., Corr, S.C., McManus, G., Ryan, D., Jacobs, H.T., Szibor, M., Xavier, R.J., Braun, T., Frezza, C., Murphy, M.P., O'Neill, L.A., 2016. Succinate Dehydrogenase Supports Metabolic Repurposing of Mitochondria to Drive Inflammatory Macrophages. *Cell*. <https://doi.org/10.1016/j.cell.2016.08.064>

Mills, E.L., Kelly, B., O'Neill, L.A.J., 2017. Mitochondria are the powerhouses of immunity. *Nat. Immunol.* <https://doi.org/10.1038/ni.3704>

Mills, E.L., Ryan, D.G., Prag, H.A., Dikovskaya, D., Menon, D., Zaslona, Z., Jedrychowski, M.P., Costa, A.S.H., Higgins, M., Hams, E., Szpyt, J., Runtsch, M.C., King, M.S., McGouran, J.F., Fischer, R., Kessler, B.M., McGettrick, A.F., Hughes, M.M., Carroll, R.G., Booty, L.M., Knatko, E. V., Meakin, P.J., Ashford, M.L.J., Modis, L.K., Brunori, G., Sévin, D.C., Fallon, P.G., Caldwell, S.T., Kunji, E.R.S., Chouchani, E.T., Frezza, C., Dinkova-Kostova, A.T., Hartley, R.C., Murphy, M.P., O'Neill, L.A., 2018. Itaconate is an anti-inflammatory metabolite that activates Nrf2 via alkylation of KEAP1. *Nature*. <https://doi.org/10.1038/nature25986>

Mookerjee, S.A., Gerencser, A.A., Nicholls, D.G., Brand, M.D., 2017. Quantifying intracellular rates of glycolytic and oxidative ATP production and consumption using extracellular flux measurements. *J. Biol. Chem.* <https://doi.org/10.1074/jbc.M116.774471>

Mosser, D.M., Edwards, J.P., 2008. Exploring the full spectrum of macrophage activation. *Nat. Rev. Immunol.* <https://doi.org/10.1038/nri2448>

Muñoz-Elías, E.J., McKinney, J.D., 2005. Mycobacterium tuberculosis isocitrate lyases 1 and 2 are jointly required for in vivo growth and virulence. *Nat. Med.*

<https://doi.org/10.1038/nm1252>

Murphy, M.P., 2015. Redox modulation by reversal of the mitochondrial nicotinamide nucleotide transhydrogenase. *Cell Metab.* <https://doi.org/10.1016/j.cmet.2015.08.012>

Murphy, M.P., 2009. How mitochondria produce reactive oxygen species. *Biochem. J.* <https://doi.org/10.1042/BJ20081386>

Murphy, M.P., Hartley, R.C., 2018. Mitochondria as a therapeutic target for common pathologies. *Nat. Rev. Drug Discov.* <https://doi.org/10.1038/nrd.2018.174>

Murray, P.J., 2017. Macrophage Polarization. *Annu. Rev. Physiol.* <https://doi.org/10.1146/annurev-physiol-022516-034339>

Namgaladze, D., Brüne, B., 2014. Fatty acid oxidation is dispensable for human macrophage IL-4-induced polarization. *Biochim. Biophys. Acta - Mol. Cell Biol. Lipids.* <https://doi.org/10.1016/j.bbalip.2014.06.007>

Newsholme, P., Curi, R., Gordon, S., Newsholme, E.A., 1986. Metabolism of glucose, glutamine, long-chain fatty acids and ketone bodies by murine macrophages. *Biochem. J.* <https://doi.org/10.1042/bj2390121>

Nicholls, D.G., Ferguson, S.J., 2013. *Bioenergetics 4*, Academic O'Ress. <https://doi.org/10.1017/CBO9781107415324.004>

Nickel, A.G., Von Hardenberg, A., Hohl, M., Löffler, J.R., Kohlhaas, M., Becker, J., Reil, J.C., Kazakov, A., Bonnekoh, J., Stadelmaier, M., Puhl, S.L., Wagner, M., Bogeski, I., Cortassa, S., Kappl, R., Pasieka, B., Lafontaine, M., Lancaster, C.R.D., Blacker, T.S., Hall, A.R., Duchon, M.R., Kästner, L., Lipp, P., Zeller, T., Müller, C., Knopp, A., Laufs, U., Böhm, M.,

Hoth, M., Maack, C., 2015. Reversal of mitochondrial transhydrogenase causes oxidative stress in heart failure. *Cell Metab.* <https://doi.org/10.1016/j.cmet.2015.07.008>

Nomura, M., Liu, J., Rovira, I.I., Gonzalez-Hurtado, E., Lee, J., Wolfgang, M.J., Finkel, T., 2016. Fatty acid oxidation in macrophage polarization. *Nat. Immunol.* <https://doi.org/10.1038/ni.3366>

Noy, R., Pollard, J.W., 2014. Tumor-Associated Macrophages: From Mechanisms to Therapy. *Immunity.* <https://doi.org/10.1016/j.immuni.2014.06.010>

O'Neill, L.A.J., Artyomov, M.N., 2019. Itaconate: the poster child of metabolic reprogramming in macrophage function. *Nat. Rev. Immunol.* <https://doi.org/10.1038/s41577-019-0128-5>

O'Neill, L.A.J., Golenbock, D., Bowie, A.G., 2013. The history of Toll-like receptors- redefining innate immunity. *Nat. Rev. Immunol.* <https://doi.org/10.1038/nri3446>

O'Neill, L.A.J., Pearce, E.J., 2016. Immunometabolism governs dendritic cell and macrophage function. *J. Exp. Med.* <https://doi.org/10.1084/jem.20151570>

Odegaard, J.I., Chawla, A., 2011. Alternative Macrophage Activation and Metabolism. *Annu. Rev. Pathol. Mech. Dis.* <https://doi.org/10.1146/annurev-pathol-011110-130138>

Odegaard, J.I., Ricardo-Gonzalez, R.R., Goforth, M.H., Morel, C.R., Subramanian, V., Mukundan, L., Eagle, A.R., Vats, D., Brombacher, F., Ferrante, A.W., Chawla, A., 2007. Macrophage-specific PPAR γ controls alternative activation and improves insulin resistance. *Nature.* <https://doi.org/10.1038/nature05894>

Olefsky, J.M., Glass, C.K., 2010. Macrophages, Inflammation, and Insulin Resistance. *Annu. Rev. Physiol.* <https://doi.org/10.1146/annurev-physiol-021909-135846>

Pagliarini, D.J., Rutter, J., 2013. Hallmarks of a new era in mitochondrial biochemistry.

Genes Dev. <https://doi.org/10.1101/gad.229724.113>

Palmieri, E.M., Baseler, W.A., Davies, L.C., Gonzalez-Cotto, M., Ghesquiere, B., Fan, T.W.M., Lane, A.N., Wink, D.A., McVicar, D.W., 2018. Nitric oxide dictates the reprogramming of carbon flux during M1 macrophage polarization. *J. Immunol.*

Palmieri, E.M., Menga, A., Martín-Pérez, R., Quinto, A., Riera-Domingo, C., De Tullio, G., Hooper, D.C., Lamers, W.H., Ghesquière, B., McVicar, D.W., Guarini, A., Mazzone, M., Castegna, A., 2017. Pharmacologic or Genetic Targeting of Glutamine Synthetase Skews Macrophages toward an M1-like Phenotype and Inhibits Tumor Metastasis. *Cell Rep.*

<https://doi.org/10.1016/j.celrep.2017.07.054>

Palmieri, F., 2013. The mitochondrial transporter family SLC25: Identification, properties and physiopathology. *Mol. Aspects Med.* <https://doi.org/10.1016/j.mam.2012.05.005>

Picca, A., Lezza, A.M.S., Leeuwenburgh, C., Pesce, V., Calvani, R., Landi, F., Bernabei, R., Marzetti, E., 2017. Fueling inflamm-aging through mitochondrial dysfunction: Mechanisms and molecular targets. *Int. J. Mol. Sci.* <https://doi.org/10.3390/ijms18050933>

Puleston, D.J., Buck, M.D., Klein Geltink, R.I., Kyle, R.L., Caputa, G., O'Sullivan, D., Cameron, A.M., Castoldi, A., Musa, Y., Kabat, A.M., Zhang, Y., Flachsmann, L.J., Field, C.S., Patterson, A.E., Scherer, S., Alfei, F., Baixauli, F., Austin, S.K., Kelly, B., Matsushita, M., Curtis, J.D., Grzes, K.M., Villa, M., Corrado, M., Sanin, D.E., Qiu, J., Pällman, N., Paz, K., Maccari, M.E., Blazar, B.R., Mittler, G., Buescher, J.M., Zehn, D., Rospert, S., Pearce, E.J., Balabanov, S., Pearce, E.L., 2019. Polyamines and eIF5A Hypusination Modulate

Mitochondrial Respiration and Macrophage Activation. *Cell Metab.*

<https://doi.org/10.1016/j.cmet.2019.05.003>

Raud, B., Roy, D.G., Divakaruni, A.S., Tarasenko, T.N., Franke, R., Ma, E.H., Samborska, B., Hsieh, W.Y., Wong, A.H., Stüve, P., Arnold-Schrauf, C., Guderian, M., Lochner, M., Rampertaap, S., Romito, K., Monsale, J., Brönstrup, M., Bensinger, S.J., Murphy, A.N., McGuire, P.J., Jones, R.G., Sparwasser, T., Berod, L., 2018. Etomoxir Actions on

Regulatory and Memory T Cells Are Independent of Cpt1a-Mediated Fatty Acid Oxidation. *Cell Metab.* <https://doi.org/10.1016/j.cmet.2018.06.002>

Reczek, C.R., Chandel, N.S., 2015. ROS-dependent signal transduction. *Curr. Opin. Cell Biol.* <https://doi.org/10.1016/j.ceb.2014.09.010>

Rich, P.R., Maréchal, A., 2010. The mitochondrial respiratory chain. *Essays Biochem.* <https://doi.org/10.1042/BSE0470001>

Robb, E.L., Hall, A.R., Prime, T.A., Eaton, S., Szibor, M., Viscomi, C., James, A.M., Murphy, M.P., 2018. Control of mitochondrial superoxide production by reverse electron transport at complex I. *J. Biol. Chem.* <https://doi.org/10.1074/jbc.RA118.003647>

Rodríguez-Prados, J.-C., Través, P.G., Cuenca, J., Rico, D., Aragonés, J., Martín-Sanz, P., Cascante, M., Boscá, L., 2010. Substrate Fate in Activated Macrophages: A Comparison between Innate, Classic, and Alternative Activation. *J. Immunol.* <https://doi.org/10.4049/jimmunol.0901698>

Rubic, T., Lametschwandtner, G., Jost, S., Hinteregger, S., Kund, J., Carballido-Perrig, N., Schwärzler, C., Junt, T., Voshol, H., Meingassner, J.G., Mao, X., Werner, G., Rot, A.,

Carballido, J.M., 2008. Triggering the succinate receptor GPR91 on dendritic cells enhances immunity. *Nat. Immunol.* <https://doi.org/10.1038/ni.1657>

Ruetz, M., Campanello, G.C., Purchal, M., Shen, H., McDevitt, L., Gouda, H., Wakabayashi, S., Zhu, J., Rubin, E.J., Warncke, K., Mootha, V.K., Koutmos, M., Banerjee, R., 2019.

Itaconyl-CoA forms a stable biradical in methylmalonyl-CoA mutase and derails its activity and repair. *Science* (80-.). <https://doi.org/10.1126/science.aay0934>

Russell, D.G., Huang, L., VanderVen, B.C., 2019. Immunometabolism at the interface between macrophages and pathogens. *Nat. Rev. Immunol.* <https://doi.org/10.1038/s41577-019-0124-9>

Ryan, D.G., Murphy, M.P., Frezza, C., Prag, H.A., Chouchani, E.T., O'Neill, L.A., Mills, E.L., 2019. Coupling Krebs cycle metabolites to signalling in immunity and cancer. *Nat. Metab.* <https://doi.org/10.1038/s42255-018-0014-7>

Sanin, D.E., Matsushita, M., Klein Geltink, R.I., Grzes, K.M., van Teijlingen Bakker, N., Corrado, M., Kabat, A.M., Buck, M.D., Qiu, J., Lawless, S.J., Cameron, A.M., Villa, M., Baixauli, F., Patterson, A.E., Hässler, F., Curtis, J.D., O'Neill, C.M., O'Sullivan, D., Wu, D., Mittler, G., Huang, S.C.C., Pearce, E.L., Pearce, E.J., 2018. Mitochondrial Membrane Potential Regulates Nuclear Gene Expression in Macrophages Exposed to Prostaglandin E2. *Immunity.* <https://doi.org/10.1016/j.immuni.2018.10.011>

Sciacovelli, M., Frezza, C., 2017. Metabolic reprogramming and epithelial-to-mesenchymal transition in cancer. *FEBS J.* <https://doi.org/10.1111/febs.14090>

Seim, G.L., Britt, E.C., John, S. V., Yeo, F.J., Johnson, A.R., Eisenstein, R.S., Pagliarini,

D.J., Fan, J., 2019. Two-stage metabolic remodelling in macrophages in response to lipopolysaccharide and interferon- γ stimulation. *Nat. Metab.* <https://doi.org/10.1038/s42255-019-0083-2>

Selak, M.A., Armour, S.M., MacKenzie, E.D., Boulahbel, H., Watson, D.G., Mansfield, K.D., Pan, Y., Simon, M.C., Thompson, C.B., Gottlieb, E., 2005. Succinate links TCA cycle dysfunction to oncogenesis by inhibiting HIF- α prolyl hydroxylase. *Cancer Cell.* <https://doi.org/10.1016/j.ccr.2004.11.022>

Shadel, G., 2012. MITOCHONDRIAL STRESS SIGNALING IN DISEASE AND AGING. *Free Radic. Biol. Med.* <https://doi.org/10.1016/j.freeradbiomed.2012.10.005>

Shaw, R.J., 2006. Glucose metabolism and cancer. *Curr. Opin. Cell Biol.* <https://doi.org/10.1016/j.ceb.2006.10.005>

Shimada, K., Crother, T.R., Karlin, J., Dagvadorj, J., Chiba, N., Chen, S., Ramanujan, V.K., Wolf, A.J., Vergnes, L., Ojcius, D.M., Rentsendorj, A., Vargas, M., Guerrero, C., Wang, Y., Fitzgerald, K.A., Underhill, D.M., Town, T., Arditi, M., 2012. Oxidized Mitochondrial DNA Activates the NLRP3 Inflammasome during Apoptosis. *Immunity.* <https://doi.org/10.1016/j.immuni.2012.01.009>

Shin, J.H., Yang, J.Y., Jeon, B.Y., Yoon, Y.J., Cho, S.N., Kang, Y.H., Ryu, D.H., Hwang, G.S., 2011. ¹H NMR-based metabolomic profiling in mice infected with *Mycobacterium tuberculosis*. *J. Proteome Res.* <https://doi.org/10.1021/pr101054m>

Sica, A., Mantovani, A., 2012. Macrophage plasticity and polarization: In vivo veritas. *J. Clin. Invest.* <https://doi.org/10.1172/JCI59643>

Sivanand, S., Viney, I., Wellen, K.E., 2018. Spatiotemporal Control of Acetyl-CoA

Metabolism in Chromatin Regulation. *Trends Biochem. Sci.*

<https://doi.org/10.1016/j.tibs.2017.11.004>

Sonoda, J., Laganière, J., Mehl, I.R., Barish, G.D., Chong, L., Li, X., Scheffler, I.E., Mock,

D.C., Bataille, A.R., Robert, F., Lee, C., Giguère, V., Evans, R.M., 2007. Nuclear receptor

ERRalpha and coactivator PGC-1beta are effectors of IFN- gamma -induced host defense.

Genes Dev. <https://doi.org/10.1101/gad.1553007.oxide>

Strelko, C.L., Lu, W., Dufort, F.J., Seyfried, T.N., Chiles, T.C., Rabinowitz, J.D., Roberts,

M.F., 2011. Itaconic acid is a mammalian metabolite induced during macrophage activation.

J. Am. Chem. Soc. <https://doi.org/10.1021/ja2070889>

Stuehr, D.J., Nathan, C.F., 1989. Nitric oxide: A macrophage product responsible for

cytostasis and respiratory inhibition in tumor target cells. *J. Exp. Med.*

<https://doi.org/10.1084/jem.169.5.1543>

Sugimoto, M., Ikeda, S., Niigata, K., Tomita, M., Sato, H., Soga, T., 2012. MMMDB: Mouse

multiple tissue metabolome database. *Nucleic Acids Res.*

<https://doi.org/10.1093/nar/gkr1170>

Tait, S.W.G., Green, D.R., 2010. Mitochondria and cell death: Outer membrane

permeabilization and beyond. *Nat. Rev. Mol. Cell Biol.* <https://doi.org/10.1038/nrm2952>

Tal, M.C., Sasai, M., Lee, H.K., Yordy, B., Shadel, G.S., Iwasaki, A., 2009. Absence of

autophagy results in reactive oxygen species-dependent amplification of RLR signaling.

Proc. Natl. Acad. Sci. U. S. A. <https://doi.org/10.1073/pnas.0S07694106>

Tan, Z., Xie, N., Cui, H., Moellering, D.R., Abraham, E., Thannickal, V.J., Liu, G., 2015.

Pyruvate Dehydrogenase Kinase 1 Participates in Macrophage Polarization via Regulating Glucose Metabolism. *J. Immunol.* <https://doi.org/10.4049/jimmunol.1402469>

Tannahill, G.M., Curtis, A.M., Adamik, J., Palsson-Mcdermott, E.M., McGettrick, A.F., Goel, G., Frezza, C., Bernard, N.J., Kelly, B., Foley, N.H., Zheng, L., Gardet, A., Tong, Z., Jany, S.S., Corr, S.C., Haneklaus, M., Caffrey, B.E., Pierce, K., Walmsley, S., Beasley, F.C., Cummins, E., Nizet, V., Whyte, M., Taylor, C.T., Lin, H., Masters, S.L., Gottlieb, E., Kelly, V.P., Clish, C., Auron, P.E., Xavier, R.J., O'Neill, L.A.J., 2013. Succinate is an inflammatory signal that induces IL-1 β through HIF-1 α . *Nature.* <https://doi.org/10.1038/nature11986>

Tavakoli, S., Downs, K., Short, J.D., Nguyen, H.N., Lai, Y., Jerabek, P.A., Goins, B., Toczek, J., Sadeghi, M.M., Asmis, R., 2017. Characterization of macrophage polarization states using combined measurement of 2-deoxyglucose and glutamine accumulation: Implications for imaging of atherosclerosis. *Arterioscler. Thromb. Vasc. Biol.*

<https://doi.org/10.1161/ATVBAHA.117.308848>

Taylor, E.B., 2017. Functional Properties of the Mitochondrial Carrier System. *Trends Cell Biol.* <https://doi.org/10.1016/j.tcb.2017.04.004>

Van den Bossche, J., Baardman, J., Otto, N.A., van der Velden, S., Neele, A.E., van den Berg, S.M., Luque-Martin, R., Chen, H.J., Boshuizen, M.C.S., Ahmed, M., Hoeksema, M.A., de Vos, A.F., de Winther, M.P.J., 2016. Mitochondrial Dysfunction Prevents Repolarization of Inflammatory Macrophages. *Cell Rep.* <https://doi.org/10.1016/j.celrep.2016.09.008>

Van den Bossche, J., O'Neill, L.A., Menon, D., 2017. Macrophage Immunometabolism:

Where Are We (Going)? Trends Immunol. <https://doi.org/10.1016/j.it.2017.03.001>

Van den Bossche, J., van der Windt, G.J.W., 2018. Fatty Acid Oxidation in Macrophages and T Cells: Time for Reassessment? Cell Metab.

<https://doi.org/10.1016/j.cmet.2018.09.018>

Vats, D., Mukundan, L., Odegaard, J.I., Zhang, L., Smith, K.L., Morel, C.R., Greaves, D.R., Murray, P.J., Chawla, A., 2006. Oxidative metabolism and PGC-1 β attenuate macrophage-mediated inflammation. Cell Metab. <https://doi.org/10.1016/j.cmet.2006.05.011>

Vijayan, V., Pradhan, P., Braud, L., Fuchs, H.R., Gueler, F., Motterlini, R., Foresti, R., Immenschuh, S., 2019. Human and murine macrophages exhibit differential metabolic responses to lipopolysaccharide - A divergent role for glycolysis. Redox Biol.

<https://doi.org/10.1016/j.redox.2019.101147>

Viola, A., Munari, F., Sánchez-Rodríguez, R., Scolaro, T., Castegna, A., 2019. The Metabolic Signature of Macrophage Responses. Front. Immunol.

<https://doi.org/10.3389/fimmu.2019.01462>

Voza, A., Parisi, G., De Leonardis, F., Lasorsa, F.M., Castegna, A., Amorese, D., Marmo, R., Calcagnile, V.M., Palmieri, L., Ricquier, D., Paradies, E., Scarcia, P., Palmieri, F., Bouillaud, F., Fiermonte, G., 2014. UCP2 transports C4 metabolites out of mitochondria, regulating glucose and glutamine oxidation. Proc. Natl. Acad. Sci. U. S. A.

<https://doi.org/10.1073/pnas.1317400111>

Walker, J.E., 2013. The ATP synthase: The understood, the uncertain and the unknown. Biochem. Soc. Trans. <https://doi.org/10.1042/BST20110773>

Wang, F., Zhang, S., Jeon, R., Vuckovic, I., Jiang, X., Lerman, A., Folmes, C.D., Dzeja, P.D., Herrmann, J., 2018a. Interferon Gamma Induces Reversible Metabolic Reprogramming of M1 Macrophages to Sustain Cell Viability and Pro-Inflammatory Activity. *EBioMedicine*. <https://doi.org/10.1016/j.ebiom.2018.02.009>

Wang, F., Zhang, S., Vuckovic, I., Jeon, R., Lerman, A., Folmes, C.D., Dzeja, P.P., Herrmann, J., 2018b. Glycolytic Stimulation Is Not a Requirement for M2 Macrophage Differentiation. *Cell Metab*. <https://doi.org/10.1016/j.cmet.2018.08.012>

Weinberg, S.E., Sena, L.A., Chandel, N.S., 2015. Mitochondria in the regulation of innate and adaptive immunity. *Immunity*. <https://doi.org/10.1016/j.immuni.2015.02.002>

West, A.P., Brodsky, I.E., Rahner, C., Woo, D.K., Erdjument-Bromage, H., Tempst, P., Walsh, M.C., Choi, Y., Shadel, G.S., Ghosh, S., 2011. TLR signalling augments macrophage bactericidal activity through mitochondrial ROS. *Nature*. <https://doi.org/10.1038/nature09973>

West, A.P., Shadel, G.S., 2017. Mitochondrial DNA in innate immune responses and inflammatory pathology. *Nat. Rev. Immunol*. <https://doi.org/10.1038/nri.2017.21>

Wiedemann, N., Pfanner, N., 2017. Mitochondrial Machineries for Protein Import and Assembly. *Annu. Rev. Biochem*. <https://doi.org/10.1146/annurev-biochem-060815-014352>

Wynn, T.A., Vannella, K.M., 2016. Macrophages in Tissue Repair, Regeneration, and Fibrosis. *Immunity*. <https://doi.org/10.1016/j.immuni.2016.02.015>

Xiao, M., Yang, H., Xu, W., Ma, S., Lin, H., Zhu, H., Liu, L., Liu, Y., Yang, C., Xu, Y., Zhao, S., Ye, D., Xiong, Y., Guan, K.L., 2012. Inhibition of α -KG-dependent histone and DNA demethylases by fumarate and succinate that are accumulated in mutations of FH and SDH

tumor suppressors. *Genes Dev.* <https://doi.org/10.1101/gad.191056.112>

Xu, W., Yang, H., Liu, Y., Yang, Y., Wang, Ping, Kim, S.H., Ito, S., Yang, C., Wang, Pu, Xiao, M.T., Liu, L.X., Jiang, W.Q., Liu, J., Zhang, J.Y., Wang, B., Frye, S., Zhang, Y., Xu, Y.H., Lei, Q.Y., Guan, K.L., Zhao, S.M., Xiong, Y., 2011. Oncometabolite 2-hydroxyglutarate is a competitive inhibitor of α -ketoglutarate-dependent dioxygenases. *Cancer Cell.*

<https://doi.org/10.1016/j.ccr.2010.12.014>

Zhang, W., Petrovic, J.M., Callaghan, D., Jones, A., Cui, H., Howlett, C., Stanimirovic, D., 2006. Evidence that hypoxia-inducible factor-1 (HIF-1) mediates transcriptional activation of interleukin-1 β (IL-1 β) in astrocyte cultures. *J. Neuroimmunol.*

<https://doi.org/10.1016/j.jneuroim.2006.01.014>

Zhong, Z., Liang, S., Sanchez-Lopez, E., He, F., Shalpour, S., Lin, X. jia, Wong, J., Ding, S., Seki, E., Schnabl, B., Hevener, A.L., Greenberg, H.B., Kisseleva, T., Karin, M., 2018. New mitochondrial DNA synthesis enables NLRP3 inflammasome activation. *Nature.*

<https://doi.org/10.1038/s41586-018-0372-z>

Zhou, B., Tian, R., 2018. Mitochondrial dysfunction in pathophysiology of heart failure. *J. Clin. Invest.* <https://doi.org/10.1172/JCI120849>

**CHAPTER 1: A single LC-MS/MS analysis to quantify CoA biosynthetic intermediates
and short-chain acyl CoAs**

Abstract: Coenzyme A (CoA) is an essential cofactor for dozens of reactions in intermediary metabolism. Dysregulation of CoA synthesis or acyl CoA metabolism can result in metabolic or neurodegenerative disease. Although several methods use liquid chromatography coupled to mass spectrometry/mass spectrometry (LC-MS/MS) to quantify acyl CoA levels in biological samples, few allow for simultaneous measurement of intermediates in the CoA biosynthetic pathway. Here we describe a simple sample preparation and LC-MS/MS method that can measure both short-chain acyl CoAs as well as biosynthetic precursors of CoA. The method does not require use of a solid phase extraction column during sample preparation and exhibits high sensitivity, precision, and accuracy. It reproduces expected changes from known effectors of cellular CoA homeostasis, helps clarify the mechanism by which excess concentrations of etomoxir reduce intracellular CoA levels, and is capable of measuring the levels of different intracellular CoA esters following addition of exogenous CoA to bone marrow-derived macrophages.

1. Introduction

Coenzyme A (CoA) is an obligatory co-factor in all organisms (Leonardi et al., 2005). It is involved in several aspects of mammalian cellular metabolism including the Krebs cycle, oxidation of fatty acids and branched chain amino acids, as well as synthesis of fatty acids and sterols. CoA acts as an acyl group carrier, forming thioester linkages with organic acids to yield acyl CoAs (e.g. acetyl CoA or palmitoyl CoA) (Leonardi *et al.*, 2005). Formation of a CoA thioester serves multiple functions. The large free energy of hydrolysis of the thioester bond serves as a means to 'charge' or 'activate' the adjoining acyl group for further metabolism. Additionally, formation of CoA esters can also aid in subcellular metabolite compartmentation. These acyl CoA esters are used as building blocks for biosynthetic reactions, substrates for post-translational modifications, or energy substrates oxidized to ultimately produce ATP (Pietrocola et al., 2015).

In mammals, de novo synthesis of CoA starts with the cellular uptake of pantothenate (vitamin B5) via the sodium-dependent multivitamin transporter (SMVT) (Prasad et al., 1998; Quick and Shi, 2015). Five enzymatic reactions convert pantothenate into CoA. Pantothenate is first phosphorylated by pantothenate kinase (PANK), the primary rate-controlling step in CoA synthesis (Robishaw and Neely, 1984). Subsequent conjugation with cysteine followed by decarboxylation results in 4'-phosphopantetheine. Lastly, 4'-phosphopantetheine is converted to CoA by the bifunctional enzyme Coenzyme A synthase (COASY). An adenylyl group from ATP is first transferred to 4'-phosphopantetheine to form dephospho-CoA, followed by phosphorylation of dephospho-CoA to form unesterified ("free") CoA (Leonardi *et al.*, 2005).

Free CoA can be used to activate carboxylic acids of differing chain lengths through the action of various CoA ligases (Rivera and Bartlett, 2018; Vessey et al., 1999). Disruption of CoA biosynthesis or short-chain CoA metabolism can result in pathological defects. For example, altering levels of short-chain acyl CoAs disrupts hepatic metabolic homeostasis (Gauthier et al., 2013), and certain forms of neurodegeneration are caused by mutations in enzymes responsible for CoA synthesis (Gregory and Hayflick, 1993; Venco et al., 2014). Short-chain acyl CoAs also have additional roles in cell biology beyond energy metabolism in post-translation modifications. In macrophages, for example, increased acetyl CoA production via ATP citrate lyase (ACLY) is associated with histone acetylation and the epigenetic changes observed during anti-inflammatory activation with interleukin-4 (IL-4) (Covarrubias et al., 2016). Further work has shown that supplementing macrophages with exogenous CoA enhances IL-4-driven macrophage activation (Divakaruni et al., 2018a). However, the precise mechanism by which this occurs – and whether CoA supplementation leads to increased abundance of other short-chain acyl CoAs – remains unclear. A single assay for measuring CoA biosynthetic intermediates as well as short-chain acyl

CoA species is therefore important to better understand CoA homeostasis in response to physiologically relevant stimuli such as macrophage activation.

Several techniques are available to measure short-chain acyl CoAs. These include fluorescence-based enzymatic assays, high performance liquid chromatography (HPLC), gas chromatography-mass spectrometry (GC-MS), and HPLC coupled with tandem mass

spectrometry-based (LC-MS/MS) assays. Of these, LC-MS/MS-based methods offer the highest selectivity and sensitivity (Neubauer et al., 2015; Tsuchiya et al., 2014).

While several published procedures detail the quantification of acyl CoAs of different chain lengths (Basu and Blair, 2012; Basu et al., 2011; Gao et al., 2007; Hayashi and Satoh, 2006; Minkler et al., 2008; Park et al., 2007; Perera et al., 2009; Snyder et al., 2015), none currently present a single method for the extraction and analysis of both short-chain acyl CoAs as well as intermediates in the CoA biosynthetic pathway. A primary challenge for this lies in the preparation of the biological sample. Many LC-MS/MS assays use halogenated carboxylic acids or oxo-acids for deproteinizing the sample (e.g. trichloroacetic acid) (Sedgwick et al., 1991). Solid phase extraction (SPE) is then used to purify acyl CoAs and remove the deproteinizing agent (Basu *et al.*, 2011; Hayashi and Satoh, 2006; Minkler *et al.*, 2008; Park *et al.*, 2007). Mechanistically, SPE works by retaining the acyl CoA species on the solid phase sorbent while the aqueous phase containing the deproteinization agent is discarded as waste (Berrueta et al., 1995). While SPE efficiently binds relatively hydrophobic acyl CoAs (e.g., propionyl CoA, isovaleryl CoA, etc.), it does not efficiently retain relatively hydrophilic CoA biosynthetic pathway intermediates such as dephospho-CoA and pantothenate. It is therefore difficult to use SPE as a method to measure both acyl CoAs and CoA biosynthetic intermediates. Their divergent polarities also create difficulty in developing a single LC-MS/MS method. More hydrophobic short-chain acyl CoAs exhibit the best chromatography when using traditional C18 columns under reverse phase conditions (Rivera and Bartlett, 2018). Under those same conditions, however, more hydrophilic species including pantothenate,

dephospho-CoA, and free CoA exhibit poor chromatographic peak shape and retention (Abranko et al., 2018; Gao *et al.*, 2007).

Here we present a single sample preparation and LC-MS/MS method that allows the extraction and quantification of both short-chain acyl CoAs as well as the CoA biosynthetic intermediates pantothenate and dephospho-CoA. We use 5-sulfosalicylic acid (SSA) for sample deproteinization, as this compound obviates the need for removal by SPE prior to LC-MS/MS analysis. This therefore retains a significant amount of pantothenate and dephospho-CoA from biological samples that would otherwise be lost following SPE-based purification. We overcome the challenge of poor chromatographic separation between the various species by carefully controlling the pH, thereby minimizing the charge on the competing positively and negatively polarizable moieties of the CoA backbone. We then further suppress and mask remaining polarization and charge with ion-pairing chromatography. When combined with an ultra-high performance liquid chromatography (UHPLC) C18 column with high theoretical plates, we observe stable and symmetric peak shape with good resolution across a range of analytes. We show this method is able to reproduce findings generated using other LC-MS/MS methods, and also helps reveal the mechanism by which excess concentrations of the carnitine palmitoyltransferase-1 (CPT-1) inhibitor etomoxir decreases intracellular CoA levels in bone marrow-derived macrophages (BMDMs).

2. Results

2.1. MRM MS/MS methods can detect both CoA biosynthetic intermediates and short-chain acyl CoAs

We initially optimized the mass spectrometry to ensure robust detection of both short-chain acyl CoAs as well as pantothenate and dephospho-CoA (Figure 1).

To optimize the MS detection of short-chain acyl CoAs, we prepared 1 $\mu\text{g/mL}$ solutions of each acyl CoA standard in the SSA extraction solution (see methods), and these standards were directly infused into the mass spectrometer for MS/MS analysis. We focused on optimizing the detection of short-chain acyl CoAs with the MS operated in positive mode, as previous studies showed that they are more efficiently ionized under these conditions (Perera *et al.*, 2009). We observed a characteristic fragmentation pattern for all acyl CoA species. The CoA portion fragments at the 3'-phosphate-adenosine-5'-diphosphate during positive mode MS/MS. This cleavage gives rise to a neutral loss of 507 atomic mass units (amu) together with a daughter ion equal to a mass-to-charge ratio (m/z) of $[M - 507 + H]^+$, where "M" is the molecular mass of the initial compound. Additionally, the phosphate-adenosine portion of each acyl CoA species fragments between the 5'-diphosphates, and gives rise to a daughter equal to 428 m/z (Palladino *et al.*, 2012) (Figure 2A). For example, acetyl CoA has a monoisotopic mass of 809.1, and therefore gives rise to an MS1 parent of 810.1 m/z . Following fragmentation, daughter ions of 303 m/z (indicating cleavage at the 3'-phosphate-adenosine-5'-diphosphate) and 428 m/z (indicating fragmentation between the 5' diphosphates) were both apparent (Figures 2B, C). We used multiple reaction monitoring (MRM) to both identify

and quantify each acyl CoA species detected with this method. For each acyl CoA, two separate transitions were monitored: (i) $[M + H]^+$ fragmenting to $[M - 507 + H]^+$ m/z was used for quantitation and (ii) $[M + H]^+$ fragmenting to 428 m/z was used for qualitative identification (Table 1).

After tuning for efficient detection of acyl CoAs, we then optimized the detection of CoA synthetic intermediates. Dephospho-CoA, similar to acyl CoAs, was efficiently detected in positive mode. The quantitative and qualitative MRM transitions of dephospho-CoA were determined empirically during tuning (Table 1). Initial efforts to optimize the detection of pantothenate in positive mode MRM were unsuccessful, and much greater sensitivity was observed using negative mode MRM. As a result, negative mode MRM was used for pantothenate, while positive mode MRM was used for all other analytes. Additional settings for each transition including declustering potential (DP), entrance potential (EP), collision energy (CE), and cell exit potential (CXP) were also optimized during tuning with reference standards. Source settings of temperature, ion spray voltage, and gas flows were likewise optimized during method development (see Methods).

2.2. Ion-pairing UHPLC chromatography produces well separated peaks for CoA biosynthetic intermediates and short-chain acyl CoAs

We next developed the chromatography parameters for CoA biosynthetic intermediates and short-chain acyl CoAs. Like other phosphorylated organic molecules, CoA can be a difficult structure to resolve using common chromatographic techniques (Abranko *et al.*, 2018). Its three phosphate groups are polar and capable of negatively ionizing at higher

pH, resulting in poor affinity for the solid phase of common, reverse phase columns like C18.

At the same time, the adenine moiety can serve as a Bronsted-Lowry base and acquire a proton at a pH below 4.0. Moreover, these polar or charged groups are offset by acyl groups of increasing non-polarity as the length of the acyl chain increases.

We first tested a standard HPLC C18 column using an acetonitrile gradient containing common modifiers such as 0.1% (v/v) formic acid or 5 mM ammonium acetate. Formic acid produced extremely poor chromatography (not shown), so ammonium acetate was used as the modifier and proton source. Unmodified ammonium acetate still produced considerable peak tailing, so the pH was carefully adjusted with acetic acid to pH 5.6. This value was selected in order to be above the pKa of adenine NH_3^+ (4.0) but below the pKa of the secondary phosphate (6.4) (). While the chromatography of the CoA species was improved, it still exhibited poor peak shape. Notably, this pH of 5.6 leaves pantothenate as an anion, and results in the primary phosphate of the CoA backbone having a negative charge, explaining the poor results at this pH.

The remaining chromatographic difficulties were resolved by ion pairing chromatography together with the use of a UHPLC C18 column with high theoretical plates. N,N-dimethylbutylamine (DMBA) is a tertiary amine that acquires a proton below pH 10.0 (), and has been used as an ion pairing agent to improve the chromatography of phosphate-containing compounds like oligonucleotides (Basiri et al., 2017). DMBA has also been used to improve the chromatography of short-chain acyl CoA species such as malonyl CoA (Gao et al., 2007). It was therefore added to the ammonium acetate solution and a Phenomenex

Kinetex ultra-high performance liquid chromatography (UHPLC) C18 column was used. The resulting chromatography produced well-separated peaks with minimal tailing for both CoA biosynthetic intermediates and short chain acyl CoAs (Figure 3).

2.3. The method displays a linear detection of analytes across a wide concentration range with sensitive lower limits of detection and quantitation.

The sensitivity and linearity of the LC-MS/MS method were determined by spiking a range of reference analytes into sample extraction solution along with the internal standard crotonoyl CoA. Calibration curves were fit by linear regression with 1/x weighting (Figure 4).

The lower limit of detection (LLOD) for each analyte was determined as the lowest concentration that produced a signal at least five times that of the corresponding noise floor. The lower limit of quantitation (LLOQ) was determined as the lowest concentration in the calibration curve for which the curve-calculated concentration was within 20% of its nominal concentration. The linearity of each calibration curve was determined as the coefficient of correlation r . For each analyte, the LC-MS/MS yielded impressively sensitive LLOD and LLOQ with $r \geq 0.95$ (Table 3).

2.4. Extraction with 2.5% SSA is suitable for analysis of acyl CoAs and CoA biosynthetic intermediates

Following refinement of the LC-MS/MS settings, we next determined an appropriate method to extract acyl CoAs and CoA biosynthetic intermediates from biological material. We first evaluated common acyl CoA extraction procedures to test their capacity to also recover dephospho-CoA and pantothenate. Acyl CoAs are commonly extracted with halogenated

forms of acetic acid [e.g. trichloroacetic acid (TCA) and trifluoroacetic acid (TFA)] followed by solid phase extraction (SPE) to remove the deproteinizing agent. After SPE purification, acyl CoAs are resuspended in a solvent favorable for LC-MS/MS analysis such as water or SSA (Basu *et al.*, 2011; Hayashi and Satoh, 2006; Park *et al.*, 2007).

To control for variabilities in the sample extraction procedure we again used crotonoyl CoA as an internal standard. Complete precision under all possible conditions for a given CoA species or biosynthetic intermediate, of course, requires a matched, isotopically labeled reference species. This can be accomplished by SILEC labeling (Basu and Blair, 2012), which exploits the lack of de novo pantothenate synthesis in mammalian and insect cells to generate such standards with provision of labeled pantothenate in cell culture medium. Although this technique is the gold standard for such assays, it can be time- and cost prohibitive for almost all non-specialist labs. We therefore use crotonyl CoA as an inexpensive and amenable standard to this straightforward method. Importantly, endogenous crotonyl CoA levels range from less than 1% (cultured cells) to an upper bound of 3% (liver tissue) of the internal standard. As such, endogenous changes in crotonyl CoA levels would only introduce marginal error when quantifying short-chain CoAs and CoA biosynthetic intermediates under most conditions. To test whether TCA followed by SPE was a suitable extraction technique, 1 nmol of standards for pantothenate, dephospho-CoA, and each acyl CoA were extracted with 200 μ L of 10%(w/v) TCA. TCA was removed by SPE, and samples were reconstituted in 2.5% SSA prior to LC-MS/MS analysis (Basu and Blair, 2012; Basu *et al.*, 2011; Snyder *et al.*, 2015). For comparison, 1 nmol of each standard was also spiked into 200 μ L of water and similarly

analyzed. Relative recovery was determined by comparing the area under the curve (AUC) of each analyte extracted with TCA with the analyte in water. While using TCA showed moderate recovery of acetyl CoA and CoA species with longer acyl tails, there was a marked decrease in recovery of free CoA and the biosynthetic intermediates (Figure 5A).

In the search for alternatives, we noted that SSA, in addition to being a commonly used solvent for reconstituting acyl CoAs for LC-MS/MS (Basu and Blair, 2012; Basu *et al.*, 2011; Snyder *et al.*, 2015), has also been used for deproteinizing biological samples (Demoz *et al.*, 1995; Khan *et al.*, 1991). We determined that 2.5%(w/v) SSA fully deproteinized biological samples without lowering the pH of the extraction solution below pH 1.0, the recommended lower threshold for the HPLC column used in this study. Indeed, extraction with 2.5% SSA showed similar recovery of hydrophobic short-chain acyl CoAs relative TCA. Additionally, we observed increased recovery of free CoA and the CoA biosynthetic precursors pantothenate and dephospho-CoA (Figure 5A). 2.5% SSA was also able to efficiently extract these metabolites from the HEK 293FT human embryonic kidney cell line and compared favorably to TCA (Figure 5B). The results demonstrate SSA is a preferred extraction solvent for our optimized LC-MS/MS method and obviates the need for solid phase extraction for these metabolites.

2.5. The sample preparation and LC-MS/MS method shows minimal matrix effect and preserves accuracy

Having shown 2.5% SSA is a suitable extraction solvent, we then determined if our method displayed minimal variability due to matrix effects across the range of analytes. A

matrix effect was determined as the percentage ratio of the AUC of analyte that had been spiked into matrix versus the LC-MS AUC of analyte that had been spiked into extraction solution alone. For each analyte apart from dephospho-CoA, the matrix effect was marginal and less than 10% ion suppression. Dephospho-CoA exhibited a consistently greater matrix effect, exhibiting ion suppression of an average of 19% across its low, medium, and high spikes into matrix.

Comparative accuracy was determined as the percent ratio of the mean, baseline-subtracted concentrations for the spikes into post-extraction matrix compared to mean concentrations of spikes into extraction solution alone. In general, the internal standard-corrected matrix effect was deemed acceptable if it produced comparative accuracy within 85%. All analytes, including dephospho-CoA achieved this average comparative accuracy. As such, despite the relatively large matrix effect of dephospho-CoA, this was partially compensated for by the internal standard when determining the concentration.

2.6. The method exhibits acceptable precision and accuracy parameters for measured analytes across their entire linear ranges.

The precision and accuracy for the sample preparation and LC-MS/MS method were determined according to guidelines provided by the FDA (Health and Services, 2001) and EMA (Smith, 2012) (Table 4). Low, medium, and high amounts of eight analytes were added to cell pellets, and the concentration was determined. Precision was reported as the relative standard deviation or coefficient of variation (CV). In general, precision was deemed acceptable with $15\% \geq CV$, and all metabolites considered fit this criterion. Accuracy was

determined by comparing the average observed concentration to the amount spiked at that concentration after baseline correction. Accuracy was deemed acceptable when mean values were within 15% of the nominal values, and all metabolites considered met this mark.

2.7. The method detects expected perturbations in levels of CoA and CoA esters

We next validated our method by assessing acyl CoA levels in cells following treatments that have been previously shown to increase and decrease steady-state levels of CoA-related metabolites. To determine if we could detect enhanced synthesis of specific acyl CoAs, we treated HepG2 cells with 1 mM propionate. Consistent with prior reports (Snyder *et al.*, 2015), we observed a more than ten-fold increase in propionyl CoA levels following treatment (Figure 6A). We then measured whether the method could detect an increase in CoA synthesis with PZ-2891, a pantazine compound that is effective in treating preclinical models of pantothenate kinase-associated neurodegeneration (PKAN) (Sharma *et al.*, 2018b). The drug increases CoA levels by stabilizing pantothenate kinase in its active conformation. Indeed, HepG2 cells treated with 10 μ M PZ-2891 caused an expected 2-fold increase in free CoA along with increased abundance of both acetyl- and propionyl CoA (Figure 6B).

Having shown that the method can detect increases in steady-state CoA levels, we then measured whether it can similarly detect decreased levels of CoA and CoA esters. We therefore treated HepG2 cells with cyclopropanecarboxylic (CPCA), which is known to decrease CoA levels in mammalian hepatocytes (Ulrich *et al.*, 2001). Indeed, CPCA treatment halved intracellular free CoA levels and reduced the levels of short-chain acyl CoAs including acetyl- and propionyl CoA (Figure 6C). As expected, cyclopropanecarboxyl-CoA levels were

readily detectable after being undetectable prior to CPCA treatment (Figure 6D), suggesting that formation of this acyl CoA is likely associated with depletion of free CoA.

Finally, we determined if our method could be used to measure incorporation of isotopically labeled substrates into short-chain acyl CoAs. Treating HepG2 cells with uniformly labelled ¹³C-glucose showed incorporation into acetyl CoA (“M2” isotopologue) that was substantially decreased in response to UK5099 (Divakaruni et al., 2017), a potent and specific inhibitor of mitochondrial pyruvate uptake (Figure 6E).

2.8. The method detects changes in the CoA metabolism in IL-4-polarized macrophages treated with excess etomoxir or exogenous CoA.

Finally, we used our method to follow-up previous studies showing the macrophage response to the anti-inflammatory cytokine IL-4 activation is inhibited by high concentrations of etomoxir and enhanced by exogenous CoA supplementation.

Previously we showed that treating macrophages with 200 μ M etomoxir depleted free CoA (as measured by colorimetric assay) and qualitatively increased levels of pantothenate (measured separately by LC-MS/MS) (Divakaruni *et al.*, 2018a). We previously speculated high concentrations of etomoxir may be sufficient to deplete steady-state CoA levels by formation of an etomoxiryl CoA ester (Divakaruni *et al.*, 2018a). However, the ability to accurately quantify pantothenate, dephospho-CoA, and short-chain CoA esters in the same method allows us to test the hypothesis that the etomoxiryl CoA ester may inhibit pantothenate kinase (PANK) similarly to feedback inhibition by other long-chain CoA esters (Rock et al.,

2002). Consistent with previous work, treatment with 200 μ M etomoxir increased intracellular pantothenate levels (Figure 7A). In addition, our LC-MS/MS method revealed dephospho-CoA and other short-chain acyl CoA abundances were also reduced (Figure 7A,B), supporting a mechanism whereby etomoxir depletes free CoA and other short-chain acyl CoAs, in part, by PANK inhibition (Figure 7C). We also used this method to determine if the addition of CoA to BMDM culture media increases the abundance of other intracellular acyl CoAs. Intriguingly, addition of CoA resulted in not only an increase in intracellular free CoA levels, but also increased abundance of other short-chain acyl CoAs including acetyl CoA and propionyl CoA (Fig 8).

3. Discussion

Here we detail an LC-MS/MS method that allows for sensitive detection of short-chain acyl CoAs and metabolites in the CoA biosynthetic pathway. Our method efficiently overcomes limitations that otherwise preclude the use of a single method to analyze CoA esters and biosynthetic precursors. In particular, use of SSA circumvents the need for solid phase extraction (SPE) (Gao *et al.*, 2007; Khan *et al.*, 1991), as this single solvent can be used as both a deproteinizing agent as well as a solvent for reconstitution of acyl CoAs.

There are multiple advantages gained from bypassing SPE with the use of SSA. SPE results in poor recovery of free CoA and biosynthetic intermediates. Although the divergent polarities between the two classes of analytes can lead to poor chromatography, this can be corrected by carefully adjusting pH, including an ion pairing agent, and using an ultra-high performance liquid chromatography column. Eliminating SPE also circumvents the need to run multiple internal standards to correct for the differential recovery of various CoA esters. Because many of these are not commercially available, intensive and specialized techniques such as generation of SILEC-labeled internal standards (Basu and Blair, 2012; Basu *et al.*, 2011). The single, SSA extraction step allows for the use of a single, commercially available internal standard (crotonyl CoA). Although we demonstrate that endogenous levels of crotonyl CoA range from below 1% (cultured cells) to 3% (murine liver tissue) of the internal standard, indicating that changes in endogenous crotonyl CoA levels would introduce minimal error when quantifying short-chain CoAs and CoA biosynthetic intermediates. However, caution should be exercised when interpreting data in model systems where steady-state crotonyl CoA

levels are high or may substantially change between experimental groups, and SILEC-generated standards may be necessary.

Proof-of-concept biological experiments show that the proposed method is sensitive and can be used to quantify CoA-related metabolism in biological samples. In addition to showing the method can be used to detect both augmentation and depletion of acyl CoAs following pharmacological perturbations, the simultaneous quantification of metabolites involved in CoA biosynthesis may have biological and clinical utility. For example, more than 50% of neurodegeneration with brain iron accumulation (NBIA) cases are caused by dysfunction of enzymes involved in CoA synthesis (Di Meo *et al.*, 2019; Venco *et al.*, 2014). Patient fibroblasts and tissues from preclinical disease models are often characterized by decreased free CoA (Dusi *et al.*, 2014; Garcia *et al.*, 2012), though mutations in both pantothenate kinase (PANK) or coenzyme A synthase (COASY) can cause NBIA (Di Meo *et al.*, 2019; Venco *et al.*, 2014). As such, a combined LC-MS/MS method detecting short-chain acyl CoAs as well as the reactants and products of enzymes involved in NBIA may be useful in better identifying the molecular basis resulting in these pathologies.

This method also proved useful in better understanding how CoA homeostasis impacts IL-4-activated macrophages (Divakaruni *et al.*, 2018a). We were able to further previous work by showing that exogenous CoA provision causes increased abundance of many intracellular short-chain CoA esters. We also demonstrated that excess concentrations of etomoxir increased intracellular pantothenate levels while dephospho-CoA was decreased, suggesting that etomoxir may disrupt CoA metabolism by inhibiting a process downstream of

pantothenate uptake but upstream of dephospho-CoA production. Given that long-chain acyl CoAs are potent inhibitors of PANK (Rock et al., 2000; Rock *et al.*, 2002), it is likely that etomoxir is converted to its CoA thioester etomoxiryl CoA to inhibit PANK and block CoA biosynthesis. This reduction in steady-state free CoA in BMDMs is also associated with a reduction in short-chain acyl CoAs such as acetyl CoA, propionyl CoA, and succinyl CoA. As these metabolites are involved in many facets of cell physiology including the Krebs cycle, sterol synthesis, post-translational modifications, and epigenetic reprogramming, the mechanism linking disrupted CoA homeostasis by etomoxir with a reduced IL-4 response remains unclear.

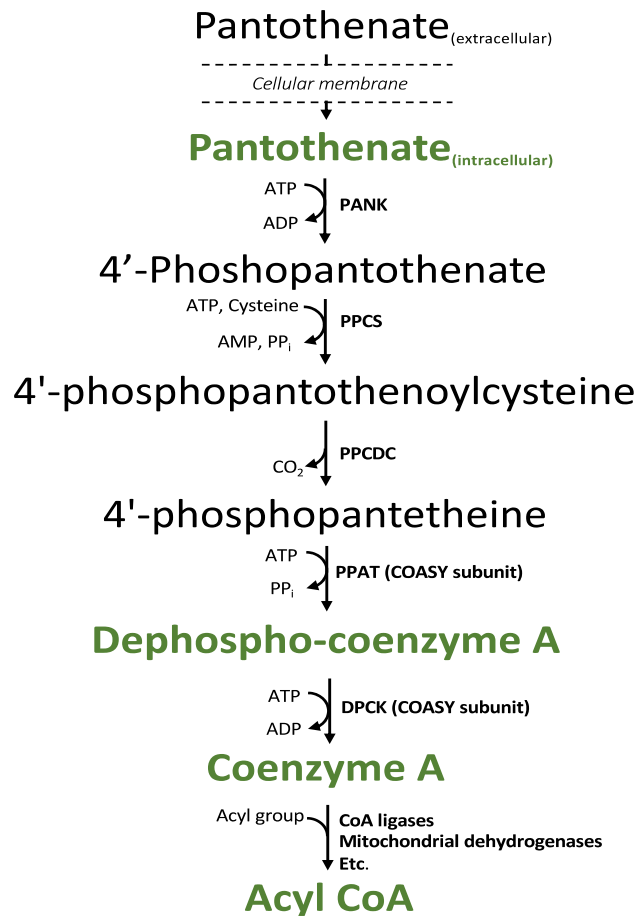


Figure 1: The CoA biosynthetic pathway.

The metabolites detected by the method detailed in this manuscript are highlighted in green.

PANK, pantothenate kinase; PPCS, phosphopantothenoylcysteine synthase; PPCDC, phosphopantothenoylcysteine decarboxylase; PPAT, phosphopantetheine adenylyl transferase; DPCK, dephosphocoenzyme A kinase. The bifunctional enzyme Coenzyme A synthase (COASY) is comprised of PPAT and DPCK.

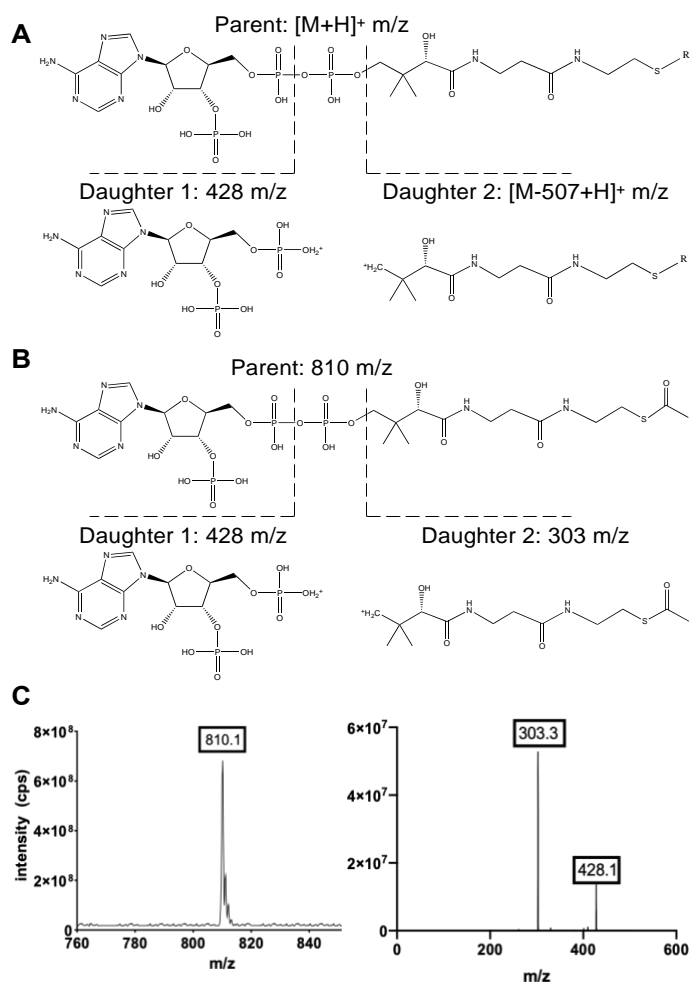


Figure 2: The common MS/MS fragmentation pattern for all CoA species.

(A) The CoA moiety of all CoA esters fragments during MS/MS at the 3'-phosphate-adenosine-5'-diphosphate. This cleavage gives rise to a daughter ion equal to $[M - 507 + H]^+$ m/z (right). "M" is the molecular mass of the starting compound. The phosphate-adenosine portion also fragments between the 5' diphosphates and gives rise to a daughter equal to 428 m/z (left).

(B) Acetyl CoA has a parent m/z of 810, with a predicted fragmentation pattern for daughter ions of 428 m/z and 303 m/z . (C) The MS1 parent and both predicted MS2 daughter ions for acetyl CoA were detected following direct infusion of 1 $\mu\text{g/mL}$ acetyl CoA into the mass spectrometer.

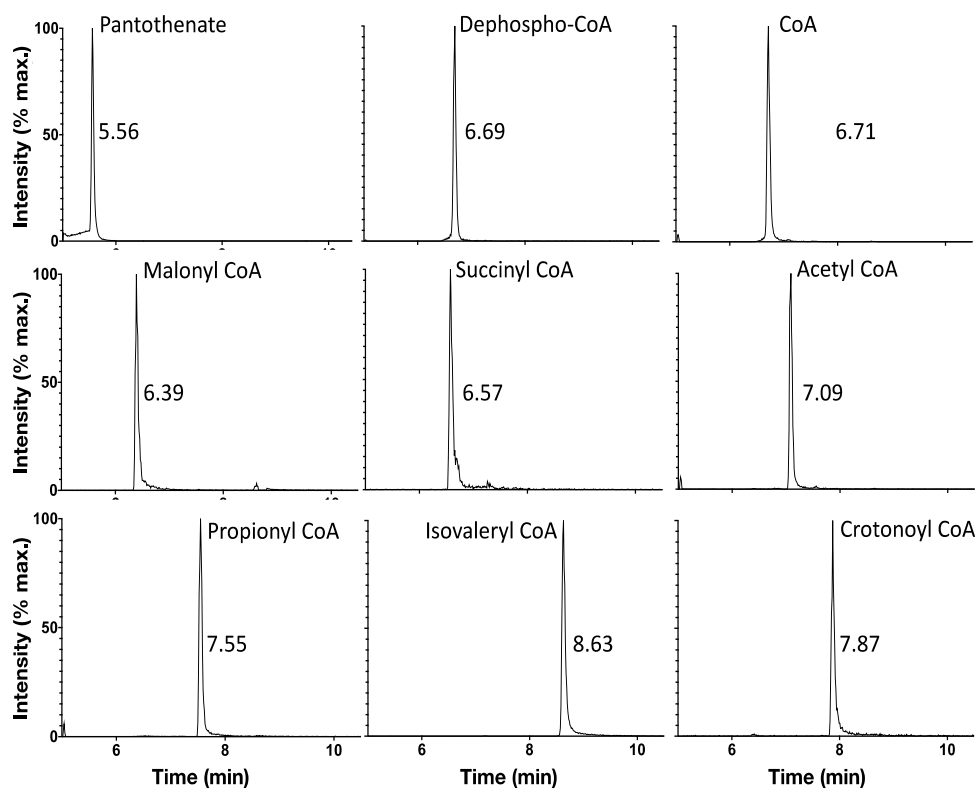


Figure 3: The LC-MS/MS method produces well-separated peaks for each analyte

All eight compounds together with the internal standard (crotonoyl CoA) were injected at 1 $\mu\text{g/mL}$ into the LC-MS/MS. Retention times are listed to the right of each peak. Liquid chromatography consisted of a reverse-phase gradient with solvents A & B (see Table 2) along with a Phenomenex Kinetex, 2.6 mm x 150 mm UHPLC C18 column. The quantitative MRM channel of each species was isolated, and retention times determined.

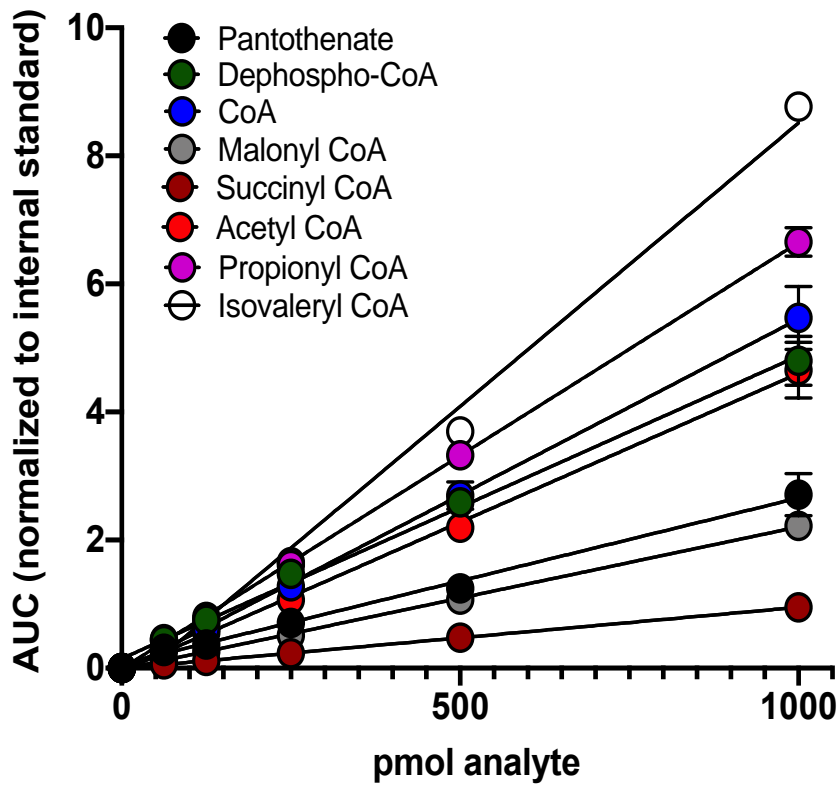


Figure 4: The method displays a linear detection of analytes

Standards were spiked into 200 μ L of extraction solution and analyzed via LC-MS/MS. Calibration curves were generated by plotting the area under the curve (AUC) for each analyte (normalized to the internal standard) against the amount of analyte contained in 200 μ L of extraction solution. Data are presented as mean \pm standard error of the mean (S.E.M.) for $n \geq 3$ technical replicates

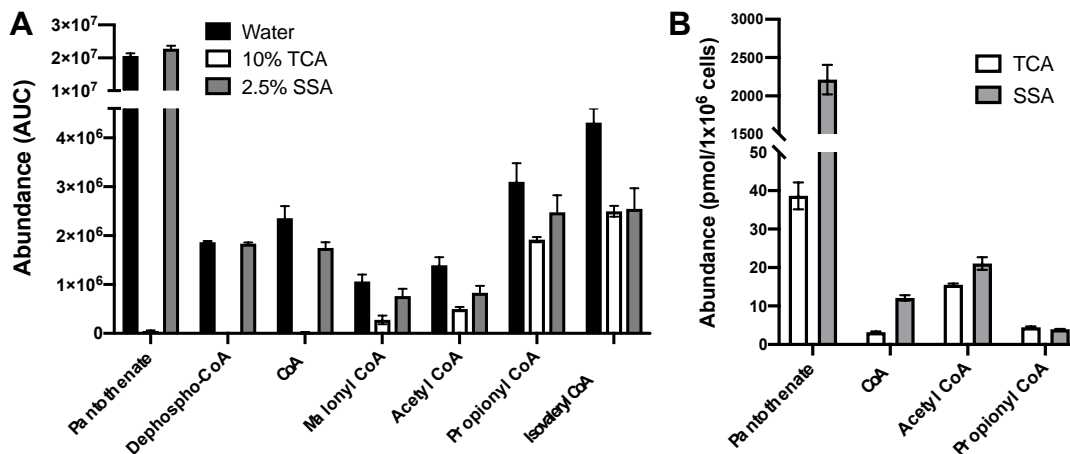


Figure 5: SSA-based sample preparation results in higher recovery of CoA-related metabolites.

(A) 1 nmol of each analyte was extracted with 200 μ L of 10% (v/v) TCA, 2.5% SSA, or spiked into 200 μ L water. The following percent recoveries were obtained relative to water, and shown as TCA vs. SSA: pantothenate (0% vs. >100%); dephospho-CoA (0% vs. >99%); CoA (1% vs. 74%); malonyl CoA (26% vs. 74%); acetyl CoA (36% vs. 59%); propionyl CoA (62% vs. 80%); isovaleryl CoA (58% vs. 59%). (B) Metabolites were extracted from HEK 293FT cells using either direct extraction with SSA or TCA followed by solid-phase extraction. All data are presented as mean \pm standard error of the mean (S.E.M.) for $n \geq 3$ technical replicates.

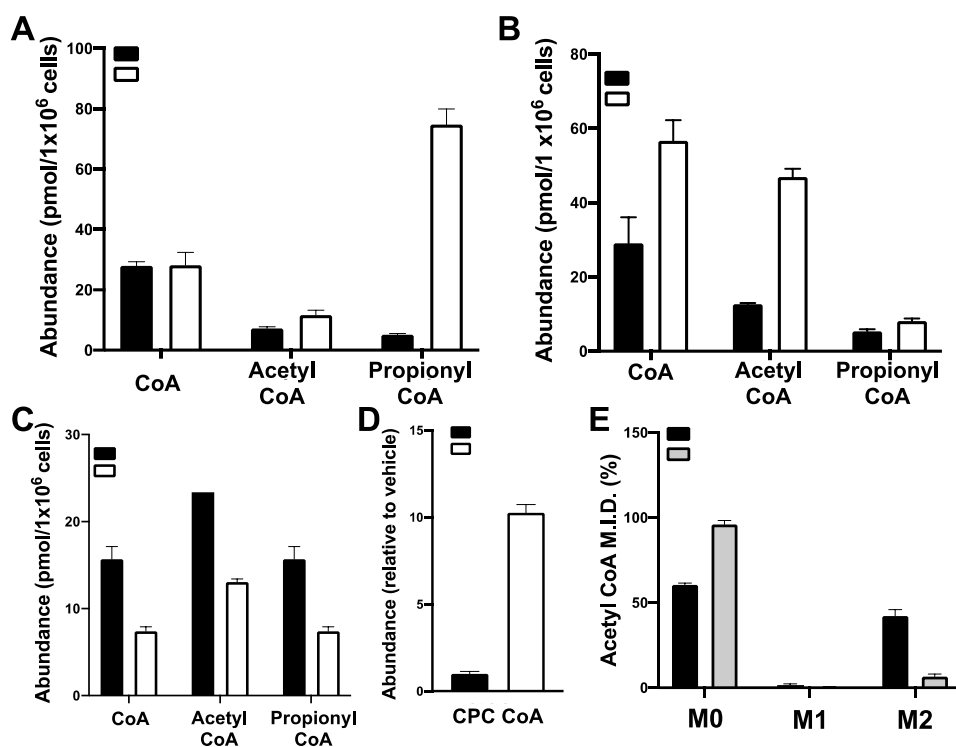


Figure 6: The method successfully detects expected perturbations in CoA metabolism.

(A-D) HepG2 cells were treated for 24 hr. with either 1mM propionate (A), 10μM PZ-2891 (B), or 1 mM cyclopropanecarboxylic acid (CPCA; C & D). CoA and short-chain acyl CoA esters were the extracted and measured as described above. (E) Mass isotopologue distribution (M.I.D.) of acetyl CoA extracted from HepG2 cells treated for 24 hr. with U-¹³C₆-glucose. All data are presented as mean ± standard error of the mean (S.E.M.) for n=3 technical replicates.

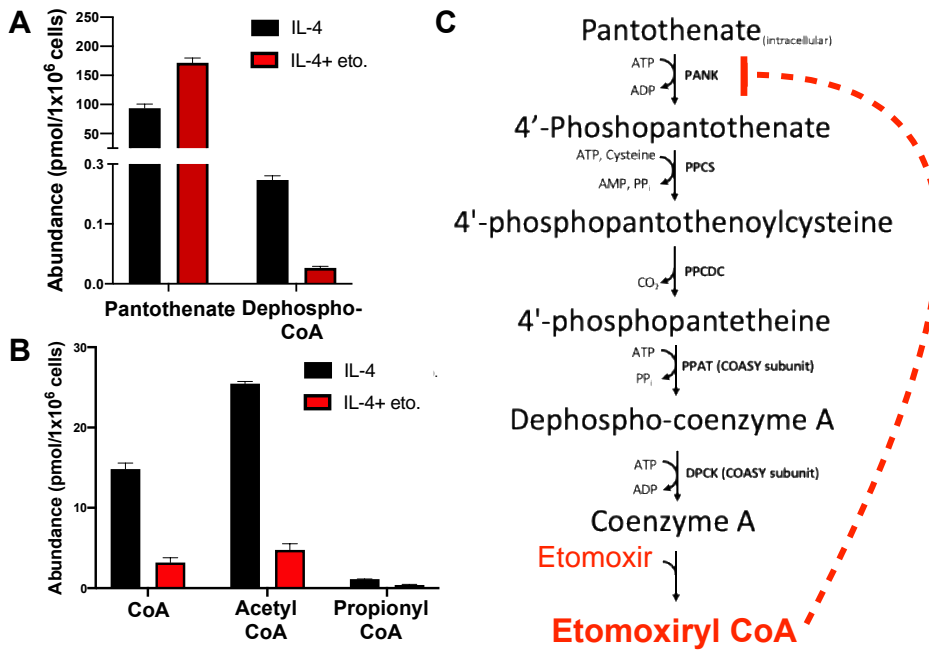


Figure 7: The method detects changes in the CoA biosynthetic pathway of etomoxir treated macrophages.

(A) and short-chain acyl CoA species (B) in IL-4-polarized macrophages following etomoxir treatment. Data are presented as mean ± standard error of the mean (S.E.M.) for $n = 3$ technical replicates.

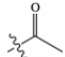
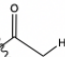
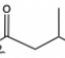
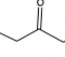
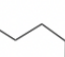
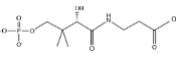
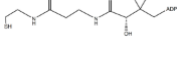
Compound Name	Acyl Group Formula	Acyl Group Structure	Parent (m/z)	Daughter 1 (m/z)	Daughter 2 (m/z)
CoA	H	H	768.1	261.1	428.1
Acetyl CoA	COCH ₃		810.1	303.1	428.1
Propionyl CoA	COCH ₂ CH ₃		824.1	317.1	428.1
Isovaleryl CoA	COCH ₂ (CH ₃) ₂		852.1	345.1	428.1
Malonyl CoA	COCH ₂ CO ₂ H		854.1	347.1	428.1
Succinyl CoA	CO(CH ₂) ₂ CO ₂ H		868.1	361.1	428.1
Compound Name	Chemical Formula	Compound Structure	Parent (m/z)	Daughter 1 (m/z)	Daughter 2 (m/z)
Pantothenate	C ₉ H ₁₇ NO ₅		218.0	88.0	145.8
Dephospho-CoA	C ₂₁ H ₃₅ N ₇ O ₁₃ P ₂ S		688.1	261.1	348.1

Table 1. Parent and daughter ion m/z for short-chain acyl CoAs, dephospho-CoA, and pantothenate.

Time (min)	%A	%B	Notes
0	98	2	Divert to waste (0–5.5 min)
1.5	98	2	
9	50	50	Divert to MS (5.5–10.5 min)
9.5	2	98	
14.5	2	98	Divert to waste (10.5–22 min)
15	98	2	
22	98	2	

Table 2. The following solvents were used during the chromatography: Solvent A, 5 mM ammonium acetate + 2.5 mM DMBA (pH 5.6) and Solvent B, 95% acetonitrile, 5% H₂O + 5 mM ammonium acetate

Compound	Linear Regression	r	LLOD (pmol)	LLOQ (pmol)
Pantothenate	$Y = 0.00264x + 0.0307$	0.98	1	7.4
Dephospho-CoA	$Y = 0.00481x + 0.0892$	0.97	0.4	3.7
CoA	$Y = 0.00546x - 0.0196$	0.97	1	3.7
Malonyl CoA	$Y = 0.00221x - 0.00851$	0.99	3	3.7
Succinyl CoA	$Y = 0.00095x - 0.0011$	0.95	1	7.4
Acetyl CoA	$Y = 0.00461x - 0.0163$	0.97	1	3.7
Propionyl CoA	$Y = 0.00660x + 0.0367$	0.99	2	3.7
Isovaleryl CoA	$Y = 0.00864x - 0.1853$	0.99	1	7.4

Table 3. The lower limits of detection (LLOD) and quantitation (LLOQ) are calculated as described in the text.

	Standards (pmol)	Calculated concentration (pmol/1x10 ⁶ cells)	SEM	Precision CV (%)	Accuracy (% of nominal value)
Pantothenate	0	969.15	7.74	1.60	NA
	62.5	1231.50	48.44	7.87	119.37
	250	1421.00	78.83	11.10	116.56
	1000	2244.50	31.47	2.80	113.98
Dephospho-CoA	0	1.68	0.08	9.78	NA
	62.5	57.39	4.78	16.64	89.41
	250	228.81	23.02	20.12	90.91
	1000	961.96	24.63	5.12	96.03
CoA	0	49.98	4.67	18.68	NA
	62.5	143.03	4.81	6.73	127.16
	250	277.50	16.61	11.97	92.51
	1000	865.48	7.02	1.62	82.43
Acetyl CoA	0	65.67	1.81	5.52	NA
	62.5	127.05	8.85	13.94	99.13
	250	356.48	14.96	8.40	112.93
	1000	1402.79	32.15	4.58	131.63
Propionyl CoA	0	7.95	0.20	5.03	NA
	62.5	75.03	5.98	15.93	106.49
	250	277.52	4.06	2.92	107.59
	1000	1132.35	59.58	10.52	112.34
Isovaleryl CoA	0	3.17	0.21	13.19	NA
	62.5	67.53	6.33	18.76	102.82
	250	314.52	4.34	2.76	124.23
	1000	1383.19	50.47	7.30	137.88
Malonyl CoA	0	2.45	0.18	14.84	NA
	62.5	62.03	2.94	9.48	95.50
	250	265.98	20.15	15.15	105.36
	1000	1077.85	69.21	12.84	107.52
Succinyl CoA	0	208.61	11.79	11.31	NA
	62.5	295.38	22.62	15.32	108.96
	250	507.42	25.24	9.95	110.64
	1000	1279.86	71.49	11.17	105.90

Table 4. Precision and accuracy determination

4. References

Abranko, L., Williamson, G., Gardner, S., Kerimi, A., 2018. Comprehensive quantitative analysis of fatty-acyl-Coenzyme A species in biological samples by ultra-high performance liquid chromatography-tandem mass spectrometry harmonizing hydrophilic interaction and reversed phase chromatography. *J Chromatogr A* 1534, 111-122.

Basiri, B., Murph, M.M., Bartlett, M.G., 2017. Assessing the Interplay between the Physicochemical Parameters of Ion-Pairing Reagents and the Analyte Sequence on the Electrospray Desorption Process for Oligonucleotides. *J Am Soc Mass Spectrom* 28 (8), 1647-1656.

Basu, S.S., Blair, I.A., 2012. SILEC: a protocol for generating and using isotopically labeled coenzyme A mass spectrometry standards. *Nature Protocols* 7 (1), 1-11.

Basu, S.S., Mesaros, C., Gelhaus, S.L., Blair, I.A., 2011. Stable isotope labeling by essential nutrients in cell culture for preparation of labeled coenzyme A and its thioesters. *Anal Chem* 83 (4), 1363-1369.

Berrueta, L.A., Gallo, B., Vicente, F., 1995. A review of solid phase extraction: Basic principles and new developments. *Chromatographia* 40 (7), 474-483.

Covarrubias, A.J., Aksoylar, H.I., Yu, J., Snyder, N.W., Worth, A.J., Iyer, S.S., Wang, J., Ben-Sahra, I., Byles, V., Polynne-Stapornkul, T., Espinosa, E.C., Lamming, D., Manning, B.D., Zhang, Y., Blair, I.A., Horng, T., 2016. Akt-mTORC1 signaling regulates Acly to integrate metabolic input to control of macrophage activation. *Elife* 5.

Demoz, A., Garras, A., Asiedu, D.K., Netteland, B., Berge, R.K., 1995. Rapid method for the separation and detection of tissue short-chain coenzyme A esters by reversed-phase high-performance liquid chromatography. *J Chromatogr B Biomed Appl* 667 (1), 148-152.

Di Meo, I., Carecchio, M., Tiranti, V., 2019. Inborn errors of coenzyme A metabolism and neurodegeneration. *J Inherit Metab Dis* 42 (1), 49-56.

Divakaruni, A.S., Hsieh, W.Y., Minarrieta, L., Duong, T.N., Kim, K.K.O., Desousa, B.R., Andreyev, A.Y., Bowman, C.E., Caradonna, K., Dranka, B.P., Ferrick, D.A., Liesa, M., Stiles, L., Rogers, G.W., Braas, D., Ciaraldi, T.P., Wolfgang, M.J., Sparwasser, T., Berod, L., Bensinger, S.J., Murphy, A.N., 2018. Etomoxir Inhibits Macrophage Polarization by Disrupting CoA Homeostasis. *Cell Metab* 28 (3), 490-503 e497.

Divakaruni, A.S., Wallace, M., Buren, C., Martyniuk, K., Andreyev, A.Y., Li, E., Fields, J.A., Cordes, T., Reynolds, I.J., Bloodgood, B.L., Raymond, L.A., Metallo, C.M., Murphy, A.N., 2017. Inhibition of the mitochondrial pyruvate carrier protects from excitotoxic neuronal death. *J Cell Biol* 216 (4), 1091-1105.

Dusi, S., Valletta, L., Haack, T.B., Tsuchiya, Y., Venco, P., Pasqualato, S., Goffrini, P., Tigano, M., Demchenko, N., Wieland, T., Schwarzmayr, T., Strom, T.M., Invernizzi, F., Garavaglia, B., Gregory, A., Sanford, L., Hamada, J., Bettencourt, C., Houlden, H., Chiapparini, L., Zorzi, G., Kurian, M.A., Nardocci, N., Prokisch, H., Hayflick, S., Gout, I., Tiranti, V., 2014. Exome sequence reveals mutations in CoA synthase as a cause of neurodegeneration with brain iron accumulation. *Am J Hum Genet* 94 (1), 11-22.

Gao, L., Chiou, W., Tang, H., Cheng, X., Camp, H.S., Burns, D.J., 2007. Simultaneous quantification of malonyl-CoA and several other short-chain acyl-CoAs in animal tissues by ion-pairing reversed-phase HPLC/MS. *J Chromatogr B Analyt Technol Biomed Life Sci* 853 (1-2), 303-313.

Garcia, M., Leonardi, R., Zhang, Y.M., Rehg, J.E., Jackowski, S., 2012. Germline deletion of pantothenate kinases 1 and 2 reveals the key roles for CoA in postnatal metabolism. *PLoS One* 7 (7), e40871.

Gauthier, N., Wu, J.W., Wang, S.P., Allard, P., Mamer, O.A., Sweetman, L., Moser, A.B., Kratz, L., Alvarez, F., Robitaille, Y., Lépine, F., Mitchell, G.A., 2013. A liver-specific defect of Acyl-CoA degradation produces hyperammonemia, hypoglycemia and a distinct hepatic Acyl-CoA pattern. *PLoS One* 8 (7), e60581.

Gregory, A., Hayflick, S.J., 1993. Pantothenate Kinase-Associated Neurodegeneration, in: Adam, M.P., Ardinger, H.H., Pagon, R.A., Wallace, S.E., Bean, L.J.H., Mirzaa, G., Amemiya, A. (Eds.), *GeneReviews*(®). University of Washington, Seattle

Copyright © 1993-2021, University of Washington, Seattle. GeneReviews is a registered trademark of the University of Washington, Seattle. All rights reserved., Seattle (WA).

Hayashi, O., Satoh, K., 2006. Determination of acetyl-CoA and malonyl-CoA in germinating rice seeds using the LC-MS/MS technique. *Biosci Biotechnol Biochem* 70 (11), 2676-2681.

Health, U.D.o., Services, H., 2001. Guidance for industry, bioanalytical method validation. <http://www.fda.gov/cder/guidance/index.htm>.

Khan, K., Blaak, E., Elia, M., 1991. Quantifying intermediary metabolites in whole blood after a simple deproteinization step with sulfosalicylic acid. *Clin Chem* 37 (5), 728-733.

Leonardi, R., Zhang, Y.M., Rock, C.O., Jackowski, S., 2005. Coenzyme A: back in action. *Prog Lipid Res* 44 (2-3), 125-153.

Minkler, P.E., Kerner, J., Ingalls, S.T., Hoppel, C.L., 2008. Novel isolation procedure for short-, medium-, and long-chain acyl-coenzyme A esters from tissue. *Anal Biochem* 376 (2), 275-276.

Neubauer, S., Chu, D.B., Marx, H., Sauer, M., Hann, S., Koellensperger, G., 2015. LC-MS/MS-based analysis of coenzyme A and short-chain acyl-coenzyme A thioesters. *Anal Bioanal Chem* 407 (22), 6681-6688.

Palladino, A.A., Chen, J., Kallish, S., Stanley, C.A., Bennett, M.J., 2012. Measurement of tissue acyl-CoAs using flow-injection tandem mass spectrometry: acyl-CoA profiles in short-chain fatty acid oxidation defects. *Molecular Genetics and Metabolism* 107 (4), 679-683.

Park, J.W., Jung, W.S., Park, S.R., Park, B.C., Yoon, Y.J., 2007. Analysis of intracellular short organic acid-coenzyme A esters from actinomycetes using liquid chromatography-electrospray ionization-mass spectrometry. *J Mass Spectrom* 42 (9), 1136-1147.

Perera, M.A., Choi, S.Y., Wurtele, E.S., Nikolau, B.J., 2009. Quantitative analysis of short-chain acyl-coenzymeAs in plant tissues by LC-MS-MS electrospray ionization method. *J Chromatogr B Analyt Technol Biomed Life Sci* 877 (5-6), 482-488.

Pietrocola, F., Galluzzi, L., Bravo-San Pedro, J.M., Madeo, F., Kroemer, G., 2015. Acetyl coenzyme A: a central metabolite and second messenger. *Cell Metab* 21 (6), 805-821.

Prasad, P.D., Wang, H., Kekuda, R., Fujita, T., Fei, Y.J., Devoe, L.D., Leibach, F.H., Ganapathy, V., 1998. Cloning and functional expression of a cDNA encoding a mammalian sodium-dependent vitamin transporter mediating the uptake of pantothenate, biotin, and lipoate. *J Biol Chem* 273 (13), 7501-7506.

Quick, M., Shi, L., 2015. The sodium/multivitamin transporter: a multipotent system with therapeutic implications. *Vitam Horm* 98, 63-100.

Rivera, L.G., Bartlett, M.G., 2018. Chromatographic methods for the determination of acyl-CoAs. *Analytical Methods* 10 (44), 5252-5264.

Robishaw, J.D., Neely, J.R., 1984. Pantothenate kinase and control of CoA synthesis in heart. *Am J Physiol* 246 (4 Pt 2), H532-541.

Rock, C.O., Calder, R.B., Karim, M.A., Jackowski, S., 2000. Pantothenate kinase regulation of the intracellular concentration of coenzyme A. *J Biol Chem* 275 (2), 1377-1383.

Rock, C.O., Karim, M.A., Zhang, Y.M., Jackowski, S., 2002. The murine pantothenate kinase (Pank1) gene encodes two differentially regulated pantothenate kinase isozymes. *Gene* 291 (1-2), 35-43.

Sedgwick, G.W., Fenton, T.W., Thompson, J.R., 1991. Effect of protein precipitating agents on the recovery of plasma free amino acids. *Canadian Journal of Animal Science* 71 (3), 953-957.

Sharma, L.K., Subramanian, C., Yun, M.K., Frank, M.W., White, S.W., Rock, C.O., Lee, R.E., Jackowski, S., 2018. A therapeutic approach to pantothenate kinase associated neurodegeneration. *Nat Commun* 9 (1), 4399.

Smith, G., 2012. European Medicines Agency guideline on bioanalytical method validation: what more is there to say? *Bioanalysis* 4 (8), 865-868.

Snyder, N.W., Basu, S.S., Worth, A.J., Mesaros, C., Blair, I.A., 2015. Metabolism of propionic acid to a novel acyl-coenzyme A thioester by mammalian cell lines and platelets. *J Lipid Res* 56 (1), 142-150.

Tsuchiya, Y., Pham, U., Gout, I., 2014. Methods for measuring CoA and CoA derivatives in biological samples. *Biochem Soc Trans* 42 (4), 1107-1111.

Ulrich, R.G., Bacon, J.A., Brass, E.P., Cramer, C.T., Petrella, D.K., Sun, E.L., 2001. Metabolic, idiosyncratic toxicity of drugs: overview of the hepatic toxicity induced by the anxiolytic, panadiplon. *Chem Biol Interact* 134 (3), 251-270.

Venco, P., Dusi, S., Valletta, L., Tiranti, V., 2014. Alteration of the coenzyme A biosynthetic pathway in neurodegeneration with brain iron accumulation syndromes. *Biochem Soc Trans* 42 (4), 1069-1074.

Vessey, D.A., Kelley, M., Warren, R.S., 1999. Characterization of the CoA ligases of human liver mitochondria catalyzing the activation of short- and medium-chain fatty acids and xenobiotic carboxylic acids. *Biochim Biophys Acta* 1428 (2-3), 455-462.

Chapter 2: MyD88-linked TLRs enhance the IL-4 response

ABSTRACT

CoA homeostasis has been demonstrated to be important for interleukin-4 (IL-4)-mediated macrophage polarization. Previously we have shown that coenzyme A (CoA) homeostasis was associated with the IL-4 response. However, the role of CoA during alternative activation was entirely unclear. In this study, we show that exogenous CoA synergizes with IL-4 by increasing the expression of genes associated with alternative macrophage activation *in vitro*. Provision of CoA is also able to increase markers of alternative activation *in vivo*. We determined that CoA acts as a weak toll-like receptor 4 agonist, which enhances the IL-4 response through activation of the MyD88 signaling cascade. This work demonstrates that activation of the MyD88 pathway is sufficient to enhance alternative activation both *in vitro* and *in vivo*.

1.Introduction

Macrophages are innate immune cells that execute a variety of functions including detecting and removing foreign pathogens, facilitating adaptive immune cell function, and maintaining tissue homeostasis. *In vivo*, these cells integrate multiple external cues to determine which inflammatory program they must adopt to maintain organismal homeostasis. This process is known as macrophage activation or ‘polarization’ (Glass and Natoli, 2016; Murray, 2017). While *in vivo* activation likely occurs on a continuum, *in vitro* mechanistic studies can be aided by simplifying macrophage activation into two rigid states, namely classical and alternative activation (Gordon and Martinez, 2010; Martinez and Gordon, 2014).

Classical activation is characterized by the expression of the pro-inflammatory cytokines such as *Il1b*, *Tnf*, and *Il12* (Murray, 2017). This functional state occurs when macrophages detect the presence of pathogen-associated molecular patterns (PAMPs) or damage-associated molecular patterns (DAMPs) (Akira and Takeda, 2004; Takeuchi and Akira, 2010). Many common bacterial and viral PAMPs are recognized by toll-like receptors (TLRs). Following the binding of a PAMP/DAMP to its cognate TLR, the receptor activates adaptor protein-mediated signaling pathways, ultimately leading to increased activity of transcription factors responsible for pro-inflammatory gene expression.

TLR adaptor protein-linked signaling cascades can broadly be divided into two pathways. The Myeloid differentiation primary response 88 (MyD88)-dependent pathway is utilized by all TLRs except TLR3, while the TIR-domain-containing adapter-inducing

interferon- β (TRIF) pathway is only used by TLR3 and TLR4. Activation of these different adaptor proteins leads to expression of a divergent set of pro-inflammatory genes. MyD88 pathway stimulation results in the activation of Nuclear factor kappa-light-chain-enhancer of activated B cells (NF- κ B) and mitogen-activated protein kinase (MAPK) pathways, while activation of the TRIF pathway causes the production of type-I interferons (Akira and Takeda, 2004; Kawai and Akira, 2010).

Macrophages can also be polarized to the alternatively activated state, which is characterized by the expression of anti-inflammatory genes including *Mrc1*, *Mgl2*, and *Arg1* (Gordon and Martinez, 2010; Martinez et al., 2013; Murray, 2017). While classical activation can occur following TLR activation, alternative activation is achieved when macrophages are exposed to either interleukin-4 (IL-4) or interleukin-13 (IL-13) (Chomarat and Banchereau, 1998). Mechanistically, binding of either of these cytokines to their respective receptors leads to downstream activation of the transcription factor signal transducer and activator of transcription 6 (STAT6) (Glass and Natoli, 2016; Gordon and Martinez, 2010; Heller et al., 2008). STAT6 then synergizes with other transcription factors such as peroxisome proliferator-activated receptors (PPARs) and Kruppel-like factor 4 (KLF4) to efficiently induce the expression of genes associated with alternative activation (Sica and Mantovani, 2012).

In addition to enhancing the expression of inflammatory genes, macrophages also alter their metabolism in response to activation cues (Jones and Divakaruni, 2020; Van den Bossche et al., 2017). Classical activation is associated with increased aerobic glycolysis and decreased mitochondrial oxidative phosphorylation (Haschemi et al., 2012; Tannahill et al.,

2013). Pharmacologic inhibition of these metabolic processes decreases classical activation markers *in vitro* and *in vivo* (Tannahill et al., 2013). On the other hand, alternative activation is characterized by having increased rates of oxidative phosphorylation (Divakaruni et al., 2018b; Huang et al., 2016; Vats et al., 2006). We have previously shown that disrupting CoA homeostasis decreases alternative activation, while supplementing macrophages with exogenous CoA enhances this activation (Divakaruni *et al.*, 2018b; Jones et al., 2021). However, precisely how CoA instructs macrophage activation is unknown.

Investigations of macrophage biology often focus on uncovering the mechanisms by which a single class of stimuli causes change in the macrophage activation state. However, it is well appreciated that *in vivo* macrophage activation occurs in the presence of a diverse milieu of stimuli that can induce both classical and alternative activation (Murray, 2017). Further, cooperation between classical and alternatively activated macrophage states are often necessary to achieve the desired physiological response *in vivo* (Arnold et al., 2007; Chazaud, 2020; Hesketh et al., 2017). These points underlie the importance of investigating the mechanisms by which classical and alternative activation signals can converge to modify macrophage activation.

Here, we investigated the mechanism by which exogenous CoA addition enhances alternative activation. Surprisingly, CoA doesn't boost alternative activation by enhancing the metabolic hallmarks of the IL-4 response. Rather, we demonstrate that CoA enhances alternative activation by acting as a weak toll-like receptor 4 (TLR4) agonist. As a TLR4 agonist, CoA increases MyD88 pathway activation, which synergizes with IL-4 to enhance

alternative activation. Further, we show that activating MyD88 pathway signaling is sufficient to enhance alternative activation *in vitro* and *in vivo*. In summary, by utilizing CoA as a tool to better understand the mechanisms regulating alternative activation, we discovered that activation of the MyD88 pathway synergizes with IL-4 to enhance alternative macrophage activation.

2.Results

2.1 Exogenous CoA enhances alternative macrophage activation

Our previous work established that addition of exogenous Coenzyme A (CoA) to macrophage culture media enhances the abundance of cell surface markers associated with alternative activation (Divakaruni *et al.*, 2018b). We aimed to follow up on these findings by more thoroughly investigating how CoA addition affects the alternative activation program.

First, we assessed whether CoA could enhance the expression of IL-4-stimulated genes. To address this, we stimulated mouse bone marrow-derived macrophages (BMDMs) with IL-4 alone or in combination with CoA. Gene expression analysis revealed that CoA cooperates with IL-4 to enhance the expression of *Mgl2*, *Pdcd1gl2*, *Arg1*, *Mrc1*, and *Fizz1* (**Figure 1A**), genes associated with alternative macrophage activation (Liu *et al.*, 2017; Sanin *et al.*, 2018). Although CoA synergized with IL-4 to increase expression of these genes, it did not stimulate their expression in the absence of IL-4 (**Figure 1A**). Flow cytometry analysis revealed that CoA cooperates with IL-4 to increase the abundance of CD206 and CD301 on the BMDM cell-surface (**Figure 1 B&C**). Similarly, co-stimulation with as little as 62.5 μ M CoA increased the population of CD206⁺/CD71⁺ and CD206⁺/CD301⁺ BMDMs (**Figure 1B&D**). Congruent with gene expression studies, exogenous CoA was not able to enhance the presence of these cell-surface markers in the absence of IL-4 (**Figures 1B-1D**).

Next, we wanted to determine if addition of CoA could enhance alternative macrophage effector function. Since mannose receptor activity is essential for the initiation of

the T_H2 response during the helminth infection (van Die and Cummings, 2017; van Liempt et al., 2007), we tested if CoA was able to enhance its activity. Mannose receptor activity was assessed using a FITC-dextran binding assay, as this fluorescently labeled polysaccharide is a ligand of the receptor (Sallusto et al., 1995). Using high-content imaging, we demonstrated that CoA further enhances IL-4-dependent increases in mannose receptor activity (**Figures 1E and 1F**).

To assess whether CoA could enhance alternative activation *in vivo*, we treated mice with an intraperitoneal injection of IL-4 complex (IL-4c) alone or following treatment with CoA. Indeed, CoA synergized with IL-4c to increase the population of CD206⁺/CD71⁺ peritoneal macrophages *in vivo* (**Figure 1G**). Taken together, these results demonstrate that exogenous CoA synergizes with IL-4 to enhance alternative activation *in vitro* and *in vivo*.

2.2 CoA does not enhance alternative macrophage activation by boosting known metabolic hallmarks of the IL-4 response.

Having shown that exogenous CoA enhances alternative activation, we next sought to determine the mechanism by which CoA elicits this effect. It has become increasingly clear that changes in cellular metabolism are associated with alternative activation of macrophages (Van den Bossche *et al.*, 2017). Specifically, stimulation with IL-4 has been demonstrated to increase mitochondrial respiratory capacity (Huang et al., 2014; Puleston et al., 2019; Van den Bossche et al., 2016), mitochondrial glucose oxidation (Huang *et al.*, 2016; Jha et al., 2015), and lipid synthesis (Bidault et al., 2021; Huang *et al.*, 2014). Since CoA is a necessary cofactor for each of these metabolic pathways (Gout, 2018; Leonardi *et al.*, 2005; Pietrocola *et al.*, 2015), we asked if exogenous CoA enhanced the IL-4 response by increasing flux through one of these metabolic pathways.

Before testing if CoA could enhance IL-4-driven metabolic rewiring, we first determined if exogenous CoA could be incorporated into the intracellular CoA pool to be utilized as a cofactor for cellular metabolic reactions. Predictably, supplying cells with CoA-supplemented

culture media increased the intracellular abundance of CoA and acetyl CoA (**Figure 2A**). After demonstrating that exogenous CoA could be used to increase the levels intracellular acyl CoAs, we moved forward with testing if CoA addition enhanced IL-4-driven metabolic changes. Initially we asked whether CoA could boost IL-4-prompted increases in ATP-linked respiration, maximal respiration, and glycolytic rate in BMDMs (Huang *et al.*, 2014; Huang *et al.*, 2016; Van den Bossche *et al.*, 2016). Like others, we observed an IL-4-mediated increase in these parameters (**Figure 2B-2D**); however, addition of CoA did not further enhance these metabolic changes (**Figure 2B-2D**). Surprisingly, CoA addition resulted in a significant reduction in the maximal respiration of cells stimulated with IL-4 (**Figure 2B and 2C**).

Addition of CoA did not enhance the mitochondrial respiration rate of alternatively activated macrophages, though many IL-4-mediated metabolic changes can occur without appreciable changes in the rate of oxidative phosphorylation. Alternatively activated cells have been demonstrated to have increased abundance of some TCA cycle metabolites and enhanced mitochondrial glucose and glutamine oxidation (Huang *et al.*, 2016; Jha *et al.*, 2015; Sanin *et al.*, 2018), so we decided to employ metabolomics and stable isotope tracing studies to understand if CoA could enhance these IL-4 driven changes. Metabolomics revealed that exogenous CoA did not increase the abundance of TCA cycle intermediates in alternatively activated BMDMs (**Figure 2E**). Consistent with the previous results, CoA provision did not enhance ¹³C-glucose or ¹³C-glutamine labelling of TCA cycle intermediates (**Figure 2F**) or *de novo* lipogenesis in alternatively activated macrophages (**Figure 2G**).

Since exogenous CoA didn't seem to enhance alternative activation by increasing known metabolic hallmarks of the IL-4 response, we asked if simply toggling intracellular CoA levels could truly impact alternative activation. To answer this question, we utilized two pharmacological compounds that reciprocally impact intracellular CoA levels. We treated IL-4-stimulated BMDMs with cyclopropane carboxylic acid (CPCA), which decreases the abundance of intracellular "free" CoA. This occurs as CPCA utilizes large amounts of intracellular CoA to synthesize its cognate thioester Cyclopropanecarboxyl-coenzyme A

(CPC-CoA) (Jones *et al.*, 2021) (**Figure 2H**). On the other hand, we treated IL-4-polarized cells with the small molecule PZ-2891(Sharma *et al.*, 2018a), which increases intracellular CoA levels by acting as a pantothenate kinase agonist (**Figure 2H**). As expected, addition of CPCA decreased intracellular levels of CoA and acetyl CoA (**Figure 2I and Supplemental Figure 2F**), while PZ-2891 increased their intracellular abundance (**Figure 2I**). Despite causing significant changes to bulk intracellular CoA levels, addition of these compounds had no impact on alternative activation (**Figure 2J**). Thus, exogenous CoA augments alternative activation by a mechanism other than enhancing IL-4-driven changes in macrophage metabolism. More broadly, these results suggest that enhancement of the IL-4 response can occur without further augmentation of metabolic pathways associated with alternative activation.

2.4 Exogenous CoA induces a pro-inflammatory response in BMDMs

Having shown that CoA provision doesn't enhance IL-4-dependent changes in macrophage metabolism, we set out to more completely understand how CoA impacts the transcriptome of alternatively activated macrophages. To do this, we performed bulk RNA sequencing (RNA-seq) on macrophages that were stimulated with IL-4 alone or co-stimulated with exogenous CoA. As expected, IL-4-treated cells increased the expression of genes associated with alternative activation such as *Mgl2*, *Pdcd1gl2*, *Arg1*, and *Fizz1* (**Figure 3A, left, blue**). These cells also displayed decreased expression of genes associated with classical activation including *I11b*, *Tnf*, *Nos2*, and *I112b*, (**Figure 3A, left, red**).

In line with our earlier gene expression results, RNA-seq showed that CoA synergized with IL-4 to further increase markers of alternative activation (**Figure 3A, right, blue**). Unexpectedly, CoA addition also caused a marked increase in the expression markers of classical activation that were not observed with IL-4 treatment (**Figure 3A, right, red**). Pathway analysis also showed that following exposure to CoA, alternatively activated

macrophages upregulated the expression of genes belonging to TLR signaling pathways **(Figure 3B)**.

These unbiased approaches suggested that although CoA enhances alternative activation, it may elicit a pro-inflammatory response in BMDMs. To confirm this, we assessed whether CoA could provoke a pro-inflammatory response in the absence of IL-4. CoA was able to induce expression of several MyD88-linked pro-inflammatory genes including *Il1b*, *Tnf*, *Nos2*, and *Irg1* in the absence of the IL-4 **(Figure 3C)**. CoA also increased expression of the interferon-stimulated gene *Mx1* **(Figure 3D)**. Since the *Irg1* gene encodes the aconitate decarboxylase, which is responsible for the synthesis of the itaconate, we tested if CoA could stimulate the synthesis of this pro-inflammatory metabolite. Indeed, CoA was able to increase the intracellular abundance of itaconate **(Figure 3E)**.

Finally, we investigated if CoA could elicit a similar response *in vivo*. Indeed, intraperitoneal administration of CoA caused increased expression of *Il1b* and *Tnf* in peritoneal leukocytes **(Figure 3E)** and increased the abundance of IL-1B, TNF- α , IL-6, and CXCL1 in the peritoneal lavage fluid **(Figure 3E)**. Taken together, these results demonstrate that although CoA enhances alternative activation, it elicits a pro-inflammatory *in vitro* and *in vivo*.

2.5 Exogenous CoA elicits a pro-inflammatory response by acting as a TLR4 agonist

After demonstrating that CoA elicits a pro-inflammatory response, we next sought to determine if this was mediated by a pattern recognition receptor. Since pathway analysis showed that genes associated with TLR signaling were increased following CoA supplementation, we hypothesized that CoA could increase pro-inflammatory gene expression by acting as a ligand for a specific toll-like receptor.

The MyD88 adaptor protein is necessary for the full activation of all but one murine TLRs (Snyder et al., 2013), so our first approach was to ask if CoA could provoke an inflammatory response in BMDMs lacking this essential TLR signaling adaptor. Indeed, CoA-treated Myd88^{-/-} BMDMs showed significantly decreased expression of inflammatory genes

(Figure 4A) and itaconate synthesis **(Figure 4D)**. This suggested that the CoA inflammatory response was mediated by a MyD88-linked ligand receptor.

Although inflammatory gene expression was significantly decreased in *Myd88*^{-/-} BMDMs, CoA was still able to induce residual expression of *Il1b*, *Tnf*, and *Irg1* **(Figure 4A)**. Additionally, itaconate synthesis was still observed following treatment of *Myd88*^{-/-} BMDMs with CoA **(Figure 4D)**. This suggested that CoA elicited its pro-inflammatory response by triggering both MyD88-dependent and MyD88-independent signaling cascades. These findings are consistent with our earlier experiments that showed CoA induced expression of MyD88-dependent genes, as well as interferon stimulated genes (ISGs).

Toll-like receptor 4 (TLR4) elicits its inflammatory response by activating both MyD88-dependent and MyD88-independent signaling cascades (Fitzgerald and Kagan, 2020). Activation of the MyD88-dependent arm of TLR4 causes increases expression of cytokines such as *Il1b* (Kawai et al., 1999). Additionally, activation of the TRIF arm, the MyD88-independent signaling arm of TLR4, leads to increased expression of type-I interferons along with the induction of ISGs (Kawai et al., 2001; Toshchakov et al., 2002). Since our results demonstrated that CoA induced both a MyD88-dependent and a MyD88-independent response, we hypothesized that CoA may cause pro-inflammatory activation by acting as a TLR4 agonist.

To assess if CoA was a TLR4 agonist, we utilized commercially available HEK-Blue hTLR4 reporter cells. These cells show increased secreted embryonic alkaline phosphatase (SEAP) activity following exposure to TLR4 agonists such as lipopolysaccharide (LPS) and monophosphoryl lipid A (MLPA) (Sosa et al., 2021). Addition of CoA caused significant activation of hTLR4 reporter cell lines **(Figure 4C)**. Importantly, CoA did not stimulate activity of reporter cells expressing other Myd88-linked TLRs, such as TLR2 and TLR7 **(Figure 4C and Supplemental Figure 4A)**. Interpolation of the hTLR4 reporter cell data showed that 1mM CoA, which we used to drive a pro-inflammatory response in BMDMs, was equivalent to activation with roughly 0.1ng/mL LPS **(Figure 4B)**. These data indicated that CoA acts as a

relatively weak TLR4 agonist. To confirm that CoA was indeed a TLR4 agonist, we treated *Tlr4*^{-/-} BMDMs with CoA and assessed markers of classical activation. As expected, CoA failed to induce pro-inflammatory gene expression or itaconate synthesis in TLR4-deficient BMDMs (**Figure 4E and 4D**). Since the commercially provided CoA used in this study was of yeast origin, we wanted to confirm that CoA itself, and not yeast-derived PAMPs, were responsible for the inflammatory effect. Indeed, cells treated with CoA derived from chemical synthesis rather than biological origin was also capable of eliciting a potent inflammatory response in BMDMs. Further, both yeast-derived and synthetically derived CoA was demonstrated to be endotoxin free. In total, these data demonstrate that CoA induces an inflammatory response by acting as a weak TLR4 agonist.

Having shown that CoA is a weak TLR4 agonist that synergizes with IL-4 to significantly enhance alternative activation, we next determined if a small concentration of a validated TLR4 agonist could cooperate with IL-4 to enhance alternative activation. To answer this, we stimulated cells with IL-4 alone or in combination with 0.1 ng/mL LPS and assessed alternative activation by flow cytometry. Co-treatment with LPS was able to significantly increase the expression of IL-4 dependent cell-surface markers (**Figure 5A and 5B**).

Since stimulation of TLR4 leads to activation of both MyD88 and TRIF signaling cascades, we reasoned that activation of either of these pathways could mediate the LPS-driven enhancement of the IL-4 response. To determine which adaptor protein signaling pathway was causing this effect, we co-stimulated alternatively activated macrophages with TLR ligands that exclusively activate MyD88 or TRIF signaling.

Co-stimulation of IL-4 treated cells with the TLR2 ligand Pam3CSK4, which exclusively activates the MyD88-dependent pathway, increased expression of cell surface markers associated alternatively activation (**Figure 5A and 5B**). On the other hand, combining IL-4 with Poly: IC, which activates the TRIF pathway, decreased the markers of the IL-4 response (**Figure 5A and 5B**). This suggested that activation of the MyD88 pathway enhanced the expression of IL-4-dependent cell-surface markers. To further confirm this, we co-stimulated

alternatively activated macrophages with other TLR agonist that stimulate MyD88 pathway activity. Both the TLR5 agonist flagellin and the TLR7 agonist imiquimod increased the population of CD206⁺/CD301⁺ BMDMs (**Figure 5A and 5B**).

2.5 Myd88-linked TLR-ligands enhance IL-4 response

We next confirmed that MyD88 signaling also impacts the expression of alternative activation genes. Indeed, addition of LPS or Pam3CSK4 to IL-4-polarized macrophages resulted in increased expression of alternative activation genes (**Figure 5C**). Similar to CoA, LPS and Pam3CSK4 enhanced the IL-4-prompted increase in mannose receptor activity (**Figure 5D**). Further, treatment with LPS or Pam3CSK4 enhanced the IL-4 response *in vivo*, while addition of Poly: IC did not enhance this response (**Figure 5E**).

Lastly, we wished to confirm that the enhancement of the IL-4 response by Pam3CSK4 and LPS was MyD88-dependent. To this end, we treated MyD88^{-/-}BMDMs with IL-4 alone or in combination with either of these agonists. As expected, addition of LPS or Pam3CSK4 was no longer able to enhance the expression of IL-4-associated cell-surface markers (**Figure 5F**) or genes (**Figure 5F**) in BMDMs lacking this adaptor protein. Collectively, these results demonstrate that activation of the MyD88 pathway is able to enhance alternative activation *in vitro* and *in vivo*.

3. Discussion

Here we show that in addition to increasing IL-4-driven cell-surface marker levels, CoA enhances the expression of many IL-4-associated genes and increases the IL-4-dependent activity of the mannose receptor. We further show that CoA is able to enhance markers of alternative activation *in vivo*. These results are in line with previous studies showing that addition of other exogenous metabolic products can alter alternative activation. Although CoA is able to enhance alternative activation, we demonstrate that this compound is also able to elicit a pro-inflammatory response *in vitro* and *in vivo* by acting as a TLR4 agonist. This is in

agreement with a recent study that shows CoA increases the expression of pro-inflammatory genes in a TLR dependent manner (Timblin et al., 2022). Recently published studies support our finding that MyD88 signaling enhance the IL-4 response. First, Dang et al. noted that the CLP fungal effector, which enhances BMDM alternative activation in a TLR4-dependent fashion, failed to promote alternative activation in MyD88^{-/-} BMDMs. Moreover, Faas and colleagues have recently uncovered a link between IL-33, which activates MyD88 signaling, and alternative activation (Faas et al., 2021). Taken together, these studies further support our discovery that MyD88 signaling is sufficient to enhance alternative activation.

4. Methods

Isolation and differentiation of mouse bone marrow-derived macrophages

BMDMs from WT, *Myd88*^{-/-}, and *Tlr4*^{-/-} mice were prepared as previously described (Divakaruni et al., 2018b; Jones et al., 2021). Briefly, bone marrow cells were first isolated from the femurs and tibiae of mice by flushing with phosphate buffered saline (PBS). Following the removal of red blood cells, bone marrow cells were differentiated in BMDM media for 6 days at 37°C in a humidified 5% CO₂ incubator. BMDM media consisted of high-glucose DMEM (Gibco 11965) supplemented with 10% fetal bovine serum (FBS) (Hyclone), 2mM L-glutamine, 500µM sodium pyruvate, and 1% penicillin/streptomycin. CMG-14-12 conditioned media 10%(v/v) was added to BMDM media as a source of macrophage colony stimulate factor (M-CSF).

***In vivo* activation of peritoneal macrophages**

To determine if CoA was able to induce a pro-inflammatory response *in vivo*, WT C57BL/6 mice were split into two groups and treated with either PBS or CoA (40mg/kg) for 6 h Following treatment, peritoneal macrophages were collected by rinsing the peritoneal cavity with 5mL of

PBS. Following centrifugation, the supernatant was used to estimate cytokine levels with the LEGENDplex multiplex ELISA kit, while peritoneal exudate cells were lysed for gene expression analysis.

To induce alternative activation *in vivo*, mice were treated with the IL-4 complex (IL-4c). IL-4c consisted of 2:1 molar ratio of IL-4 (Peprotech, 214-14) and anti-IL-4 mAb (clone 11B11; BioXcell). Each IL-4c treated mouse received 5 μ g IL-4 and 25 μ g of anti-IL-4 antibody. For experiments determining if CoA enhanced alternative activation *in vivo*, WT C57BL/6 mice were split into 3 groups. The mice were treated with either PBS, an initial pretreatment with PBS for 6 hours followed by injection of IL-4c, or an initial pretreatment with CoA(40mg/kg) for 6 hours followed by administration of IL-4c. Following 24hr. stimulation with IL-4c, peritoneal macrophages were collected by rinsing the peritoneal cavity with 5mL of PBS. Alternative activation markers of CD11b and F4/80 double positive macrophages were assessed using flow cytometry.

To determine if TLR agonist could enhance the IL-4 response, mice were split into 5 experimental groups. Mice were treated with either PBS, an initial pretreatment with PBS for 24 hours followed by injection of IL-4c, or an initial pretreatment with the indicated TLR agonist for 24 hours followed by administration of IL-4c. Following 24hr. stimulation with IL-4c, peritoneal macrophages were collected and assessed for alternative activation as mentioned above.

BMDM stimulation

BMDMs that were differentiated for 6 days were scraped with a cell lifter and counted. The cells were then diluted in BMDM media and placed into the appropriate tissue culture plates for each assay. Two days later, cells were stimulated with the compounds indicated in the figure legends and below.

For experiments aimed at determining if CoA could enhance the IL-4 response, BMDMs were stimulated with CoA(1mM), IL-4(20ng/mL), or IL-4 in combination with CoA (1mM) for 48 h.

To assess if toll-like receptor ligands could enhance alternative activation, BMDMs were stimulated with IL-4(20ng/mL) alone or IL-4 in combination with LPS(0.1ng/mL), Pam3CSK4(5ng/mL), imiquimod (10 μ M), flagellin (100ng/mL), or Poly(I:C) (1 μ g/mL) for 48 h.

To determine if CoA increased expression of pro-inflammatory genes *in vitro*, BMDMs were stimulated with CoA(1mM) for 4 h. Each experimental group listed above also contained an unstimulated control.

Gene expression analysis

For qPCR, day 6 BMDMS were seeded at 3.0 x10⁵ cells per well in 12-well plates two days prior to stimulation. Following stimulation for the indicated time period, RNA was extracted from BMDMs using the RNeasy Mini Kit (Qiagen, 74106) according to the manufacturer's protocol. cDNA was synthesized using high-capacity cDNA reverse transcription kit (Applied Biosystems, 4368814) according to the manufacturer's protocol. qPCR was performed with PowerUp SYBR green master mix (Applied Biosystems, A25743) on a QuantStudio 5 RT-

PCR (Applied Biosystems). Relative gene expression values were calculated using the delta-delta Ct method and Rplp0 was used as the control gene.

Flow cytometry analysis

Day 6 BMDMs were seeded at 3.0×10^5 cells per well in 12-well plates two days prior to stimulation. Following stimulation, BMDMs were lifted off the plate by scraping in 450 μ L of Accutase. Cells were washed with FACS buffer (PBS+ 2%FBS+1mM EDTA) and then incubated with a 1:500 dilution of TruStain FCX (Biolegend, 101320) for 5 minutes. Cells were then stained with a 1:300 dilution of antibodies raised against mouse CD206(Biolegend,141710), CD301(Biorad, MCA2392A647T), and CD71(Biolegend, 113812) for 30 mins on ice. After washing, cells were resuspended in FACS buffer containing 1 μ g/mL DAPI for live/dead cell discrimination. Flow cytometry data was captured on an Attune NXT flow cytometer and analyzed using the FlowJo X software.

Mannose receptor endocytosis assay

3×10^4 day 6 BMDMs were seeded in 96-well plates two days prior to stimulation. Following 48hr. stimulation, cellular uptake of FITC-dextran was quantified by high-content imaging. First, stimulation media was removed and replaced with high-glucose DMEM containing 1mg/mL FITC-dextran (Sigma, FD40) and 10ng/mL Hoechst 3342. Following a 1hr. incubation at 37°C, cells were washed twice with PBS and fixed with 4% paraformaldehyde (PFA). Images were captured with a PerkinElmer Operetta, while FITC positive foci per cell were calculated using Harmony software

Quantification of short-chain acyl CoAs

Experiments were performed as previously described (Jones *et al.*, 2021). Briefly, day 6 BMDMs were seeded in 10cm dishes at 5×10^6 cells/dish two days prior to stimulation. Following 48hr. stimulation, intracellular acyl CoAs were extracted. Cells were rinsed with PBS twice, scraped into 1.5mL centrifuge tubes, and pelleted via centrifugation. 200 μ L of extraction solution was added to each cell pellet on ice and mixed. The extraction solution consisted of 2.5% (w/v) 5-sulfosalicylic acid (SSA) along with 1 μ M Crotonoyl CoA internal standard. Following extraction, the samples were centrifuged at 18,000 g for 15 min. Supernatants containing short-chain acyl CoAs were then removed and transferred to glass LC-MS vials for analysis.

Respirometry and lactate efflux

Day 6 BMDMs were plated at 3.0×10^4 cells/well in XF96 plates two days prior to stimulation. Following 48 hr. stimulation, respirometry assays were conducted with an Agilent Seahorse XFe96. Oligomycin (2 μ M), two injections of FCCP (750 nM each), and rotenone (200 nM) with antimycin A (1 μ M) were added acutely to the wells, and respiratory parameters calculated as mentioned previously (Divakaruni *et al.*, 2014). Cells were assayed in standard conditions of DMEM media (Sigma) supplemented with 5 mM HEPES, 8 mM glucose, 2 mM glutamine, and 2 mM pyruvate. Lactate efflux was measured by correcting rates of extracellular acidification for microplate sensor coverage and confounding respiratory acidification (Desousa *et al.*, 2022).

Metabolomics and stable isotope tracing Extraction

Day 6 BMDMs were plated at 1×10^6 cells/ well in 6-well dishes in normal BMDM media two days prior to stimulation. Two days later, cells were stimulated in BMDM media supplemented with 10mM uniformly labeled $^{13}\text{C}_6$ -glucose. Following 48 stimulation, cells were harvested and extracted for GC/MS analysis using established methods(Cordes and Metallo, 2019). Briefly, cell plates were placed on ice and washed twice with ice-cold 0.9% (w/v) NaCl. 500 μL of ice-cold methanol and 200 μL water containing 1 μg of the internal standard norvaline was added to cells. Cells were then scraped and placed in 1.5 mL centrifuge tubes kept on ice. Next, 500 μL of chloroform was added and the samples were vortexed for 1 min and then spun at 10,000 g for 5 min at 4°C . The aqueous layer containing the polar metabolites was transferred to a GC/MS sample vial and dried overnight using a refrigerated CentriVap. Once dry, the samples were resuspended in 20 μL of 2% (w/v) methoxyamine in pyridine and incubated at 37°C for 45 minutes. This was followed by addition of 20 μL of MTBSTFA + 1% TBDMSCI (Ntert-Butyldimethylsilyl-N-methyltrifluoroacetamide with 1% tertButyldimethylchlorosilane). Following a second 45-minute incubation at 37°C , samples were run as previously described(Cordes and Metallo, 2019). Samples were analyzed using Agilent MassHunter software and stable isotope tracing data was corrected for natural abundance of heavy isotopes with FluxFix software using a reference set of unlabeled metabolite standards(Trefely et al., 2016).

De novo lipogenesis quantification

Day 6 BMDMs were plated at 1×10^5 cells/ well in 24-well dishes in normal BMDM media. Following 2 days of rest, cells were stimulated in BMDM media which was supplemented with 10mM uniformly labeled $^{13}\text{C}_6$ -glucose. Extraction of labeled fatty acids was performed as previously described (Argus et al., 2018; Hsieh et al., 2021; Williams et al., 2013). Isotopomer spectral analysis (ISA) was conducted using an Agilent 5975C mass spectrometer coupled to a 7890 Gas Chromatograph as previously described (Hsieh *et al.*, 2021; Williams *et al.*, 2013)

Human TLR reporter cell line assays

HEK-Blue hTLR2/4/7 reporter cells (InvivoGen) were maintained according to the manufacturer's instructions. To establish dose-response curves, 2.5×10^3 reporter cells were resuspended in HEK-Blue detection medium and stimulated with increasing concentration of the appropriate agonist. Following a 24hr. incubation, SEAP reporter activity was determined by reading the OD_{630} with a plate reader. To determine if CoA acted as a TLR ligand, hTLR reporter cells were treated with 1mM CoA for 24hr. and the OD_{630} was determined. The OD_{630} of CoA treated cells was then compared to the maximal OD_{630} for each hTLR cell line.

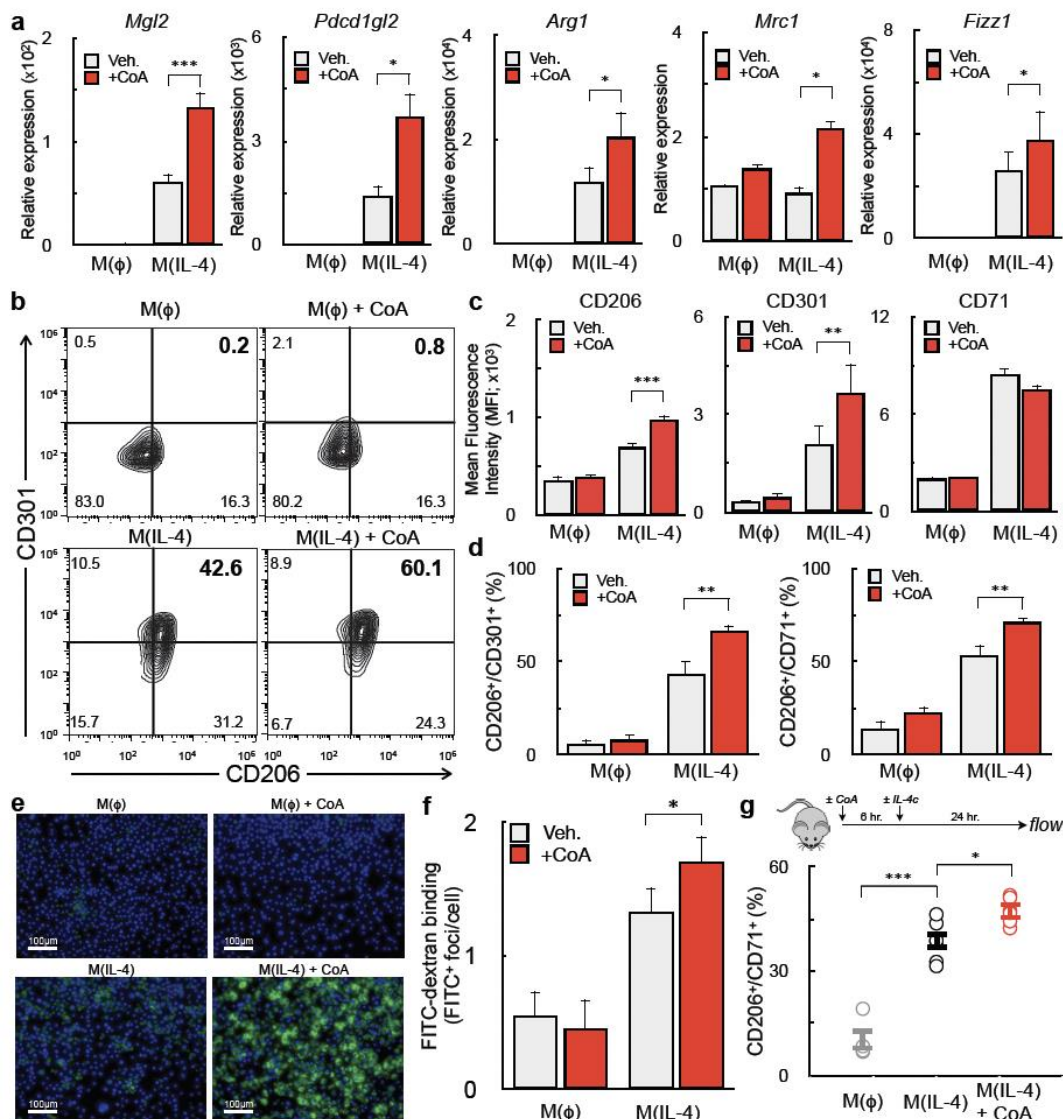


Figure 1: Exogenous CoA enhances alternative macrophage activation

(A) qPCR analysis of the IL-4-associated genes *Mgl2*, *Pdc1gl2*, *Arg1*, *Mrc1* and *Arg1* in BMDMs left unstimulated or treated with CoA(1mM), IL-4(20ng/mL), or CoA + IL-4 for 48h (n \geq 9 independent biological replicates). **(B-D)** Flow cytometric analysis of the IL-4-associated cell surface markers CD206, CD301, and CD71 in after the indicated treatment. Cells were stimulated for 48 h with CoA, IL-4, or IL-4+CoA. **(B)** Contour plots, the percentage of cells

expressing both CD206 and CD301 is indicated in the upper right quadrant. These data shown are from a single experiment and representative of a total of nine independent biological replicates. **(C)** Mean fluorescence intensity of CD206, CD301, and CD71 in BMDMs following the indicated treatment. (n=9 independent biological replicates). **(D)** Percentage of CD206⁺/CD301⁺ and CD206⁺/CD71⁺ populations following 48 h treatment (n=9 independent biological replicates). **(E)** Representative high-content images of BMDMs incubated with FITC-Dextran (1mg/mL, green) and Hoechst 3342 (10ng/mL, blue) for 1hr following stimulation with indicated compounds for 48 h (representative of n=3 independent biological replicates). **(F)** Aggregate image analysis data for BMDMs stained with FITC-Dextran. Data is shown as FITC⁺ foci per cell (n=3 independent biological replicates). **(G)** Quantification of CD206⁺/CD71⁺ peritoneal macrophages from mice that were exposed to vehicle (PBS), CoA(40mg/kg), IL-4c (5µg IL-4/25µg anti-IL-4 monoclonal antibody), or the combination of IL-4c + CoA. (n≥3 mice were used for each group). All data are presented as mean ± SEM. *p < 0.05; **p < 0.01; ***p < 0.001.

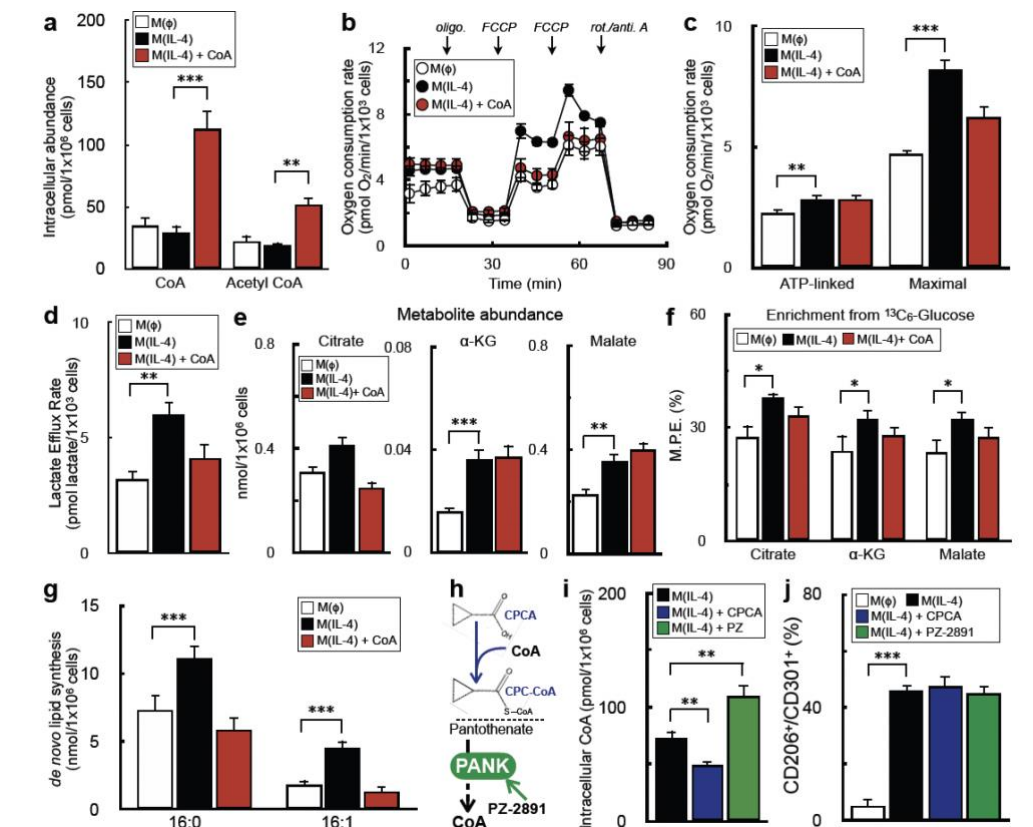


Figure 2: CoA does not enhance alternative macrophage activation by boosting known metabolic hallmarks of the IL-4 response.

(A) Intracellular CoA and acetyl CoA levels of BMDMs measured by LC-MS/MS. Cells were treated with either IL-4 or IL-4+CoA for 48 h (n=3 independent biological replicates). **(B)** Respirometry trace of BMDMs treated with IL-4 alone or in combination with CoA for 48hrs. (n=5 technical replicates). These data shown are from a single experiment and representative of a total of eight independent biological replicates. **(C)** ATP-linked and FCCP-stimulated respiration in intact BMDMs after stimulation with IL-4 or IL-4+CoA for 48 h. Cells were offered media containing 8mM glucose, 2mM pyruvate, and 2mM glutamine in the experimental medium (n=8 independent biological replicates). **(D)** Lactate efflux rate from respirometry

experiments in (C) (n=8 independent biological replicates). **(E)** Metabolite abundances of citrate, alpha-ketoglutarate(α -KG), and malate in BMDMs exposed to the indicated treatments (n=7 independent biological replicates). **(F)** Enrichment from [U- $^{13}\text{C}_6$] glucose into the TCA cycle intermediates citrate, α -ketoglutarate, and malate in BMDMs treated as in (E) (n=8 independent biological replicates). **(G)** Quantification of synthesized palmitic acid (16:0) and palmitoleic acid (16:1) from BMDMs stimulated with IL-4 alone or in combination with CoA for 48h (data shown as n=8 technical replicates from n=2 independent biological replicates). **(H)** Schematic depicting the mechanism of action of cyclopropane carboxylic acid (CPCA) and PZ-2891. **(I)** Intracellular CoA levels of BMDMs stimulated with IL-4, IL-4+ CPCA(1mM), or IL-4+PZ-2891(10 μM) for 48 h (n=5 independent biological replicates). **(J)** Flow cytometric quantification of the CD206 $^+$ /CD301 $^+$ population for BMDMs treated as in (I) (n=5 independent biological replicates). All data are presented as mean \pm SEM. *p < 0.05; **p < 0.01; ***p < 0.001.

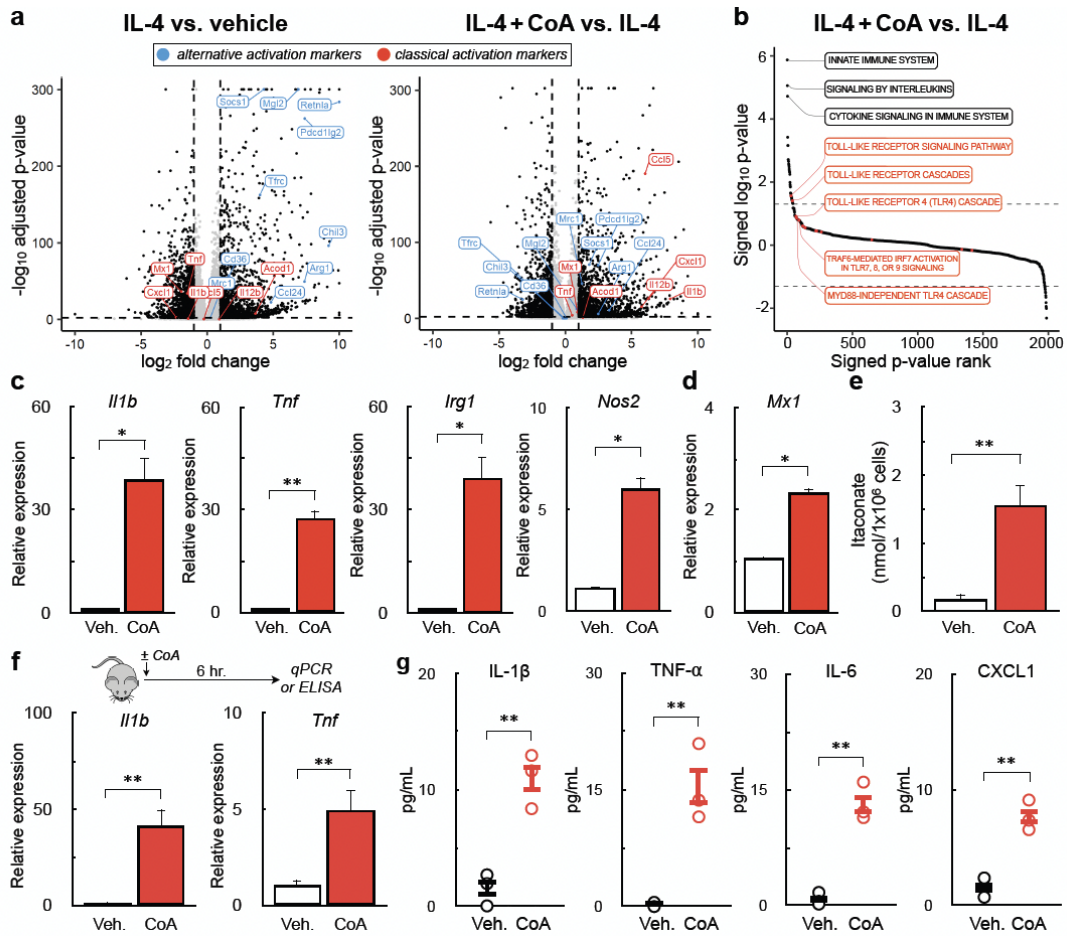


Figure 3: Exogenous CoA induces a pro-inflammatory response in BMDMs

(A) Volcano plot depicting bulk RNA sequencing data from BMDMs treated with NT, IL-4, or IL-4+CoA for 48 h. Comparisons include IL-4 vs. NT and IL-4+CoA vs. IL-4. Genes associated with classical activation are depicted in red, while genes indicative of alternative activation are shown in blue. **(B)** Pathway analysis of genes upregulated in BMDMs treated with IL-4+CoA vs. IL-4 alone. **(C)** qPCR analysis of the classical activation markers *Il1b*, *Tnf*, *Irg1*, and *Nos2* in BMDMs stimulated with CoA(1mM) for 4 h (n=4 independent biological replicates). **(D)** qPCR analysis of the interferon-stimulated gene *Mx1* in BMDMs stimulated with CoA for 24 h (n=4 independent biological replicates). **(E)** Abundance of the pro-inflammatory metabolite itaconate upon stimulation of BMDMs with CoA for 48 h (n=6 independent biological

replicates). **(F)** qPCR analysis of *Il1b* and *Tnf* in the peritoneal exudate cells (PECs) of mice treated with CoA 6 h prior to collection (n≥5 mice were used for each group). **(G)** Multiplexed ELISA quantification of cytokines in the peritoneal lavage fluid (PLF) of mice treated with CoA 6 h prior to collection (n=3 mice were used for each group). All data are presented as mean ± SEM. *p < 0.05; **p < 0.01.

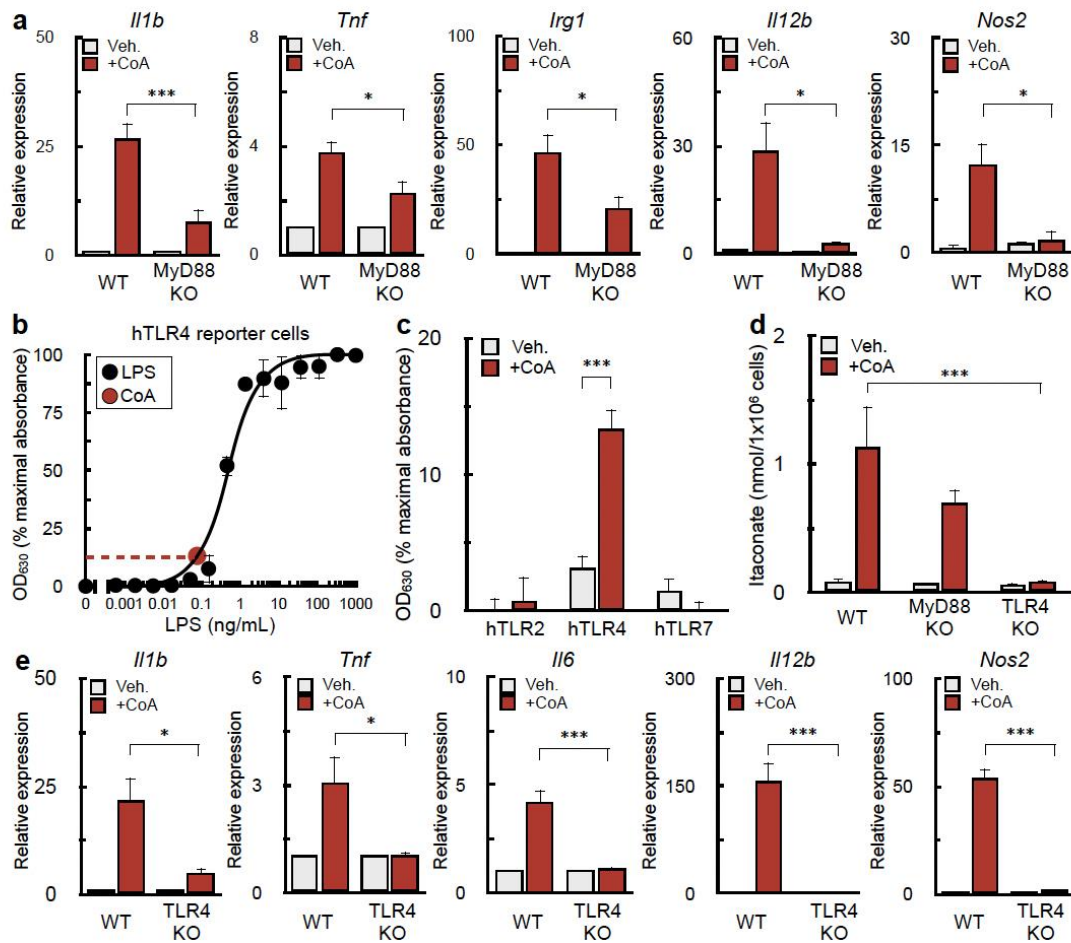


Figure 4: CoA is a toll-like receptor 4 agonist

(A) qPCR analysis of *Il1b*, *Tnf*, *Irg1*, *Il12b*, and *Nos2* in WT and MyD88^{-/-}BMDMs stimulated with CoA for 4 h (n≥3 independent biological replicates). **(B)** Concentration-response curve of hTLR4 reporter cells exposed to increasing concentrations of LPS (black dots). SEAP reporter response is determined by measuring the OD₆₃₀. The red dot and dashed lines represent the OD₆₃₀ observed when hTLR4 reporter cells were exposed to CoA (1mM) (n=4 independent biological replicates). **(C)** Aggregated data showing the activation of hTLR2, hTLR4, and hTLR7 reporter cells following exposure to CoA (1mM) (n≥3 independent biological replicates). **(D)** Abundance of itaconate upon stimulating WT, MyD88^{-/-}, and Tlr4^{-/-} BMDMs with CoA for 48 h n≥5 independent biological replicates). **(E)** qPCR analysis of *Il1b*, *Tnf*, *Il6*, *Il12b*,

and *Nos2* in WT and *Tlr4*^{-/-} BMDMs following treatment with CoA for 4 h (n=3 independent biological replicates). All data are presented as mean ± SEM. *p < 0.05; ***p < 0.001.

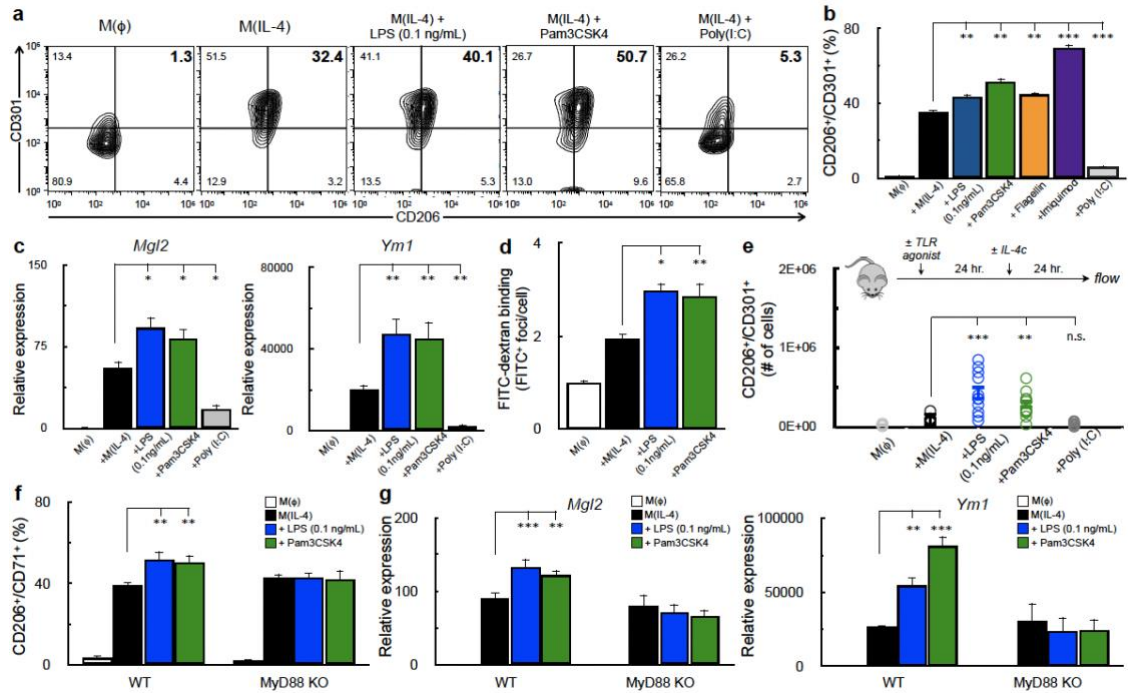


Figure 5. Myd88-linked TLR-ligands enhance IL-4 response

(A-B) Flow cytometric analysis of the IL-4-associated cell surface markers CD206 and CD301 in BMDMs after the indicated treatment. Cells were stimulated with IL-4 alone or IL-4 in combination with LPS(0.1ng/mL), pam3CSK4(5ng/mL), imiquimod (10 μ M), flagellin (100ng/mL), or poly(I:C) (1 μ g/mL) for 48 h **(A)** Contour plots showing the percentage of cells expressing both CD206 and CD301 in the upper right quadrant. These data shown are from a single experiment and representative of a total of eight independent biological replicates. **(B)** Percentage of CD206⁺/CD301⁺ populations following 48 h treatment (n=8 independent biological replicates). **(C)** qPCR analysis of the IL-4-responsive genes *Mgl2* and *Ym1* in BMDMs stimulated with IL-4 alone or IL-4 in combination with LPS, pam3CSK4, or Poly(I:C) for 48h (n \geq 3 independent biological replicates). **(D)** Aggregate high-content image analysis data for BMDMs stained with FITC-Dextran. Data is shown as FITC⁺ foci per cell (n=4 independent biological replicates). **(E)** Quantification of CD206⁺/CD71⁺ peritoneal

125

macrophages from mice that were exposed to vehicle, IL-4c, IL-4c+LPS (125µg), IL-4c+Pam3(50µg), or IL-4c + Poly(I:C) (200µg). (n≥9 mice were used for each group). **(F)** Percentage of CD206⁺/CD301⁺ populations in WT and MyD88^{-/-}BMDMs stimulated with IL-4 alone or in combination with the indicated TLR agonists for 48 h (n=8 independent biological replicates). **(G)** qPCR analysis of *Mgl2* and *Ym1* in WT and MyD88^{-/-}BMDMs exposed to the indicated treatments for 48 h (n=4 independent biological replicates). All data are presented as mean ± SEM. *p < 0.05; **p < 0.01; ***p < 0.001; ns, not significant.

5. References

- Akira, S., and Takeda, K. (2004). Toll-like receptor signalling. *Nat Rev Immunol* 4, 499-511. 10.1038/nri1391.
- Argus, J.P., Wilks, M.Q., Zhou, Q.D., Hsieh, W.Y., Khialeeva, E., Hoi, X.P., Bui, V., Xu, S., Yu, A.K., Wang, E.S., et al. (2018). Development and Application of FASA, a Model for Quantifying Fatty Acid Metabolism Using Stable Isotope Labeling. *Cell Rep* 25, 2919-2934.e2918. 10.1016/j.celrep.2018.11.041.
- Arnold, L., Henry, A., Poron, F., Baba-Amer, Y., van Rooijen, N., Plonquet, A., Gherardi, R.K., and Chazaud, B. (2007). Inflammatory monocytes recruited after skeletal muscle injury switch into antiinflammatory macrophages to support myogenesis. *J Exp Med* 204, 1057-1069. 10.1084/jem.20070075.
- Bidault, G., Virtue, S., Petkevicius, K., Jolin, H.E., Dugourd, A., Guénantin, A.C., Leggat, J., Mahler-Araujo, B., Lam, B.Y.H., Ma, M.K., et al. (2021). SREBP1-induced fatty acid synthesis depletes macrophages antioxidant defences to promote their alternative activation. *Nat Metab* 3, 1150-1162. 10.1038/s42255-021-00440-5.
- Chazaud, B. (2020). Inflammation and Skeletal Muscle Regeneration: Leave It to the Macrophages! *Trends Immunol* 41, 481-492. 10.1016/j.it.2020.04.006.
- Chomarat, P., and Banchereau, J. (1998). Interleukin-4 and interleukin-13: their similarities and discrepancies. *Int Rev Immunol* 17, 1-52. 10.3109/08830189809084486.

Cordes, T., and Metallo, C.M. (2019). Quantifying Intermediary Metabolism and Lipogenesis in Cultured Mammalian Cells Using Stable Isotope Tracing and Mass Spectrometry.

Methods Mol Biol 1978, 219-241. 10.1007/978-1-4939-9236-2_14.

Cruz, C.M., Rinna, A., Forman, H.J., Ventura, A.L., Persechini, P.M., and Ojcius, D.M.

(2007). ATP activates a reactive oxygen species-dependent oxidative stress response and secretion of proinflammatory cytokines in macrophages. *J Biol Chem* 282, 2871-2879.

10.1074/jbc.M608083200.

Csóka, B., Selmeczy, Z., Koscsó, B., Németh, Z.H., Pacher, P., Murray, P.J., Kepka-

Lenhart, D., Morris, S.M., Jr., Gause, W.C., Leibovich, S.J., and Haskó, G. (2012).

Adenosine promotes alternative macrophage activation via A2A and A2B receptors. *Faseb j* 26, 376-386. 10.1096/fj.11-190934.

Dang, E.V., Lei, S., Radkov, A., Volk, R.F., Zaro, B.W., and Madhani, H.D. (2022). Secreted fungal virulence effector triggers allergic inflammation via TLR4. *Nature* 608, 161-167.

10.1038/s41586-022-05005-4.

Desousa, B.R., Kim, K.K.O., Hsieh, W.Y., Jones, A.E., Swain, P., Morrow, D.H., Ferrick,

D.A., Shirihai, O.S., Neilson, A., Nathanson, D.A., et al. (2022). Calculating ATP production rates from oxidative phosphorylation and glycolysis during cell activation. *bioRxiv*,

2022.2004.2016.488523. 10.1101/2022.04.16.488523.

Dichtl, S., Sanin, D.E., Koss, C.K., Willenborg, S., Petzold, A., Tanzer, M.C., Dahl, A., Kabat,

A.M., Lindenthal, L., Zeitler, L., et al. (2022). Gene-selective transcription promotes the

inhibition of tissue reparative macrophages by TNF. *Life Sci Alliance* 5.

10.26508/lisa.202101315.

Divakaruni, A.S., Hsieh, W.Y., Minarrieta, L., Duong, T.N., Kim, K.K.O., Desousa, B.R.,

Andreyev, A.Y., Bowman, C.E., Caradonna, K., Dranka, B.P., et al. (2018). Etomoxir Inhibits Macrophage Polarization by Disrupting CoA Homeostasis. *Cell Metab* 28, 490-503.e497.

10.1016/j.cmet.2018.06.001.

Divakaruni, A.S., Paradyse, A., Ferrick, D.A., Murphy, A.N., and Jastroch, M. (2014).

Analysis and interpretation of microplate-based oxygen consumption and pH data. *Methods Enzymol* 547, 309-354. 10.1016/b978-0-12-801415-8.00016-3.

Faas, M., Ipseiz, N., Ackermann, J., Culemann, S., Grüneboom, A., Schröder, F., Rothe, T.,

Scholtyssek, C., Eberhardt, M., Böttcher, M., et al. (2021). IL-33-induced metabolic reprogramming controls the differentiation of alternatively activated macrophages and the resolution of inflammation. *Immunity* 54, 2531-2546.e2535. 10.1016/j.immuni.2021.09.010.

Fitzgerald, K.A., and Kagan, J.C. (2020). Toll-like Receptors and the Control of Immunity.

Cell 180, 1044-1066. 10.1016/j.cell.2020.02.041.

Glass, C.K., and Natoli, G. (2016). Molecular control of activation and priming in macrophages. *Nat Immunol* 17, 26-33. 10.1038/ni.3306.

Gordon, S., and Martinez, F.O. (2010). Alternative Activation of Macrophages: Mechanism and Functions. *Immunity* 32, 593-604. <https://doi.org/10.1016/j.immuni.2010.05.007>.

Gout, I. (2018). Coenzyme A, protein CoAlation and redox regulation in mammalian cells.

Biochem Soc Trans 46, 721-728. 10.1042/bst20170506.

Haschemi, A., Kosma, P., Gille, L., Evans, C.R., Burant, C.F., Starkl, P., Knapp, B., Haas, R., Schmid, J.A., Jandl, C., et al. (2012). The sedoheptulose kinase CARKL directs macrophage polarization through control of glucose metabolism. *Cell Metab* 15, 813-826. 10.1016/j.cmet.2012.04.023.

Heller, N.M., Qi, X., Junttila, I.S., Shirey, K.A., Vogel, S.N., Paul, W.E., and Keegan, A.D. (2008). Type I IL-4Rs selectively activate IRS-2 to induce target gene expression in macrophages. *Sci Signal* 1, ra17. 10.1126/scisignal.1164795.

Hesketh, M., Sahin, K.B., West, Z.E., and Murray, R.Z. (2017). Macrophage Phenotypes Regulate Scar Formation and Chronic Wound Healing. *Int J Mol Sci* 18. 10.3390/ijms18071545.

Hsieh, W.Y., Williams, K.J., Su, B., and Bensinger, S.J. (2021). Profiling of mouse macrophage lipidome using direct infusion shotgun mass spectrometry. *STAR Protoc* 2, 100235. 10.1016/j.xpro.2020.100235.

Huang, S.C., Everts, B., Ivanova, Y., O'Sullivan, D., Nascimento, M., Smith, A.M., Beatty, W., Love-Gregory, L., Lam, W.Y., O'Neill, C.M., et al. (2014). Cell-intrinsic lysosomal lipolysis is essential for alternative activation of macrophages. *Nat Immunol* 15, 846-855. 10.1038/ni.2956.

Huang, S.C., Smith, A.M., Everts, B., Colonna, M., Pearce, E.L., Schilling, J.D., and Pearce, E.J. (2016). Metabolic Reprogramming Mediated by the mTORC2-IRF4 Signaling Axis Is Essential for Macrophage Alternative Activation. *Immunity* 45, 817-830. 10.1016/j.immuni.2016.09.016.

Jha, A.K., Huang, S.C., Sergushichev, A., Lampropoulou, V., Ivanova, Y., Loginicheva, E., Chmielewski, K., Stewart, K.M., Ashall, J., Everts, B., et al. (2015). Network integration of parallel metabolic and transcriptional data reveals metabolic modules that regulate macrophage polarization. *Immunity* 42, 419-430. 10.1016/j.immuni.2015.02.005.

Jones, A.E., Arias, N.J., Acevedo, A., Reddy, S.T., Divakaruni, A.S., and Meriwether, D. (2021). A Single LC-MS/MS Analysis to Quantify CoA Biosynthetic Intermediates and Short-Chain Acyl CoAs. *Metabolites* 11. 10.3390/metabo11080468.

Jones, A.E., and Divakaruni, A.S. (2020). Macrophage activation as an archetype of mitochondrial repurposing. *Mol Aspects Med* 71, 100838. 10.1016/j.mam.2019.100838.

Kawai, T., Adachi, O., Ogawa, T., Takeda, K., and Akira, S. (1999). Unresponsiveness of MyD88-deficient mice to endotoxin. *Immunity* 11, 115-122. 10.1016/s1074-7613(00)80086-2.

Kawai, T., and Akira, S. (2010). The role of pattern-recognition receptors in innate immunity: update on Toll-like receptors. *Nat Immunol* 11, 373-384. 10.1038/ni.1863.

Kawai, T., Takeuchi, O., Fujita, T., Inoue, J., Mühlradt, P.F., Sato, S., Hoshino, K., and Akira, S. (2001). Lipopolysaccharide stimulates the MyD88-independent pathway and results in activation of IFN-regulatory factor 3 and the expression of a subset of lipopolysaccharide-inducible genes. *J Immunol* 167, 5887-5894. 10.4049/jimmunol.167.10.5887.

Kusnadi, A., Park, S.H., Yuan, R., Pannellini, T., Giannopoulou, E., Oliver, D., Lu, T., Park-Min, K.H., and Ivashkiv, L.B. (2019). The Cytokine TNF Promotes Transcription Factor SREBP Activity and Binding to Inflammatory Genes to Activate Macrophages and Limit Tissue Repair. *Immunity* 51, 241-257.e249. 10.1016/j.immuni.2019.06.005.

Leonardi, R., Zhang, Y.M., Rock, C.O., and Jackowski, S. (2005). Coenzyme A: back in action. *Prog Lipid Res* 44, 125-153. 10.1016/j.plipres.2005.04.001.

Liu, P.S., Wang, H., Li, X., Chao, T., Teav, T., Christen, S., Di Conza, G., Cheng, W.C., Chou, C.H., Vavakova, M., et al. (2017). α -ketoglutarate orchestrates macrophage activation through metabolic and epigenetic reprogramming. *Nat Immunol* 18, 985-994.

10.1038/ni.3796.

Liu, S.X., Gustafson, H.H., Jackson, D.L., Pun, S.H., and Trapnell, C. (2020). Trajectory analysis quantifies transcriptional plasticity during macrophage polarization. *Sci Rep* 10, 12273. 10.1038/s41598-020-68766-w.

Luan, B., Yoon, Y.-S., Le Lay, J., Kaestner, K.H., Hedrick, S., and Montminy, M. (2015). CREB pathway links PGE2 signaling with macrophage polarization. *Proceedings of the National Academy of Sciences* 112, 15642-15647. doi:10.1073/pnas.1519644112.

Lucas, T., Waisman, A., Ranjan, R., Roes, J., Krieg, T., Müller, W., Roers, A., and Eming, S.A. (2010). Differential Roles of Macrophages in Diverse Phases of Skin Repair. *The Journal of Immunology* 184, 3964-3977. 10.4049/jimmunol.0903356.

Major, J., Fletcher, J.E., and Hamilton, T.A. (2002). IL-4 pretreatment selectively enhances cytokine and chemokine production in lipopolysaccharide-stimulated mouse peritoneal macrophages. *J Immunol* 168, 2456-2463. 10.4049/jimmunol.168.5.2456.

Martinez, F.O., and Gordon, S. (2014). The M1 and M2 paradigm of macrophage activation: time for reassessment. *F1000Prime Rep* 6, 13. 10.12703/p6-13.

Martinez, F.O., Helming, L., Milde, R., Varin, A., Melgert, B.N., Draijer, C., Thomas, B., Fabbri, M., Crawshaw, A., Ho, L.P., et al. (2013). Genetic programs expressed in resting and IL-4 alternatively activated mouse and human macrophages: similarities and differences. *Blood* 121, e57-69. 10.1182/blood-2012-06-436212.

Midwood, K., Sacre, S., Piccinini, A.M., Inglis, J., Trebault, A., Chan, E., Drexler, S., Sofat, N., Kashiwagi, M., Orend, G., et al. (2009). Tenascin-C is an endogenous activator of Toll-like receptor 4 that is essential for maintaining inflammation in arthritic joint disease. *Nat Med* 15, 774-780. 10.1038/nm.1987.

Ming-Chin Lee, K., Achuthan, A.A., De Souza, D.P., Lupancu, T.J., Binger, K.J., Lee, M.K.S., Xu, Y., McConville, M.J., de Weerd, N.A., Dragoljevic, D., et al. (2022). Type I interferon antagonism of the JMJD3-IRF4 pathway modulates macrophage activation and polarization. *Cell Rep* 39, 110719. 10.1016/j.celrep.2022.110719.

Murray, P.J. (2017). Macrophage Polarization. *Annu Rev Physiol* 79, 541-566. 10.1146/annurev-physiol-022516-034339.

O'Brien, E.M., and Spiller, K.L. (2022). Pro-inflammatory polarization primes Macrophages to transition into a distinct M2-like phenotype in response to IL-4. *J Leukoc Biol* 111, 989-1000. 10.1002/jlb.3a0520-338r.

Okamura, Y., Watari, M., Jerud, E.S., Young, D.W., Ishizaka, S.T., Rose, J., Chow, J.C., and Strauss, J.F., 3rd (2001). The extra domain A of fibronectin activates Toll-like receptor 4. *J Biol Chem* 276, 10229-10233. 10.1074/jbc.M100099200.

Pelka, K., Bertheloot, D., Reimer, E., Phulphagar, K., Schmidt, S.V., Christ, A., Stahl, R., Watson, N., Miyake, K., Hacohen, N., et al. (2018). The Chaperone UNC93B1 Regulates Toll-like Receptor Stability Independently of Endosomal TLR Transport. *Immunity* 48, 911-922.e917. 10.1016/j.immuni.2018.04.011.

Pietrocola, F., Galluzzi, L., Bravo-San Pedro, J.M., Madeo, F., and Kroemer, G. (2015). Acetyl coenzyme A: a central metabolite and second messenger. *Cell Metab* 21, 805-821. 10.1016/j.cmet.2015.05.014.

Puleston, D.J., Buck, M.D., Klein Geltink, R.I., Kyle, R.L., Caputa, G., O'Sullivan, D., Cameron, A.M., Castoldi, A., Musa, Y., Kabat, A.M., et al. (2019). Polyamines and eIF5A Hypusination Modulate Mitochondrial Respiration and Macrophage Activation. *Cell Metab* 30, 352-363.e358. 10.1016/j.cmet.2019.05.003.

Rao, A.J., Gibon, E., Ma, T., Yao, Z., Smith, R.L., and Goodman, S.B. (2012). Revision joint replacement, wear particles, and macrophage polarization. *Acta Biomater* 8, 2815-2823. 10.1016/j.actbio.2012.03.042.

Rifkin, I.R., Leadbetter, E.A., Busconi, L., Viglianti, G., and Marshak-Rothstein, A. (2005). Toll-like receptors, endogenous ligands, and systemic autoimmune disease. *Immunol Rev* 204, 27-42. 10.1111/j.0105-2896.2005.00239.x.

Sallusto, F., Cella, M., Danieli, C., and Lanzavecchia, A. (1995). Dendritic cells use macropinocytosis and the mannose receptor to concentrate macromolecules in the major histocompatibility complex class II compartment: downregulation by cytokines and bacterial products. *J Exp Med* 182, 389-400. 10.1084/jem.182.2.389.

Sanin, D.E., Matsushita, M., Klein Geltink, R.I., Grzes, K.M., van Teijlingen Bakker, N., Corrado, M., Kabat, A.M., Buck, M.D., Qiu, J., Lawless, S.J., et al. (2018). Mitochondrial Membrane Potential Regulates Nuclear Gene Expression in Macrophages Exposed to Prostaglandin E2. *Immunity* 49, 1021-1033.e1026. 10.1016/j.immuni.2018.10.011.

Sharma, L.K., Subramanian, C., Yun, M.-K., Frank, M.W., White, S.W., Rock, C.O., Lee, R.E., and Jackowski, S. (2018). A therapeutic approach to pantothenate kinase associated neurodegeneration. *Nature Communications* 9, 4399. 10.1038/s41467-018-06703-2.

Sica, A., and Mantovani, A. (2012). Macrophage plasticity and polarization: in vivo veritas. *J Clin Invest* 122, 787-795. 10.1172/jci59643.

Snyder, G.A., Cirl, C., Jiang, J., Chen, K., Waldhuber, A., Smith, P., Römmler, F., Snyder, N., Fresquez, T., Dürr, S., et al. (2013). Molecular mechanisms for the subversion of MyD88 signaling by TcpC from virulent uropathogenic *Escherichia coli*. *Proceedings of the National Academy of Sciences* 110, 6985-6990. doi:10.1073/pnas.1215770110.

Sosa, R.A., Terry, A.Q., Kaldas, F.M., Jin, Y.P., Rossetti, M., Ito, T., Li, F., Ahn, R.S., Naini, B.V., Groyberg, V.M., et al. (2021). Disulfide High-Mobility Group Box 1 Drives Ischemia-Reperfusion Injury in Human Liver Transplantation. *Hepatology* 73, 1158-1175. 10.1002/hep.31324.

Takeuchi, O., and Akira, S. (2010). Pattern recognition receptors and inflammation. *Cell* 140, 805-820. 10.1016/j.cell.2010.01.022.

Tannahill, G.M., Curtis, A.M., Adamik, J., Palsson-McDermott, E.M., McGettrick, A.F., Goel, G., Frezza, C., Bernard, N.J., Kelly, B., Foley, N.H., et al. (2013). Succinate is an

inflammatory signal that induces IL-1 β through HIF-1 α . *Nature* 496, 238-242.

10.1038/nature11986.

Timblin, G.A., Tharp, K.M., Hoeve, J.t., Baydemir, I., Khantwal, C., Farahzad, J.N.,

Domínguez-Andrés, J., Vance, R.E., and Weaver, V.M. (2022). Coenzyme A governs proinflammatory macrophage metabolism. *bioRxiv*, 2022.2008.2030.505732.

10.1101/2022.08.30.505732.

Toshchakov, V., Jones, B.W., Perera, P.Y., Thomas, K., Cody, M.J., Zhang, S., Williams,

B.R., Major, J., Hamilton, T.A., Fenton, M.J., and Vogel, S.N. (2002). TLR4, but not TLR2,

mediates IFN-beta-induced STAT1alpha/beta-dependent gene expression in macrophages.

Nat Immunol 3, 392-398. 10.1038/ni774.

Trefely, S., Ashwell, P., and Snyder, N.W. (2016). FluxFix: automatic isotopologue

normalization for metabolic tracer analysis. *BMC Bioinformatics* 17, 485. 10.1186/s12859-016-1360-7.

Van den Bossche, J., Baardman, J., Otto, N.A., van der Velden, S., Neele, A.E., van den

Berg, S.M., Luque-Martin, R., Chen, H.J., Boshuizen, M.C., Ahmed, M., et al. (2016).

Mitochondrial Dysfunction Prevents Repolarization of Inflammatory Macrophages. *Cell Rep* 17, 684-696. 10.1016/j.celrep.2016.09.008.

Van den Bossche, J., O'Neill, L.A., and Menon, D. (2017). Macrophage Immunometabolism:

Where Are We (Going)? *Trends Immunol* 38, 395-406. 10.1016/j.it.2017.03.001.

van Die, I., and Cummings, R.D. (2017). The Mannose Receptor in Regulation of Helminth-

Mediated Host Immunity. *Front Immunol* 8, 1677. 10.3389/fimmu.2017.01677.

van Liempt, E., van Vliet, S.J., Engering, A., García Vallejo, J.J., Bank, C.M., Sanchez-Hernandez, M., van Kooyk, Y., and van Die, I. (2007). Schistosoma mansoni soluble egg antigens are internalized by human dendritic cells through multiple C-type lectins and suppress TLR-induced dendritic cell activation. *Mol Immunol* 44, 2605-2615.

10.1016/j.molimm.2006.12.012.

Vats, D., Mukundan, L., Odegaard, J.I., Zhang, L., Smith, K.L., Morel, C.R., Wagner, R.A., Greaves, D.R., Murray, P.J., and Chawla, A. (2006). Oxidative metabolism and PGC-1beta attenuate macrophage-mediated inflammation. *Cell Metab* 4, 13-24.

10.1016/j.cmet.2006.05.011.

Vénéreau, E., Ceriotti, C., and Bianchi, M.E. (2015). DAMPs from Cell Death to New Life. *Front Immunol* 6, 422. 10.3389/fimmu.2015.00422.

Williams, K.J., Argus, J.P., Zhu, Y., Wilks, M.Q., Marbois, B.N., York, A.G., Kidani, Y., Pourzia, A.L., Akhavan, D., Lisiero, D.N., et al. (2013). An essential requirement for the SCAP/SREBP signaling axis to protect cancer cells from lipotoxicity. *Cancer Res* 73, 2850-2862. 10.1158/0008-5472.Can-13-0382-t.

Conclusions and Future Directions

A shift in the macrophage polarization state has been demonstrated in a variety of pathologies. Because of this, changing the macrophage activation state has gained interest as a possible therapeutic strategy. Since defined metabolic changes are associated with different activation states, altering macrophage metabolism is an attractive therapeutic target. Our previous studies demonstrated that disrupting CoA homeostasis negatively impacted alternative activation, while adding exogenous CoA increased the expression of some cell-surface markers associated with the IL-4 response.

Initially, we sought to understand if addition of exogenous CoA increased the synthesis of specific intracellular acyl-CoAs in alternatively activated macrophages. To do this, we developed a MS/MS method that allows for the detection of short-chain acyl-CoAs and the CoA biosynthetic intermediates. This method allowed us to use a single method to analyze CoA esters and biosynthetic precursors. Following validation, we utilized our method to understand how CoA homeostasis impacts IL-4-activated macrophages. We showed that supplementing BMDM culture media with CoA increased the abundance of many intracellular short-chain CoA esters including acetyl CoA and propionyl CoA. Because these metabolites are involved in many facets of cell physiology, the mechanism linking exogenous CoA supplementation with an enhanced IL-4 response still remained unclear.

Our follow-up study aimed at determining the mechanism by which CoA enhances alternative activation. First, we demonstrated that CoA was able to enhance the expression of alternative activation markers *in vitro* and *in vivo*. In addition to increasing IL-4-driven cell-surface marker levels, CoA enhanced the expression of many IL-4-associated genes and

increased the IL-4-dependent activity of the mannose receptor. These results are in line with other studies showing that addition of metabolites, such as prostaglandin E2 (PGE2), is able to affect alternative activation markers by influencing mitochondrial membrane potential and cyclic AMP-responsive element binding (CREB) signaling (Luan *et al.*, 2015; Sanin *et al.*, 2018). Addition of exogenous purine and TCA cycle metabolites have also been demonstrated to enhance alternative activation (Csóka *et al.*, 2012; Liu *et al.*, 2017). While loss-of-function studies have proven useful, we believe that further gain-of-function studies that investigate how exogenous compounds can be used to further enhance alternative activation may be of greater therapeutic relevance.

Surprisingly, we found that addition of CoA does not augment alternative activation by increasing flux through metabolic pathways associated with IL-4 activation. While the link between macrophage activation and changes in cellular metabolism have been thoroughly established (Van den Bossche *et al.*, 2017), much of the work investigating these pathways has focused on showing that disruption of metabolism diminishes the basal response to IL-4. Our results suggest that alternative activation of macrophages may require reaching an initial metabolic checkpoint, but further increases in metabolism do not need to occur to reach a heightened activation state. This is supported by a recent study showing that addition of exogenous prostaglandins can increase markers of activation while simultaneously decreasing mitochondrial oxidative metabolism (Sanin *et al.*, 2018). Increased spare respiratory capacity is also associated with the IL-4 response; however, we previously demonstrated that mitochondrial respiration is not necessary for some markers of alternative

activation (Divakaruni *et al.*, 2018b). In support of this, our current data shows that CoA increases a wide range of markers associated with the IL-4 response, while also significantly decreasing uncoupler-stimulated respiration in BMDMs. We conclude that precisely determining the role of metabolism during the initial IL-4 response as well as during conditions that enhance IL-4 activation is of keen interest.

Although CoA is able to amplify alternative activation, we show that it is also able to elicit a pro-inflammatory response. This is in agreement with a recent study showing that CoA is capable of increasing the expression of pro-inflammatory genes such as *I11b*, *Tnf* and *Nos2* in mouse and human macrophages (Timblin *et al.*, 2022). We show that CoA elicits a pro-inflammatory effect by activating TLR4 signaling. While not specifically identifying CoA as a TLR4 agonist, Timblin *et al.* show that CoA is no longer able to induce an inflammatory response in BMDMs with a triple knockout of TLR2, TLR4, and the TLR chaperone protein Uncb93b1 (Pelka *et al.*, 2018).

TLR4 has been well characterized for its ability to respond to ligands that are derived from microbes and the role of this PRR in sensing endogenous ligands is also becoming more appreciated (Rifkin *et al.*, 2005). Endogenous proteins including tenascin 1 and high-mobility group box 1 (HMGB1) have recently been shown to induce TLR4-dependent inflammatory response (Midwood *et al.*, 2009; Okamura *et al.*, 2001; Sosa *et al.*, 2021), but the ability of non-protein metabolites to cause TLR4 activation is understudied. Since intracellular CoA levels are as high as 140 μ M in the cytosol and 5mM in the mitochondria (Gout, 2018; Leonardi *et al.*, 2005), we posit that a large occurrence of cell injury or death may allow for the release

of sufficient quantities of CoA to trigger a TLR4-mediated inflammatory response in nearby innate immune cells. This newfound ability of CoA to act as a DAMP is conceivable, as other intracellular metabolites function as DAMPs following their cell death-induced release (Cruz et al., 2007; Vénéreau et al., 2015).

The importance of the cooperation between classically and alternatively activated macrophages *in vivo* cannot be overstated. Healing processes such as muscle and skin repair are both characterized by an initial influx of pro-inflammatory macrophages followed by a later increase in the presence of alternatively activated cells (Arnold *et al.*, 2007; Hesketh *et al.*, 2017). Inhibition of the initial pro-inflammatory response also dampens the later expression of alternative activation markers and decreases wound healing (Lucas et al., 2010). The first instance of synergy between classical and alternative macrophage activation was demonstrated more than 20 years ago, with studies demonstrating that addition of IL-4 enhances the LPS-stimulated expression of pro-inflammatory genes (Major et al., 2002). Until recently there have been few studies investigating whether classical activation stimuli can enhance the IL-4 response. These more modern reports demonstrate that TLR4 agonist such as LPS and the fungal effector CLP1 both enhance the IL-4 response (Dang et al., 2022; Liu et al., 2020; O'Brien and Spiller, 2022; Rao et al., 2012). However, the mechanism by which TLR4 agonism synergizes with IL-4 signaling remained unclear. This synergy could be mediated by the activation of MyD88-dependent or the TRIF-dependent signaling cascades.

In addition to our findings, other studies are in line with the idea that the MyD88 signaling arm of TLR4 is what enhances the IL-4 response. Studies utilizing a fungal-derived

TLR4 agonist demonstrated that MyD88 was necessary to promote alternative activation. Moreover, the MyD88-linked ligand IL-33 has recently been associated with alternative activation (Faas *et al.*, 2021). Contrary to data showing MyD88 can enhance alternative activation, compounds that stimulate interferon signaling, similar to TRIF activation, actually decrease the IL-4 response. For example, stimulating alternatively activated macrophages with TNF- α or interferon- β decreases the expression of cell surface markers and genes associated with alternative activation (Dichtl *et al.*, 2022; Kusnadi *et al.*, 2019; Ming-Chin Lee *et al.*, 2022). Taken together, these studies further support our discovery that MyD88 signaling is sufficient to enhance alternative activation. We believe that future studies determining precisely how MyD88 signaling enhances the IL-4 response are of much importance. Unraveling these mechanisms may lead to the development of a new class of therapeutics for muscle generation, wound healing, and helminth infections.

References:

- Arnold, L., Henry, A., Poron, F., Baba-Amer, Y., van Rooijen, N., Plonquet, A., Gherardi, R.K., and Chazaud, B. (2007). Inflammatory monocytes recruited after skeletal muscle injury switch into antiinflammatory macrophages to support myogenesis. *J Exp Med* 204, 1057-1069. 10.1084/jem.20070075.
- Cruz, C.M., Rinna, A., Forman, H.J., Ventura, A.L., Persechini, P.M., and Ojcius, D.M. (2007). ATP activates a reactive oxygen species-dependent oxidative stress response and secretion of proinflammatory cytokines in macrophages. *J Biol Chem* 282, 2871-2879. 10.1074/jbc.M608083200.
- Csóka, B., Selmeczy, Z., Koscsó, B., Németh, Z.H., Pacher, P., Murray, P.J., Kepka-Lenhart, D., Morris, S.M., Jr., Gause, W.C., Leibovich, S.J., and Haskó, G. (2012). Adenosine promotes alternative macrophage activation via A2A and A2B receptors. *Faseb j* 26, 376-386. 10.1096/fj.11-190934.
- Dang, E.V., Lei, S., Radkov, A., Volk, R.F., Zaro, B.W., and Madhani, H.D. (2022). Secreted fungal virulence effector triggers allergic inflammation via TLR4. *Nature* 608, 161-167. 10.1038/s41586-022-05005-4.
- Dichtl, S., Sanin, D.E., Koss, C.K., Willenborg, S., Petzold, A., Tanzer, M.C., Dahl, A., Kabat, A.M., Lindenthal, L., Zeitler, L., et al. (2022). Gene-selective transcription promotes the inhibition of tissue reparative macrophages by TNF. *Life Sci Alliance* 5. 10.26508/lsa.202101315.

Divakaruni, A.S., Hsieh, W.Y., Minarrieta, L., Duong, T.N., Kim, K.K.O., Desousa, B.R., Andreyev, A.Y., Bowman, C.E., Caradonna, K., Dranka, B.P., et al. (2018). Etomoxir Inhibits Macrophage Polarization by Disrupting CoA Homeostasis. *Cell Metab* 28, 490-503.e497. 10.1016/j.cmet.2018.06.001.

Faas, M., Ipseiz, N., Ackermann, J., Culemann, S., Grüneboom, A., Schröder, F., Rothe, T., Scholtyssek, C., Eberhardt, M., Böttcher, M., et al. (2021). IL-33-induced metabolic reprogramming controls the differentiation of alternatively activated macrophages and the resolution of inflammation. *Immunity* 54, 2531-2546.e2535. 10.1016/j.immuni.2021.09.010.

Gout, I. (2018). Coenzyme A, protein CoAlation and redox regulation in mammalian cells. *Biochem Soc Trans* 46, 721-728. 10.1042/bst20170506.

Hesketh, M., Sahin, K.B., West, Z.E., and Murray, R.Z. (2017). Macrophage Phenotypes Regulate Scar Formation and Chronic Wound Healing. *Int J Mol Sci* 18. 10.3390/ijms18071545.

Kusnadi, A., Park, S.H., Yuan, R., Pannellini, T., Giannopoulou, E., Oliver, D., Lu, T., Park-Min, K.H., and Ivashkiv, L.B. (2019). The Cytokine TNF Promotes Transcription Factor SREBP Activity and Binding to Inflammatory Genes to Activate Macrophages and Limit Tissue Repair. *Immunity* 51, 241-257.e249. 10.1016/j.immuni.2019.06.005.

Leonardi, R., Zhang, Y.M., Rock, C.O., and Jackowski, S. (2005). Coenzyme A: back in action. *Prog Lipid Res* 44, 125-153. 10.1016/j.plipres.2005.04.001.

Liu, P.S., Wang, H., Li, X., Chao, T., Teav, T., Christen, S., Di Conza, G., Cheng, W.C., Chou, C.H., Vavakova, M., et al. (2017). α -ketoglutarate orchestrates macrophage activation

through metabolic and epigenetic reprogramming. *Nat Immunol* 18, 985-994.

10.1038/ni.3796.

Liu, S.X., Gustafson, H.H., Jackson, D.L., Pun, S.H., and Trapnell, C. (2020). Trajectory analysis quantifies transcriptional plasticity during macrophage polarization. *Sci Rep* 10, 12273. 10.1038/s41598-020-68766-w.

Luan, B., Yoon, Y.-S., Le Lay, J., Kaestner, K.H., Hedrick, S., and Montminy, M. (2015). CREB pathway links PGE2 signaling with macrophage polarization. *Proceedings of the National Academy of Sciences* 112, 15642-15647. doi:10.1073/pnas.1519644112.

Lucas, T., Waisman, A., Ranjan, R., Roes, J., Krieg, T., Müller, W., Roers, A., and Eming, S.A. (2010). Differential Roles of Macrophages in Diverse Phases of Skin Repair. *The Journal of Immunology* 184, 3964-3977. 10.4049/jimmunol.0903356.

Major, J., Fletcher, J.E., and Hamilton, T.A. (2002). IL-4 pretreatment selectively enhances cytokine and chemokine production in lipopolysaccharide-stimulated mouse peritoneal macrophages. *J Immunol* 168, 2456-2463. 10.4049/jimmunol.168.5.2456.

Midwood, K., Sacre, S., Piccinini, A.M., Inglis, J., Trebault, A., Chan, E., Drexler, S., Sofat, N., Kashiwagi, M., Orend, G., et al. (2009). Tenascin-C is an endogenous activator of Toll-like receptor 4 that is essential for maintaining inflammation in arthritic joint disease. *Nat Med* 15, 774-780. 10.1038/nm.1987.

Ming-Chin Lee, K., Achuthan, A.A., De Souza, D.P., Lupancu, T.J., Binger, K.J., Lee, M.K.S., Xu, Y., McConville, M.J., de Weerd, N.A., Dragoljevic, D., et al. (2022). Type I

interferon antagonism of the JMJD3-IRF4 pathway modulates macrophage activation and polarization. *Cell Rep* 39, 110719. 10.1016/j.celrep.2022.110719.

O'Brien, E.M., and Spiller, K.L. (2022). Pro-inflammatory polarization primes Macrophages to transition into a distinct M2-like phenotype in response to IL-4. *J Leukoc Biol* 111, 989-1000. 10.1002/jlb.3a0520-338r.

Okamura, Y., Watari, M., Jerud, E.S., Young, D.W., Ishizaka, S.T., Rose, J., Chow, J.C., and Strauss, J.F., 3rd (2001). The extra domain A of fibronectin activates Toll-like receptor 4. *J Biol Chem* 276, 10229-10233. 10.1074/jbc.M100099200.

Pelka, K., Bertheloot, D., Reimer, E., Phulphagar, K., Schmidt, S.V., Christ, A., Stahl, R., Watson, N., Miyake, K., Hacohen, N., et al. (2018). The Chaperone UNC93B1 Regulates Toll-like Receptor Stability Independently of Endosomal TLR Transport. *Immunity* 48, 911-922.e917. 10.1016/j.immuni.2018.04.011.

Rao, A.J., Gibon, E., Ma, T., Yao, Z., Smith, R.L., and Goodman, S.B. (2012). Revision joint replacement, wear particles, and macrophage polarization. *Acta Biomater* 8, 2815-2823. 10.1016/j.actbio.2012.03.042.

Rifkin, I.R., Leadbetter, E.A., Busconi, L., Viglianti, G., and Marshak-Rothstein, A. (2005). Toll-like receptors, endogenous ligands, and systemic autoimmune disease. *Immunol Rev* 204, 27-42. 10.1111/j.0105-2896.2005.00239.x.

Sanin, D.E., Matsushita, M., Klein Geltink, R.I., Grzes, K.M., van Teijlingen Bakker, N., Corrado, M., Kabat, A.M., Buck, M.D., Qiu, J., Lawless, S.J., et al. (2018). Mitochondrial

Membrane Potential Regulates Nuclear Gene Expression in Macrophages Exposed to Prostaglandin E2. *Immunity* 49, 1021-1033.e1026. 10.1016/j.immuni.2018.10.011.

Sosa, R.A., Terry, A.Q., Kaldas, F.M., Jin, Y.P., Rossetti, M., Ito, T., Li, F., Ahn, R.S., Naini, B.V., Groysberg, V.M., et al. (2021). Disulfide High-Mobility Group Box 1 Drives Ischemia-Reperfusion Injury in Human Liver Transplantation. *Hepatology* 73, 1158-1175.

10.1002/hep.31324.

Timblin, G.A., Tharp, K.M., Hoeve, J.t., Baydemir, I., Khantwal, C., Farahzad, J.N., Domínguez-Andrés, J., Vance, R.E., and Weaver, V.M. (2022). Coenzyme A governs proinflammatory macrophage metabolism. *bioRxiv*, 2022.2008.2030.505732.

10.1101/2022.08.30.505732.

Van den Bossche, J., O'Neill, L.A., and Menon, D. (2017). Macrophage Immunometabolism: Where Are We (Going)? *Trends Immunol* 38, 395-406. 10.1016/j.it.2017.03.001.

Vénéreau, E., Ceriotti, C., and Bianchi, M.E. (2015). DAMPs from Cell Death to New Life. *Front Immunol* 6, 422. 10.3389/fimmu.2015.00422.